# INFORMATION TO USERS

This manuscript has been reproduced from the microfilm master. UMI films the text directly from the original or copy submitted. Thus, some thesis and dissertation copies are in typewriter face, while others may be from any type of computer printer.

**The quality of this reproduction is dependent upon the quality of the copy submitted.** Broken or indistinct print, colored or poor quality illustrations and photographs, print bleedthrough, substandard margins, and improper alignment can adversely affect reproduction.

In the unlikely event that the author did not send UMI a complete manuscript and there are missing pages, these will be noted. Also, if unauthorized copyright material had to be removed, a note will indicate the deletion.

Oversize materials (e.g., maps, drawings, charts) are reproduced by sectioning the original, beginning at the upper left-hand corner and continuing from left to right in equal sections with small overlaps.

Photographs included in the original manuscript have been reproduced xerographically in this copy. Higher quality 6" x 9" black and white photographic prints are available for any photographs or illustrations appearing in this copy for an additional charge. Contact UMI directly to order.

ProQuest Information and Learning
300 North Zeeb Road, Ann Arbor, MI 48106-1346 USA
800-521-0600

# New development in ICP spectrometry: Low flow torch for axial viewing ICP-AES & Studies in semiconductor analysis by ICP-MS

by

**Towhid Hasan**

A dissertation submitted to the graduate faculty

in partial fulfillment of the requirements for the degree of

DOCTOR OF PHILOSOPHY

Major: Analytical Chemistry

Program of Study Committee:
R. S. Houk, Major Professor
Dennis C. Johnson
Marc D. Porter
Keith L. Woo
David Laird

Iowa State University

Ames, Iowa

2001

ProQuest Information and Learning Company
300 North Zeeb Road
P.O. Box 1346
Ann Arbor, MI 48106-1346

Graduate College
Iowa State University

This is to certify that the doctoral dissertation of

Towhid Hasan

has met the dissertation requirements of Iowa State University

Signature was redacted for privacy.

Major Professor

Signature was redacted for privacy.

For the Major Program

# TABLE OF CONTENTS

## ABSTRACT

A low argon flow torch has been developed for axially viewed ICP-AES. Outer argon flow has been drastically reduced by cooling the torch wall with air passing through a cooling jacket added to the outside of a Fassel torch. The outer argon gas flow can be reduced to 7 L $min^{-1}$ with no compromise in performance or torch lifetime. The plasma is viewed axially through a cooled cone interface centered on the axial channel. The low flow plasma does not reach out of the torch; but the cooled cone interface facilitates collection of photons from the axial plasma before exposure to air. For the particular spectrometer used, the plasma exhibits the same "robustness index" and interference effects from Na as the conventional, high-flow ICP supplied with the particular spectrometer used. Although detection limits (DL) for lines at ~ 200 nm are poorer by about a factor of two, those for lines at ~ 400 nm are actually much better than values typically seen for the same lines by axial viewing of a conventional, high-flow ICP. Extraordinary detection limits of the elements with high wavelength emission lines, e.g., Ca, Ba, and could be of great value in the semiconductor industry.

Both quantitative and isotope ratio measurement of silicon in organic solvents are essential in semiconductor manufacturing process. Silicon measurement at m/z 28, 29 and 30 by ICP-MS is complicated by the spectral interference caused by organic molecular ions, nitrogen and nitrogen oxides. A method has been developed to measure silicon by reducing polyatomic interferences at m/z 28 to 30. Cryogenic desolvation of organic solvent from the wet droplets of a low flow nebulizer removes most of the solvent and makes silicon determination possible in the parts per million level by low resolution ICP-MS. Krypton and xenon have been added to the sample gas flow of plasma for further removal of polyatomic ions present in the plasma. A few

ml/min of Kr or Xe greatly reduces polyatomic ion intensity in the m/z range of 28 to 30. Isotope ratios can be measured by medium resolution (R=4000) ICP-MS by direct nebulization. To avoid deposition on the interface cone, the flow of oxygen in the spray chamber is adjusted to titrate carbon in the plasma. Despite the sharply pointed peaks at R = 4000, ratio precision of ± 0.1% RSD can be obtained using approximately 1 μg of silicon.

Detection limit of the analyte element by modern ICP-MS is generally limited by the purity of the blank. For detecting very trace contaminants in a high purity substance, like semiconductor materials, a clean blank is necessary. Electrochemically modulated liquid chromatography (EMLC) column has been adapted online with ICP-MS to clean up blanks to reduce background signals and thereby improve detection limits of analyte elements. Metal ions can be retained from the flow of blanks in the micrometer size glassy carbon particle packing with appropriate negative potential. A Ag/AgCl (satd. NaCl) reference electrode in dilute nitric acid supporting electrolyte was used for electrochemical cell combination. The supporting electrolyte is placed outside the porous stainless steel column with a Nafion ion exchange resin coating inside, so that supporting electrolyte does not contaminate the stream of blank flow through the column. Several metal ions have found to be retained with >99% extraction efficiency from the blank solution. Cleaning of the column can be done easily by stripping the deposited metal with a high positive potential.

# CHAPTER 1: GENERAL INTRODUCTION

The inductively coupled plasma (ICP) is an electrical discharge created at radio frequencies. Typically the gas is argon and the plasma is sustained at atmospheric pressure inside a quartz torch. The concept of the ICP started in the 1940s and the idea of radio frequency plasma generation emerged in the early sixties by pioneering work of Reed [1,2]. The use of inductively coupled plasmas as excitation sources for trace metal determinations was first investigated independently by Greenfield and associates [3], and by Wendt and Fassel [4]. Although their work on the ICP later revolutionized elemental analysis, there were early set backs due to the impression that technique was inherently impractical and costly. The high power capacity of the generators, large argon consumption rates used, and the difficulties sometimes experienced in coupling the radio frequency energy into the plasma contributed to that impression. However with the relentless effort of Fassel and coworkers over a decade, ICP atomic emission spectrometry (ICP-AES) emerged as a powerful tool for multi-element analysis in the early 1970s [5-7].

The history of ICP mass spectrometry goes back to the mid 1970s. Gray [8,9] showed that an atmospheric pressure capillary arc DC plasma could be used in conjunction with mass spectrometry for sensitive elemental analysis. Because of the low temperature (4000 K) and poor ionization efficiency of many elements, the DC plasma was not a practical tool of elemental analysis. The coupling of the ICP with a high temperature (7000 K) advantage was realized by Houk et al. in 1980 [10], leading to the development of the most powerful tool for elemental and isotopic analysis. The outstanding features of ICP-MS include multi-element analysis capability with high sensitivity and selectivity, detection limits even in parts per

quadrillion (ppq) level, a large linear dynamic range (8 order of magnitudes), a relatively interference free simple mass spectrum, and isotopic ratio measurement with high precision (0.01% relative standard deviation, RSD) [10-15].

Although ICP optical emission spectrometry and mass spectrometry can already perform elemental analysis at extremely low concentrations and isotopic measurement at very high precision, there are still problems and limitations for their applicability in practical situations. While detection of most of the elements and problems of common interferences have been thoroughly studied, there are still a lot of challenging dilemmas to be resolved and room for improvement in ICP techniques. One obvious obstacle of ICP techniques, in addition to their inevitable capital investment, is the high operating cost of argon (15 to 20 L/min). The popularity of ICP instruments is hindered in developing countries where argon is unavailable or too expensive. Over the years, tremendous efforts have been made by the commercial instrument manufacturers to reduce the capital cost of their instruments, while little has been done to reduce the running cost.

An additional limitation of ICP techniques is their poor performance when handling excess of organic matrices, which also produce polyatomic mass interference in ICP-MS. Silicon is an important element, whose measurement is interfered by polyatomic ions in the m/z range 28 to 30.

With advances in instrumentation especially with introduction of magnetic sector mass analyzer, ICP-MS has gained a tremendous power to detect ultra trace elements present in solution matrices. However, full utilization of its detection ability is somewhat limited by elemental impurities present in the background and blank. To take advantage of the extreme capability of modern ICP-MS instruments it is necessary to obtain a clean blank or

background. With an ever increasing demand for lower detection limits for elements, especially in the semiconductor industry, these problems have to be addressed.

## Operation of an ICP

The ICP torch consists of three concentric quartz-tubes (figure 1). Through the tubes three flows of argon gas (outer flow through outer tube, intermediate flow through intermediate tube and nebulizer flow through injector tube) comprise 15 to 20 L/min in total. At the open end, the torch is encircled by a water cooled copper tube, called the load coil. A RF power of 800 to 2000 W is supplied to the load coil from a generator operated at 27 or 40 MHz. The plasma is ignited by a spark from a Tesla coil, which produces seed electrons to interact with the fluctuating magnetic field converting electrical energy into kinetic energy of electrons. High energy electrons then ionize argon from the outer gas flow (13-18 L/min) forming a stable plasma in the induction zone. The aerosol gas flow punches a hole, referred to as the central channel, and delivers sample aerosol through the center of the plasma. Although the central channel is cooler than the induction region, it is hot enough to dissociate, atomize and ionize to form singly charged atomic ions from sample aerosol. The intermediate flow of argon (1 L/min), introduced through the intermediate tube, helps stabilize the plasma and pushes it forward to keep it from melting the injector tube.

This stable plasma consists of three distinct bodies: the inductive region, the central channel and the plasma tail. The inductive region is mainly where energy coupling occurs. As a sample or droplet travels through the central channel, it will undergo desolvation, vaporization, atomization, ionization and excitation. The central channel consists of three

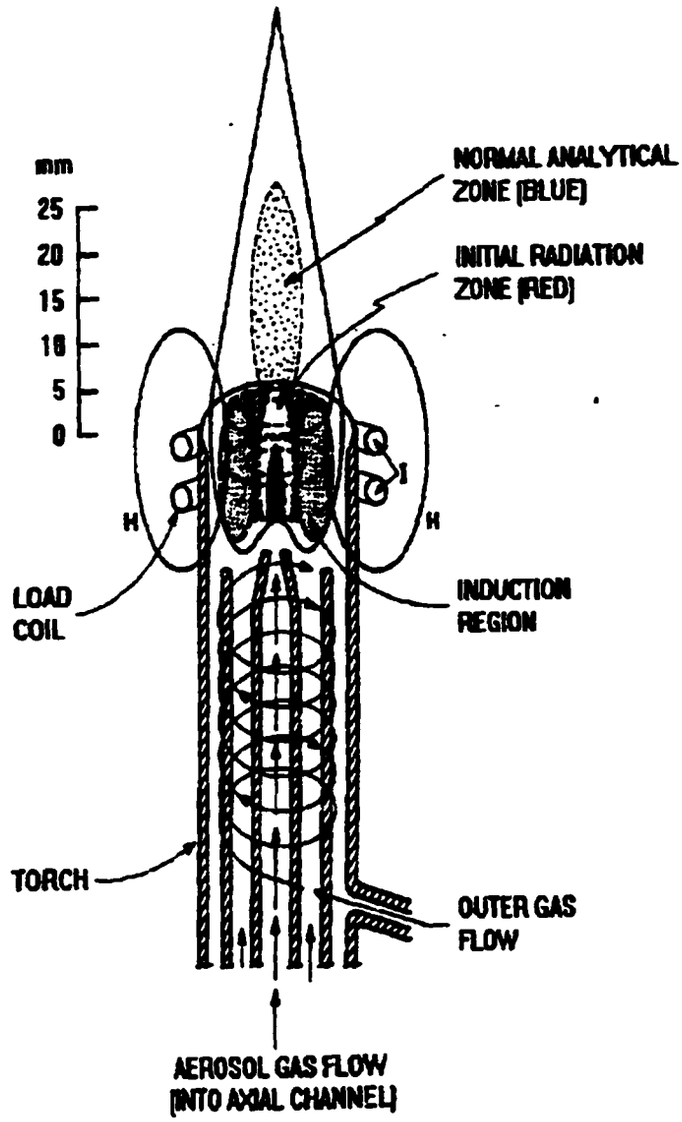


Figure 1: Schematic diagram of ICP [16]

zones; the initial radiation zone (IRZ), normal analytical zone (NAZ) and the plasma plume. The NAZ is the plasma region of greatest analytical utility in ICP-MS and ICP-AES.

## Axial Viewing of ICP-AES

In optical emission spectrometry the emitted radiation from the analyte zone of the ICP is viewed in two basic configurations. Conventional ICP viewing is lateral (also known as side on or radial viewing), the optical axis is orthogonal to the central channel. The other configuration is axial (the optical axis is coincident with the central channel), also known as end-on. In many of the commercial ICP-AE instruments, the collected radiation is dispersed by an echelle grating and analyte emission lines are detected simultaneously by array CCD detectors.

The magnification factor of the spectrometer and the height of the entrance slit of the spectrometer define the vertical extent of the plasma viewed. Analyte emission in the central channel of the plasma as well as emission from the surrounding plasma sheath (primarily background radiation consisting of argon atomic emission, recombination continuum and molecular band emission) is observed in this arrangement. Analytical performance advantages in viewing ICP axially were first reported by Lichte and Koirtyohann [17]. The plasma was viewed horizontally and a vertical flow of gas just past the tip was used to protect the optics from the hot plasma and to remove cooler absorbing atoms in the tail plume of the plasma, which might cause self-absorption resulting in lower dynamic range. With this viewing arrangement, an increase in analyte signal intensities, 10 fold reduction of background, lower in linear dynamic range, reduced molecular band emission, and increased matrix effects were observed [17-19]. The increase in analyte emission intensity in axial

viewing can be justified from the following theoretical concepts [20]. The intensity of an atomic emission signal, $B_E$, is directly dependent upon the source path length.

$$B_E = \frac{A_{ji} h c g_j n_M l e^{-E_j/kT}}{4\pi\lambda_m Z(T)}$$

where

$B_E$ = Total line radiance

$A_{ji}$ = Einstein's coefficient for spontaneous emission ($s^{-1}$)

$n_M$ = Total number of free atoms /$cm^3$

l = Observation/excitation length

Z(T) = Partition function

$\lambda_m$ = Wavelength (line center)

$E_j$ = Excitation energy

$g_j$ = Statistical weight factor

By viewing axially, $B_E$ is increased for longer path length of excitation resulting in higher sensitivity.

## Low Flow Torch for ICP-AES

Early ICP torches required as much as 40 L/min argon flow and very high RF power (15 kW) for its operation. Fassel et al.[6] introduced a three-tube torch that can be operated with a total flow of 15-20L/min and less than 2 kW power. Although argon consumption is still high, this Fassel-type torch has been widely used for most of the ICP instruments. An

estimate shows that the average cost of argon for a typical ICP system in the U.S. is approximately $20,000 per year based on regular usage (40 hours per week). This high running cost of ICP instruments triggered several studies of torch design during the last two decades.

Most of the argon consumption is outer gas flow (14-16 L/min) which is introduced tangentially through the outer annular space to sustain the plasma and cool the torch. This flow produces a high-speed vorticular stream of gas to shield the plasma from the outer tube and prevent the torch from melting, and also reduces air entrainment into the plasma. The reduction of outer gas flow has been the main focus in all torch design studies since the majority of this flow is simply wasted to create the protective shield for the torch. Moreover, a large fraction of RF power is wasted through heating this excessive flow [21].

In earlier investigations, several approaches were reported [22,23] to reduce the argon flow for the successful operation of the ICP for analytical purposes. The low flow of argon can be achieved by miniaturization of the torch and external cooling. Miniaturization of the torch dimensions reduces the argon flow to about 8 L/min. Externally cooled torches have been developed to reduce the argon flow substantially to 3-4 L/min [22-24]. Torches with external cooling can be distinguished in air-cooled, water-cooled and radiatively cooled torches. Although the argon flow was reduced significantly, the performance of these very low flow torches was not as good as the conventional torches. Most of the designs often suffered from instability of plasma, arcing and high reflected RF power.

To be useful for analytical applications the plasma needs to be a proper torodoial shape. A clear axial channel sets a lower limit to outer gas flow. If the flow rate is too low, the plasma collapses into spherical shape instead of torodoial and proper atomization of

elements is not occurred [25]. The radial air-cooling was technically difficult and prone to electrical arcing problem [26]. Water is extreme cooling medium, with a heat transfer coefficient of $10^4$ $W/m^2K$ from water to silica [13]. Water has been used successfully to cool the torch, which reduce outer gas flow substantially [27]. Although water-cooled torches operate at very low outer gas flow, most of the input power is uselessly drained away through heating the water and it was susceptible to form bubble inside the water tube that might explode and cause serious hazards. Application of radiatively cooled torches was limited by the physical properties of the ceramic materials available [28,29]. In addition to other operational problems, plasma in the externally cooled torches was not robust [30] and exhibited poorer analytical performance. Overall detection sensitivity is poor and non-easily-ionizable elements suffer severely from loss of sensitivity. These low flow torches have satisfied the economical criteria in terms of argon consumption, but the analytical capabilities of these plasmas have always been poorer than that of conventional torches. Low flow torches will become widely used only when there is no sacrifice in analytical performance.

Our laboratory recently reported an externally air-cooled low flow torch for ICP-MS that has the same analytical performance as a conventional torch and that can be easily adapted and used in most ICP-MS devices [31]. The plasma generated in this torch at ~ 5 L $min^{-1}$ outer Ar flow has the same basic shape and appearance as a conventional ICP, but does not stream out of the torch into the air. Fortunately, in ICP-MS the sampling cone can be inserted flush with or inside the end of the torch. The ions can thus be extracted before the plasma is cooled by entrained air. Based on this concept an analogous design can be envisioned for ICP-AES. Figure 2 shows the concept of the externally air-cooled torch for axially viewed ICP-AES presented in this study.

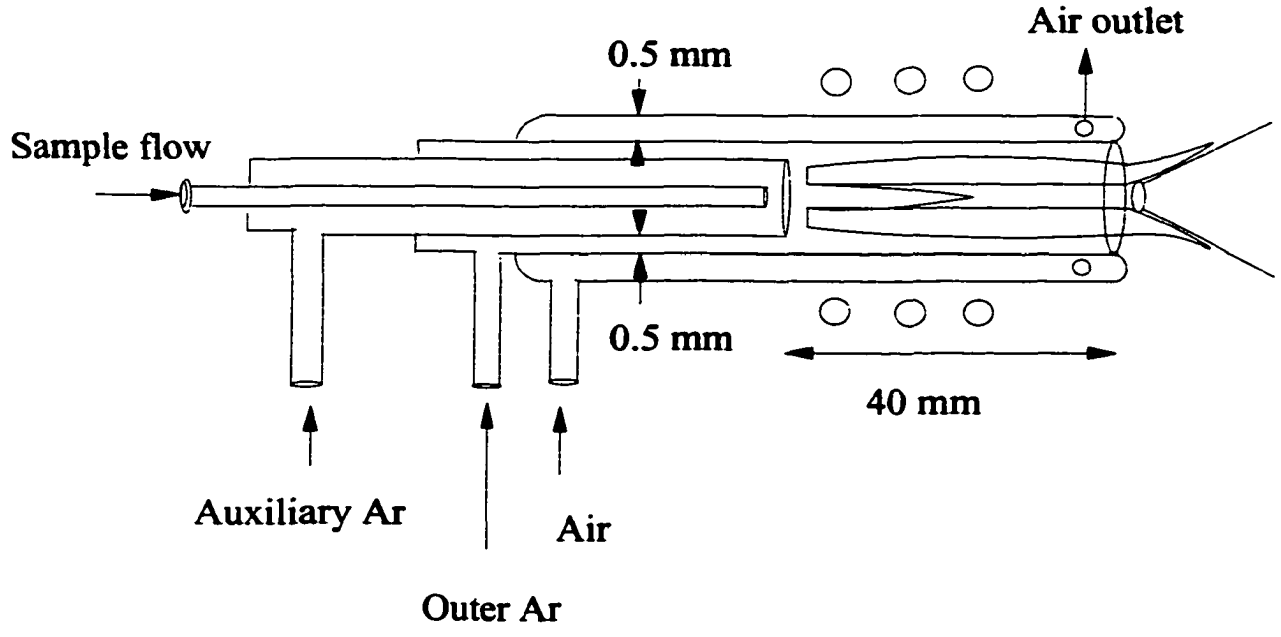


Figure 2: Externally air cooled torch for ICP-AES

**Cooled Cone Interface for ICP-AES**

Axially viewing of ICP provides better atomic emission signal by viewing a longer excitation path length. If not viewed properly, it also reduces the linear dynamic range due to self-absorption at the cooler end of plasma. Conventional axial viewing of ICP in some commercial instruments is done with a shear gas interface, where air or $N_2$ at 30 –70 L/min cuts off the plasma plume. Although this shear gas interface helps keep the spectrometer

away from the plasma and removes most of the cooler plume out of the observation volume, it may cause some additional adverse effects, such as increased molecular emission, air entraintment and disturbance by blowing gas. Besides, the shear gas interface removes the cooler plume incompletely and hence still high background is observed in emission spectrum. Reduction of background emission and stability of plasma is desired to boost the performance of the analytical technique as it can be clarified through the following concept. Total noise, $N_{total}$ of an atomic emission system using a high background excitation source, such as ICP, is given by [32]-

$$N_{total} = (N^2_{shot} + N^2_{flicker})^{1/2}$$

$N_{shot}$ is the shot noise at the photo detector output, which depends on the total light flux on to the detector. $N_{flicker}$ is the noise excess of shot noise due to the instability of the plasma, which usually result from fluctuations in either the plasma gas flows, the RF power or the aerosol transport rate. Because of the unique toroidal shape of the ICP, proper axial viewing should mask off high background outer region to be able to view effectively the background free central channel, thereby decreasing $N_{shot}$.

Earlier Houk et al. [33,34] introduced a cooled metal cone into the ICP axially to detect vacuum ultraviolet radiation directly through an optical sampling orifice. Figure 3 schematically shows the concept of the cooled cone inserted into the plasma. The inserted cone also deflects the cooler plasma plume outwards away from the optical path. To keep the plume out of the cone orifice, a small counter flow of argon or helium can be passed which forms a bubble at the tip. This counter flow also prevents arcing, keeps the plasma undisturbed, limits deposition of solid, and keeps the orifice clean. Such a torch – sampler

combination combines the improved detection limits of axial viewing with wide linear dynamic range.

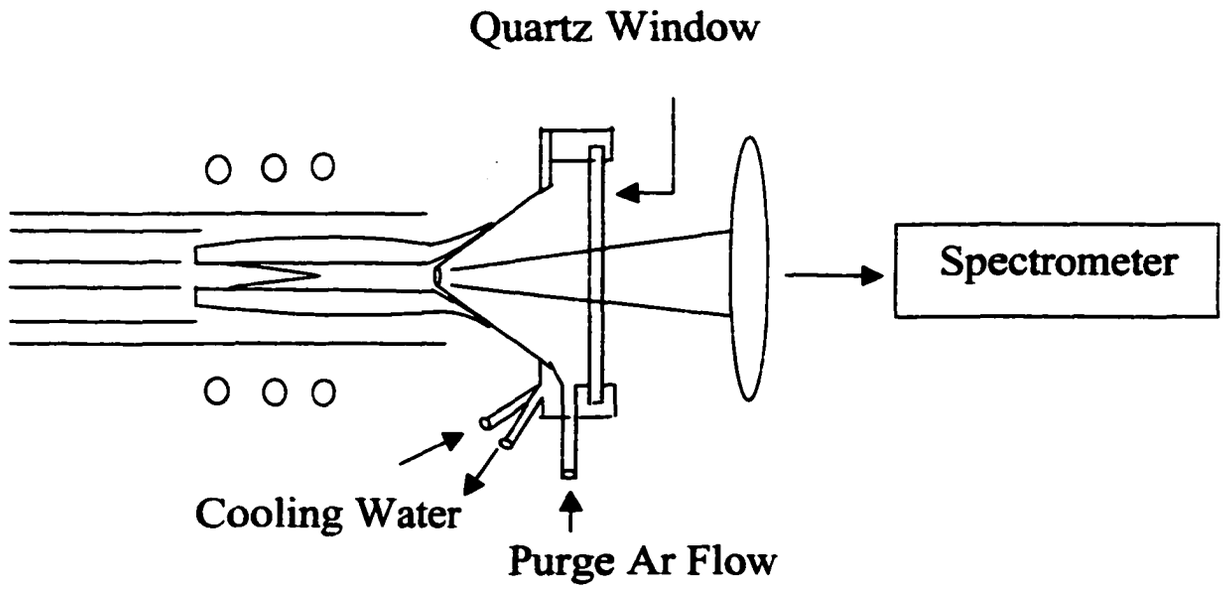


Figure 3: A cooled cone counter flow interface for axially viewed ICP-AES

With low argon flow plasma the possibility of air entraintment is more likely, because the plasma does not reach out of the torch. Moreover, due to lower flow of outer gas, the analyte zone is not shielded from air as in regular flow plasma. Therefore the cooled cone interface should serve to collect emission from the central channel before its exposure to air maintaining improved efficiency of observation of plasma.

**Low Resolution and High Resolution ICP-MS: Capabilities and Limitations**

In the ICP, because of its high temperature and excitation energy, most elements become ionized substantially, especially metallic elements. Because of low background, collection and detection of ions are expected to provide better detection power than viewing emission. Consequently ICP-MS has emerged as the most powerful tool for elemental analysis. In ICP-MS, ions created in the atmospheric pressure plasma are extracted into a mass analyzer.

The operation of mass spectrometers stipulates that the pressure must be kept low so that ions can move without collisions, therefore, a differentially pumped vacuum chamber is necessary. The mass spectrometer consists of three pumping stages (figure 4). Ions are extracted through the sampler orifice into the first vacuum stage where the pressure is reduced to approximately 1 torr. The ion beam is extracted further by the skimmer into a second vacuum stage, where the pressure is roughly $10^{-4}$ torr. Analyte ions from the extracted beam are subsequently focused and transported through a series of ion lenses into the third vacuum stage where the pressure is typically maintained less than $10^{-5}$ torr. Ions are resolved according to their mass to charge ratios in the mass analyzer situated in the high vacuum chamber. Although different mass analyzers can be coupled with ICP, the extraction of ions into the mass spectrometer follows similar concepts.

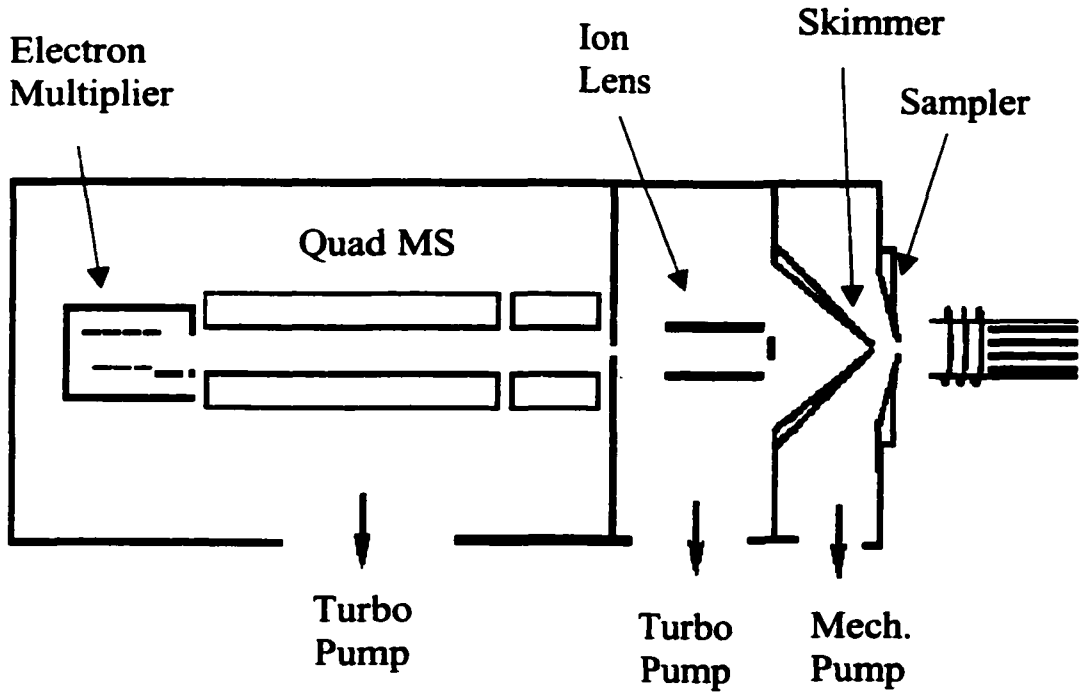


Figure 4: ICP-MS with quadrupole mass analyzer

Most mass analyzers used in commercial ICP-MS instruments are quadrupoles (figure 4). These devices provide unit mass resolution and usually cannot separate chemically different ions at the same nominal m/z value. The resolution obtainable with a quadrupole instrument in the usual stability region is 400 (m/Δm) maximum. One of the main reasons for tremendous popularity of quadrupole instruments is low cost. Besides, quadrupole mass analyzer provides very fast scan rate (30,000 –50,000 mass unit/s). Because of its fast scan capability it edges out other analyzers in real time mass signal acquisition. Although this type of analyzer does not provide flat top and stable peak shapes, still they can perform reasonably well for precise isotope analysis of element for interference free isotopes.

Despite the tremendous capabilities of a quadrupole-based ICP-MS for trace elemental analysis, detection power and selectivity of this analyzer are limited by its poor resolution. A significant number of isotopes of different elements are hard to detect because of overlapping of other ions at the same nominal mass position. When pure water is nebulized into the central channel of the plasma, Ar, O, H, and N atoms are the most important elements in the plasma. Some of these atoms are ionized, so that $Ar^+$, $O^+$, $H^+$ and $N^+$ ions are found in the background spectrum. In addition, its ability suffers from the polyatomic ion interference [11, 35-37] formed in the ICP. The most abundant polyatomic ions found in the background spectrum are $OH^+$, $OH_2^+$ $OH_3^+$, $N_2^+$, $N_2H^+$, $O_2^+$, $ArH^+$, $ArO^+$ and $Ar_2^+$. In this case of other matrix blank instead of water, additional polyatomic ions, such as $MO^+$ and $ArM^+$ are formed which interfere analyte signal more severely. Organic solvents generate $CO^+$, $ArCO^+$, $CO_2^+$, $C_xH_yO_z^+$ etc. These inferences are most common for ions below m/z 80. A resolution of 5000 at 50 % peak height definition is needed to resolve most of the major isotopic interferences in ICP-MS.

ICP-MS with a high-resolution magnetic sector mass analyzer was introduced fairly recently. Improvement of detection sensitivity of analyte element by lowering background signal leads to the development of magnetic sector ICP-MS. With resolution up to 10000, identification and removal of interferences for unambiguous and accurate elemental analysis are possible by sector instruments. Their high sensitivity and low dark noise provides very good detection limits. A schematic diagram of a double focussing sector ICP-MS is shown in figure 5.

In scanning sector instruments, the method of collection of ions from the ICP is similar to that in quadrupole mass analyzer. Figure 5 describes the double focussing reverse Nier-Johnson geometry of sector ICP-MS. The mass analyzer consists of a magnetic sector, which separates ions according to their mass to charge ratio and an electrostatic analyzer, which selects band of ions of same kinetic energy thereby reduces velocity broadening. Ions after separating according to m/z value are detected in an electron multiplier. One shortcoming of sector instruments is their low mass scan rate (3000-5000 mass unit/s). Most recently few commercial ICP-MS instrument manufacturers introduced sector instrument with multiple faraday cup detectors to make simultaneous detection possible of signals at several adjacent m/z positions. This has enhanced capabilities of accurate isotope ratio measurement and fast analysis of real time ion signals. Although the cost of high resolution ICP-MS is still quite high, it has already shown its outstanding promise to fulfill future demand of quality for isotope ratio measurements.

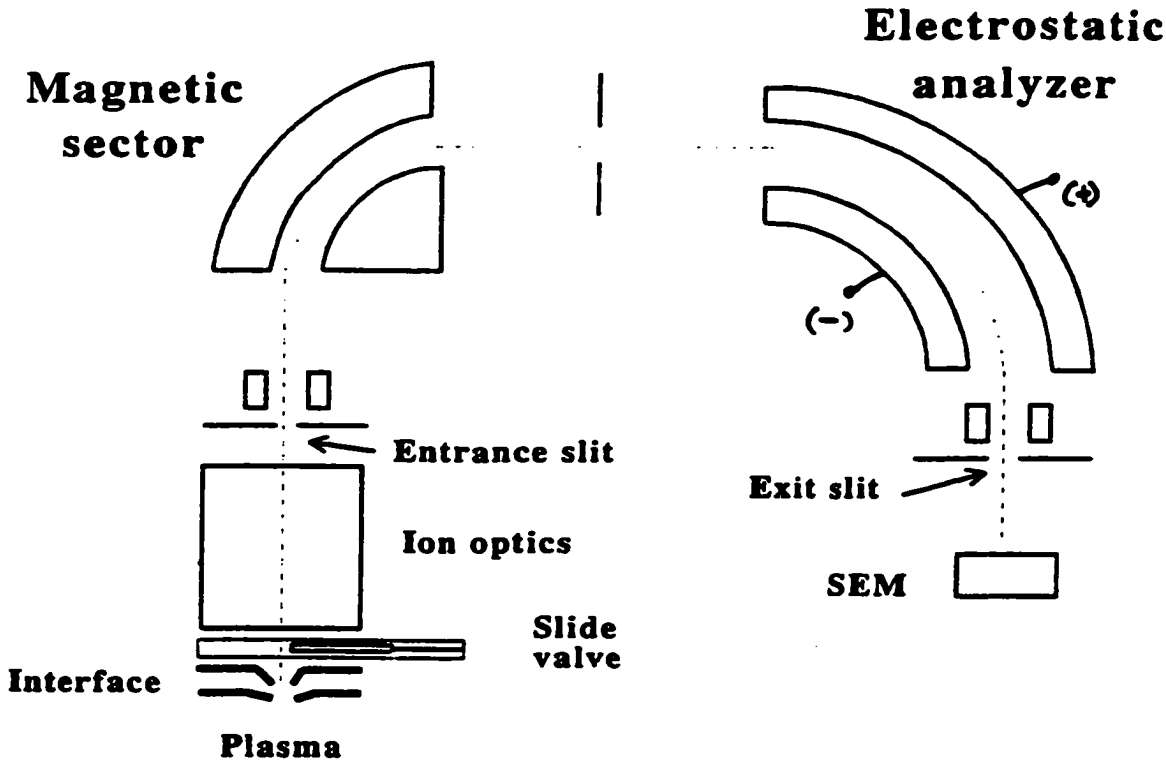


Figure 5: ICP-MS with Double Focussing Magnetic Sector Mass Analyzer [38]

## Organic Solvents in ICP-MS

The great majority of sample types are presented to the ICP as aqueous, frequently acidic, solutions. The fundamental properties of the plasma have therefore been characterized for these solvents. However, there are certain circumstances in which the introduction of organic solvents is necessary. Typical applications include determination of trace elements in petroleum products, various solvents used in chromatography, and more importantly solvents used at different stages in semiconductor manufacturing.

The problems associated with introduction of organic substances into the ICP have been reported earlier [39-44]. The primary adverse effects are

1) Overloading the plasma due to higher vapor pressure of organic solvent than water, which in turn expends more energy for heating and dissociation resulting in lower overall sensitivity and detection limit. Sensitivity and detection limits for analyte ions are usually worse than those obtained when aqueous solutions are nebulized [45,46].
2) Nebulization of organic matrix causes carbon deposition, which clogs the sampler and skimmer cones.
3) Formation of other polyatomic ions e.g., $CN^+$, $CO^+$, $COH^+$, $ArC^+$, $ArCO^+$, $CO_2^+$ etc. interferes with measurement of a number important analyte elements.

Over the last decades a number of investigators tried to characterize the ideal ICP conditions for direct introduction of organic solvent in the ICP [39-44,47]. Optimum parameters for plasma, such as RF power, nebulizer configuration, gas flow varies widely depending on the nature of solvents.

Silicon measurement by ICP-MS is hindered by interference from polyatomic ions e.g., $N_2^+$, $CO^+$ at m/z 28, $COH^+$ at m/z 29, and $NO^+$ at m/z 30. With organic matrices the polyatomic

interference at those m/z level is even more severe causing very high background for silicon measurement.

## Removal of Organic Solvent by Cryogenic Desolvation

To avoid the inevitable difficulties of organic solvent introduction into the plasma numerous attempts have been made over the years, such as cooled spray chamber, [48] a reduction in sample uptake rate, [44], increased forward paper [39] and the addition of a low oxygen flow [46]. Removal of solvent from the aerosol generated by the nebulizer is an effective solution as shown by Maessen et al. [42] for ICP emission spectrometry. Reducing the solvent load to the plasma can attenuate many polyatomic ions, avoid clogging of plasma cones, and hence give relatively interference free analyte ion signal and stability. A range of desolvation systems has been designed to remove large percentage of organic solvent prior to its reaching the plasma. During the important condensation stage, these desolvation systems have been cooled by employing a range of methods, which include pumped ice cooled water [49], pumped cooled ethylene glycol and water [50], membrane gas liquid separators [51] and thermoelectric devices [52]. Lower temperature desolvation at –40°C by peltier cooling was demonstrated by Hill et. el. [53] for removal of organic solvent. Cryogenic desolvation at –77°C coupled with ultrasonic nebulizer used by our group [47,54-57] has been proven very effective tool for desolvation of water, organic solvent, and HCl from aqueous solution. Cryogenic desolvation has also been useful to attenuate troublesome $MO^+$ ions to very low levels by removing water and reducing the corresponding concentration of oxygen in the ICP [55].

## Introduction of Inert Gases in ICP and Their Effects

Although ICP-MS spectra are simpler than emission spectra, ions spectroscopic interferences can become a significant obstacle. Interferences from polyatomic ions arising from either the plasma [58] or the matrix [59] can drastically degrade the analytical capabilities of the instruments. The instrumental operating conditions can have dramatic effect on spectroscopic interferences from polyatomic species. For instances, an all-argon ICP gives rise to major background interferences of $ArO^+$, $N_2^+$, $N_2H^+$, $ArN^+$, $NO^+$, $Ar_2^+$, etc. With the introduction of non-aqueous matrix, such as organic solvent, the diversity and severity of polyatomic interferences increase many fold. These polyatomic ions have been a subject of study with utmost importance with regards to analytical performance of ICP instruments [60].

Mixed gas plasmas were proposed to overcome some of the problems associated with polyatomic ions. Several authors [61,62] have reported that addition of small amount of nitrogen or oxygen to the nebulizer gas decreased interferences from $ArCl^+$ and $Ar_2^+$ on $As^+$ and $Se^+$. Many polyatomic ions (Ar+, $ArH^+$, $ArN^+$, $ArO^+$, $ArCl^+$, $Ar_2^+$, and $ClO^+$) were reported to be attenuated substantially upon addition of few mL of Xe in the Ar flow [63]. An evidence of charge transfer reaction between $Xe^+$ and Fe that increases the sensitivity of Fe signal was also reported [Bricker 1995]. With 1-2 mL of introduction Xe (roughly 5% ionized) can give rise to $10^{15}$ $Xe^+/cm^3$ density in the plasma [64]. Xenon is particularly desirable for polyatomic atomic interference removal because it can be added in small doses without causing gross changes in the size, shape, and spatial structure of plasma. Krypton can also be added without inducing obvious change to the plasma. It can be expected that polyatomic ions $N_2^+$, $CO^+$, $COH^+$ and $NO^+$ that occur at m/z 28 to 30 can be attenuated by addition Xe or Kr for the analysis of silicon.

## Isotope Ratio Measurement by ICP-MS

Isotope ratios are generally determined by means of thermal ionization mass spectrometry (TIMS) because of its excellent precision attainable (RSD values 0.01% or better). The need for extensive sample pretreatment imposes serious limitations on the routine use of TIMS. Although ICP-MS has shown an inferior precision in comparison with TIMS, it has some important advantages, such as a) simple sample pretreatment, b) higher sample throughput and simple sample introduction and c) widespread availability. It is increasingly being used as a tool for fast, precise and accurate isotope ratio measurement [65]. However, the use of ICP-MS for isotope ratio measurement needs some careful considerations to its fundamental characteristics of ion transmission and counting. Measurement of ions by ICP-MS is always associated with mass discrimination (i.e., a bias against low mass ions in favor of high mass ions) due to space charge effect [66], that affect isotope ratio measurement especially, when the isotopes are widely separated. The other reason which contribute to mass bias is the dead time of the ion counting detection system [67]. If the ion signal is not corrected for dead time, it deteriorates the linearity of the instrument over the range of isotope ratios. Aging of the electron multiplier significantly changes dead time. Continuous monitoring of dead time is therefore necessary for reliable measurement of isotope ratio by ICP-MS.

Quadrupole ICP-MS instrument has been used for isotope ratio measurement. Typically relative standard deviation is 0.1 % for interference free isotope signals although the precision is substantially poorer particularly for very large or very small isotope ratios [68]. The use of quadrupole instruments is however limited to only mass interference free isotopic conditions. Quadrupole mass analyzers are specifically designed for the scanning of

relatively large mass ranges and hence provide non-flat top peak shape. As such they are inherently less stable than magnetic sector mass analyzers and less well suited to highly precise and accurate isotope ratio measurement [69].

With recent introduction of magnetic sector mass analyzer, the scope of isotope ratio measurement by ICP-MS has been enhanced greatly. A precision of 0.05% RSD value can be attained at low resolution mode [70,71] and than 0.1% RSD value at resolution 4000 [72] for isotope ratios near unity. With multiple collectors ICP-MS, precision levels of 0.01% RSD [14] can be attained. However simultaneous analysis by faraday cup detector is only limited to low resolution mode. Moreover, because of its high cost, the collector instrument is yet to be very popular.

**Effect of Blank Contamination on Detection Limit of Elements by ICP-MS**

Modern ICP instruments have reached a maturity level that they can provide detection power to meet most of the present demand. Especially, with the introduction of magnetic sector mass analyzers, the detection ability of ICP-MS for various elements is below parts per trillion level of concentration. However, in reality the detection of such a low level of analyte is often impossible because of the background signal from impure blanks. Thus the actual or working detection limit of an analyte is limited by the purity of the blank solution, even though the instrument is capable of detecting much lower concentrations. Conventional ways of achieving low blank impurity or low background signal are using a clean room, and extra clean acid, water and solvent. A clean room is unaffordably costly for many laboratories. Not only the costs of ultra clean solvents and acids are high, but also they are not very available. In addition, long time storage may contaminate even the clean solvents

and acids due to leaching of element ions from the container to the liquid bulk. So cleaning up the blank on-line is the best way to improve these important figures of merit. In the present study an investigation is done to clean up blanks online with ICP-MS for improvement of detection limits of certain elements.

## Dissertation Objectives and Organization

The body of the dissertation is presented in three separate chapters, each of which stands alone as a complete scientific manuscript with accompanying references, tables and figures. A general conclusion, summarizing significant outcomes of the studies and ideas for future scope of research, is presented in the last chapter.

Chapter 2 describes the design of a low flow, externally air-cooled torch for axial viewing of emission from an ICP. Construction of a cooled cone counter flow argon interface to view the plasma axially is depicted. This interface helps to view the central channel of the low flow plasma axially deflecting the cooler plume of the plasma to avoid molecular emission interference and self-absorption. The flow of outer argon gas in this torch can be lowered to 5-6 L/min with no reduction in performance. Analytical performance and stability were investigated for the low flow plasma. The plasma is as robust as that with a conventional high flow torch. Matrix effects were also studied and interference effects of Na on emission signals of other elements was found similar to that observed from conventional regular flow plasma.

Techniques for measurements of silicon concentration by low-resolution quadrupole ICP-MS and silicon isotope ratios by high resolution ICP-MS in organic solvents are presented in chapter 3. Cryogenic desolvation has been employed to remove most of the

organic solvents and water from the nebulized aerosol, which makes silicon measurement possible at parts per million levels with low resolution instruments. For further removal of interfering polyatomic ions, inert gases, such as xenon and krypton, are introduced into the aerosol gas flow. Direct isotope ratio measurements of silicon in organic matrices are done by high-resolution magnetic sector ICP-MS. Separation of all polyatomic ions from silicon mass signal at m/z 28 to 30 is possible at resolution 4000. Introduction of oxygen to titrate carbon deposition from organic solvent on sampler and skimmer cones is described along with other acquisition parameters for accurate isotope measurements of silicon.

Chapter 4 describes the methods for cleaning background blanks for ultra trace analysis by ICP techniques. Detection limit is often limited by purity of blanks used as a background for elemental analysis. Online cleaning by liquid chromatography column is demonstrated for ICP-MS. Electrochemically modulated liquid chromatography (EMLC) column has been introduced to selectively remove analyte metal ions from the blank. The EMLC provides efficient removal of several contaminants from liquid blank introduced in the ICP. The main advantage of EMLC column lies with the fact that the column can be easily refreshed by stripping the deposited metal ions electrochemically.

## References

1. Reed, T. B., *J. Appl. Phys.*, 1961, **32**, 821
2. Reed, T. B., *Int. Sci. Technol.*, 1962, **6**, 42
3. Greenfield, S. Jones, J. L., and Berry C. T., *Analyst*, 1964, **89**, 713
4. Wendt, R. H. and Fassel, V. A., *Anal. Chem.*, 1965, **37**, 920
5. Dickinson, G. W., and Fassel, V. A., *Anal. Chem.*, 1969, **41**, 1021

6. Scott, R. H., Fassel, V. A., Kniseley, R. N., and Nixon, D. E., *Anal. Chem.*, 1974, **46**, 75

7. Fassel, V. A., and Kinsley, K. N., *Anal. Chem.*, 1974, **46**, 1110A and 1115A

8. Gray, A. L., *Proc. Soc. Anal. Chem.*, 1974, **11**, 182-183

9. Gray, A. L., *Analyst*, 1975, **100**, 289-299

10. Houk, R. S., Fassel, V. A., Flesh, G. D., Svec. H. J., Gray, A. L. and Taylor, C. E., *Anal. Chem.*, 1980, **52**, 2283

11. Houk, R. S., *Anal. Chem.*, 1986, **58**, 97A-105A

12. Jarvis K. E., Gray, A. L., Houk, R. S., Handbook of Inductively Coupled Plasma Mass Spectrometry, Chapman and Hall, New York, 1992

13. Montaser, A., Inductively Coupled Plasma Mass Spectrometry, Wiley-VCH, New York, 1998

14. Walder, A. J., Koller, D., Reed, N. M., Hutton, R. C. and Freedman, P. A., *J. Anal. At. Spectrom.*, 1993, **8**, 1037

15. Walder, A. J., Abell, I. D., Platzner, I., and Freedman, P. A., *Spectrochim. Acta., Part B*, 1993, **48**, 397

16. Fassel, V. A., *Pure. Appl. Chem.*, 1977, 49, 1533

17. Lichte, F. E., Conf. Paper No. 26, FACSS, Philadelphia, PA, 1976

18. Danielsson, A., ICP Inform. Newslett., 1978, **4**, 147

19. Demers, D. R., *Appl. Spectrosc.*, 1979, **33**, 584-591

20. Ingle, J. D., Crouch, S. R., (Ed.), Spectrochemical Analysis, 1988, Prentice Hall Inc., A Simon Schuster Company, pp., 21, 215

21. Ripson, P. A. M., and de Galan, L., *Spectrochim. Acta.*, 1983, **38B**, 707

22. Hieftje, G. M., *Spectrochim. Acta.*, 1983, **38B**, 1465.

23. Boumans, P. W. J. M., Hieftje, G. M., "Torches for Inductively Coupled Plasmas. *Inductively Coupled Plasma Emission Spectroscopy"*, Ed. P. W. J. M. Boumans, Part 1, Methodology, Instrumentation and Performance, Chap. 5, p 258. Wiley, New York, 1987.

24. de Galan, L., Vander Plas, P. S. C., "Low gas-flow torches for ICP. *Inductively Coupled Plasmas in Analytical Atomic Spectrometry"*, Ed. A. Montaser and D. W. Golightly, Chap. 14. V. C. H. Publishers, New York, 1987.

25. Vander Plas, P. S. C., de Waaij, A. C., de Galan, L., *Spectrochim. Acta.*, 1985, **40B**, 1457

26. de Loos-Vollebregt, M. T. C., Tiggelman, J. J., de Galan, L., *Spectrochim. Acta,* 1988, **43B**, 773.

27. Kornblum, G. R., van der Waa, W. and de Galan, L., *Anal. Chem.*, 1979, 51, 2378

28. Vander Plas, P. S. C., de Galan, L., *Spectrochim. Acta.*, 1987, **42B**, 1205

29. Kawaguchi, H., Tanaka, T., Miura, S., Xu, J., Mizuike, A., *Spectrochim. Acta.*, 1983, **38B**, 1319

30. Mermet, J. M., *Anal. Chim. Acta.*, 250 (1991) 85-94

31. Praphairaksit, N., Wiederin, D. R. and Houk, R. S., "Externally cooled low flow torch for ICP-MS," *Spectrochimica Acta Part B*, **55B** (2000), in press

32. Winefordner, J. D., Svoboda, V., and Cline, L. J., *CRC Crit. Rev. Anal. Chem.*, 1970, **1**, 233

33. Houk, R. S., Fassel, V. A. and LaFreniere, B. R., *Appl. Spectrosc.*, 1986, **40**, 94-100

34. LaFreniere, B. R, Houk, R. S., and Fassel, V. A, *Anal. Chem.*, 1987, **59,** 2276-2282

35. Horlick, G., Tan, S.H. Vaughan,M.A., and Rose, C.A., *Spectrochim. Acta* , 1985, **40B**, 1555

36. Horlick, G., Tan, S.H. Vaughan,M.A and Shao, Y. *Analytical Atomic Spectrometry*, eds. Montaser, A, and Golightly, D.W., VCH Publishers, New York, pp.361-398

37. Jarvis, K. E., Gray, A. L., and Houk, R.S., *Handbook of Inductively Coupled Plasma Mass Spectrometry*, Blackie & Son, Glasgow, 1992

38. Finigan Mat Element High Resolution ICP-MS, Operating manual

39. Boorn, A. W., Browner, R. F., *Anal. Chem.* 1982, **54**, 1402-1410

40. Hausler, D. W., Taylor, L. T., *Anal. Chem.*, 1981, **53**, 1223-1227

41. Hausler, D. W., Taylor, L. T., *Anal. Chem.*, 1981, **53**, 1227-1231

42. Maessen, F. J. M. J., Kreuning, G., Balke, J., *Spectrochim. Acta., Part B*, 1986, **41**, 3-25

43. Maessen, F. J. M. J., Seeverens, P. J. H., Kreuning, G., *Spectrochim. Acta., Part B*, 1984, **39**, 1171-1180

44. Brotherton, T., Barnes, B., Vela, N., Caruso, J., *J. Anal. At. Spectrosc.*, 1987, **2**, 389-396

45. Hutton, R. C., *J. Anal. At. Spectrosc.*, 1986, **1**, 259

46. Hausler, D., *Spectrochim. Acta.*, Part B, 1987, **42**, 63

47. Minnich, M. G., Houk, R. S., *J. Anal. At. Spectrom.*, 1998, **13**, 167- 174

48. Kreuning, G., Maessen, F. J. M. J., *Spectrochim. Acta., Part B*, 1987, **42**, 677

49. Brotherton, T. J., Pfannerstill, P.E., Creed, J. T., Heitkemper, D.T., Caruso, J. A., Pratsinis, S. E., J., *Anal. At. Spectrom.*, 1989, **4**, 341

50. Tsakahara, R., Kubota, N., *Spectrochim. Acta., Part B*, 1990, **45**, 581

51. Gustavsson, A., *Spectrochim. Acta., Part B*, 1988, **43**, 917

52. Weir, D. G. J., Blades, M. W., *Spectrochim. Acta., Part B*, 1990, **45**, 615

53. Hill, S. J., Hartley, J., Ebdon, L., *J. Anal. At. Spectrom.*, 1992, **7**, 895

54. Wiederin, D. R., Houk, R. S., Winge, R. K., D'Silva, A. P., *Anal. Chem.*, 1990, **62**, 1155

55. Alves, L. C., Wiederin, D. R., Houk, R. S., *Anal. Chem.* 1992, **64**, 1164

56. Alves, L. C., Allen, L. A., Houk, R. S., *Anal. Chem.* 1993, **65**, 2468

57. Alves, L. C., Minnich, M. G., Wiederin, D. R., Houk, R. S., *J. Anal. At. Spectrom.*, 1994, **9**, 399- 403

58. Tan S. H., Horlick, G., *Appl. Spectrosc.*, 1986, **40**, 445

59. Vaughan, M. A., Horlick, G., *Appl. Spectrosc.*, 1986, **40**, 434

60. Houk, R. S., Praphairaksit, N., "Dissociation of Polyatomic ions in ICP", *Spectrochim. Acta., Part B*, in press

61. Evans, E. H., Ebdon, L., *Anal. At. Spectrom.*, 1988, **4**, 299

62. Beauchemin, D., Craig, J. M., *Spectrochim. Acta., Part B*, 1991, **46**, 603

63. Smith, F. G.; Wiederin, D. R.; Houk, R. S.; *Anal. Chem.*, 1991, **63**, 1458

64. Bricker, T. M.; Smith, F. G.; Houk, R. S.; *Spectrochimica Acta, Part B*, 1995, **50**, 1325-1335

65. Vanhaecke, F., Moens, L., Dams, R., *Anal. Chem.*, 1996, **68**, 567

66. Praphairaksit, N., Houk, R. S., *Anal. Chem.*, 2000, **72**, 4435

67. Held, A., Taylor, D. P., *J. Anal. At. Spectrom.*, 1999, **14**, 1075

68. Whittaker, P. G., Barrett, J. F. R., Williams, J. G., *J. Anal. At. Spectrom.*, 1992, **7**, 109

69. Begley, I. S., Sharp, B. L., *J. Anal. At. Spectrom.*, 1997, **12**, 395

70. Becker J. S., Dietze, H. –J., *J. Anal. At. Spectrom.*, 1998, **13**, 1057

71. Latkoczy, C., Prohaska, T., Stingeder, G., Teschler- Nicola, M., *J. Anal. At. Spectrom.*, 1998, **13**, 561

72. Prohaska, T., Latkoczy, C., Stingeder, G., *J. Anal. At. Spectrom.*, 1999, **14**, 1501-1504

# CHAPTER 2. LOW FLOW, EXTERNALLY AIR COOLED TORCH FOR INDUCTIVELY COUPLED PLASMA ATOMIC EMISSION SPECTROMETRY WITH AXIAL VIEWING

A paper published in the Journal of Spectrochimica Acta Part B[1]

Towhid Hasan, Narong Praphairaksit and R. S. Houk[2]

## Abstract

The torch wall is cooled largely by air passing through a cooling jacket added to the outside of a Fassel torch. The plasma is viewed axially through a cooled cone interface centered on the axial channel. The outer argon gas flow can be reduced to 7 L $min^{-1}$ with no compromise in performance or torch lifetime. For the particular spectrometer used, the plasma exhibits the same "robustness index" and interference effects from Na as the conventional, high-flow ICP supplied with the particular spectrometer used. Detection limits (DL) for lines at ~ 200 nm are poorer by about a factor of two, while those for lines at ~ 400 nm are actually better than values typically seen for the same lines by axial viewing of a conventional, high-flow ICP.

Keywords: *Inductively coupled plasma (ICP); ICP atomic emission spectrometry (ICP-AES); ICP, torch design; ICP, axial viewing; ICP, low flow.*

---

[1] Reprinted with permission of Spectrochim. Acta. Part B, 2001, 15,

[2] Corresponding author

## 1. Introduction

Most ICPs consume argon at 15 L $min^{-1}$ or more, which represents one of the major operating costs of an ICP facility. Argon is particularly expensive in undeveloped countries. Most of the argon passes through the annular gap between the outer and intermediate tubes. This outer Ar flow has three purposes: to cool the wall of the torch, to shield the plasma flowing out of the torch from air entrainment, and to provide the proper shape to the plasma.

Several investigators have reported ways to reduce argon consumption. These generally fall into two categories: miniaturization of the torch dimensions [1,2] and cooling the outer tube by some other means [1-3]. Except for minitorches, most of these low-flow plasmas do not provide analytical performance as good as that obtained with a regular plasma and have not seen widespread use.

We recently reported an externally air-cooled low flow torch for ICP-MS that has the same analytical performance as a conventional torch and that can be easily adapted and used in most ICP-MS devices [4]. The plasma generated in this torch at ~ 5 L $min^{-1}$ outer Ar flow has the same basic shape and appearance as a conventional ICP but does not stream out of the torch into the air. Fortunately, in ICP-MS the sampling cone can be inserted flush with or inside the end of the torch. The ions can thus be extracted before the plasma is cooled by entrained air.

An analogous procedure can be used to sample photons for ICP-AES with a cooled sampling cone inserted axially into the plasma [5,6]. Such a torch – sampler combination combines the improved detection limits of axial viewing with low argon consumption. This is the subject of the present work.

## 2. Experimental

### *2.1. Torch construction*

The externally-air cooled torch is shown at the left of Fig. 1. It is similar to the low-flow torch described recently for ICP-MS [4], with the following minor differences. The inner torch is a bigger, Fassel-type variety (20 mm OD, 18 mm ID, 1.5 mm diam. injector, Precision Glassblowing of Colorado, CO) with a narrow annular gap (0.5 mm) between the outer and intermediate tubes. The tip of the outer tube is also extended to 40 mm from the end of the intermediate tube to "stretch out" the analytical emission zone for axial viewing. A 50 mm long externally-cooled torch was constructed but found to have moderately worse background equivalent concentrations (BEC) than the 40 mm one.

The external air jacket (24 mm OD, 22 mm ID, Fig. 1) is a quartz tube sealed onto the inner torch at the downstream end. The upstream end is simply glued to the base of the inner torch with ceramic cement (Sauereisen, Scientific Instrument Services, CA). The external jacket can be made and attached simply with low mechanical tolerances without spoiling the shape and symmetry of the torch or the plasma. Air is added at ~ 20 L $min^{-1}$ with a simple circulating fan. The air exits through four circular holes (2 mm diam.) drilled equally spaced at the downstream end of the cooling jacket. This air flow leaves the torch in a direction perpendicular to the Ar flow out of the torch, so it does not flow into and disturb the plasma.

### *2.2. ICP power supply, cooled cone interface, and transfer optics*

The horizontal ICP was the same one used for the initial studies of axial viewing through a sampling orifice inserted into the ICP [5,6]. The plasma was sustained with a generator (Plasma Therm HFS 3000D) different from that supplied with the spectrometer

(Optima 3000, Perkin Elmer). To test the general feasibility of the new torch for ICP-AES, it was easier to simply use this external plasma than to twist the load coil supplied with the spectrometer by 90° and install an optical sampler and additional torch mount inside the shielding box.

A water-cooled copper cone with a 3 mm diam. circular orifice was inserted axially into the plasma (Fig. 1). This cone had a quartz window at the base and was purged with Ar at 100 mL $min^{-1}$. This purge gas flow minimized deposition of solids from the samples onto the edges of the optical orifice. Because the plasma and sampler were outside the normal focal position for the spectrometer, three lenses were used to transfer the image of the central channel of the plasma to the normal object position inside the torch box. It was assumed that the image transfer optics inside the spectrometer would convey light from that point. Keeping the plasma separated from the spectrometer also mitigated RF noise problems in the detection electronics and computer.

*2.3. Samples and sample introduction*

Standard solutions of various metal ions were from Spex CertiPrep and were diluted with 1% aqueous nitric acid or deionized water. The samples were nebulized with a concentric nebulizer (Precision Glassblowing of Colorado) and the aerosol passed through a Scott spray chamber before it entered the plasma.

## 3. Results and discussion

### *3.1. Optimization experiments*

The size of the sampling orifice influences the width of the zones viewed in the plasma [5,6]. Therefore, the sampling orifice was drilled out progressively from 1 to 2 to 3 mm diameter. Measured values for signal and background are given in Table 1. As expected, both signal (S) and background (B) increase as the cone diameter increases. The S/B ratio for the Zn lines at ~ 200 nm did not change much with cone diameter, whereas S/B increased moderately at 3 mm for the Mg lines at ~ 280 nm. The 3 mm diam. orifice was therefore used for subsequent experiments.

As is the case in ICP-MS, the sampling position, aerosol gas flow, and power that maximize the signal are interrelated. Outer gas flow rate could also be important in this low-flow torch. Power was kept at 1.0 kW while the other parameters were varied. Observation position was optimized first (Fig. 2). Maximum signal and best S/B ratio were obtained for a typical "hard" line (Mg (II) 279.553 nm) at 32 mm from the load coil. Here the tip of the sampling cone is ~ 5 mm from the end of the torch.

At the best observation position (32 mm), changing the aerosol gas flow rate produced a mountain-shaped plot much like those described by Horlick in ICP-MS (Fig. 3) [7]. As described by several workers, changing the aerosol gas flow rate shifts the various emitting zones of the plasma upstream or down relative to the fixed observation volume determined by the sampler and optics. Apparently, the emitting zone for the "hard" line selected is at the optimum position relative to the sampling orifice and transfer optics at aerosol gas flow rates of 0.8 to 0.9 L $min^{-1}$. The intensity of the neutral atom line [Mg (I)

285.213 nm] maximizes at moderately higher aerosol gas flow rate, ~ 1.0 L $min^{-1}$, as expected from vertical spatial profiles of analyte emission from an ICP [8,9].

The background at ~ 280 nm does not change appreciably with aerosol gas flow rate within the range 0.7 to 1 L $min^{-1}$ (data not shown). Figure 2 also shows that the background is not particularly sensitive to observation position, as long as this parameter is kept within the optimum range. If the sampler is too far downstream (> 50 mm, Fig. 2), the background increases greatly. Either the induction region is in the optical path or the device is observing band emission caused by entrainment of air. There is not enough outer gas to keep the plasma isolated from air in the latter case. Thus, it is necessary to collect the photons before the plasma flows very far from the end of the low-flow torch described in the present work.

With the two previous conditions optimized, the effect of outer Ar flow rate on Mg emission is shown in Fig. 4. Note that this is the Ar flow through the usual outer tube of the torch, not the external cooling air. The Mg line intensities decrease slightly as outer gas flow increases. The torch does not show signs of overheating (i.e., an orange glow) until the outer gas flow is reduced to ~ 5 L $min^{-1}$. To provide a safety margin we kept the outer gas flow rate at 7 L $min^{-1}$ for the studies described below.

### *3.2. "Robustness:" Mg (II) / Mg (I) emission ratio*

The general area of "robustness' has been a weakness of low-flow torches in the past, especially if reduction in gas flow precludes operation at high power. Mermet [10] suggests measurement of the intensity ratio Mg (II) 280.270 nm / Mg (I) 285.213 nm as a quick, simple gauge of the "robustness" of the plasma. Observation position, aerosol gas flow rate, and power should be adjusted to provide a Mg (II) / Mg (I) signal ratio of 10 or higher. This

criterion assumes the two lines are measured with similar optical transmission and detection efficiency. In the Optima echelle device, these two lines are measured in different order and on different segments of the array detector, which leads to lower values of the Mg (II) / Mg (I) signal ratio than those suggested by Mermet, even when the plasma is apparently "robust". Ivaldi and Tyson [11] suggest that the Mg (II) / Mg (I) ratio measured with an Optima can be multiplied by 1.86 to compensate partly for different grating efficiency, which has been done for the data described below.

Figure 5 shows the effect of forward power on Mg (II) / Mg (I) ratio in the present work. An intensity ratio of up to ~ 6 can be obtained by increasing the power. At lower power less outer Ar flow is needed to cool the torch. At a compromise power of 1.0 kW the Mg (II) / Mg (I) ratio is ~ 5.8, which is about as high as that seen with this particular instrument using conventional lateral viewing or by others with axial viewing on other Optima instruments [11]. Therefore, the plasma generated with this low-flow torch exhibits the same "robustness" criterion as any we have used with this particular spectrometer.

### *3.3. Sensitivity, background and detection limits*

Table 2 lists values of background, sensitivity (i.e., signal per unit concentration), and relative standard deviation of background (RSDB). Table 3 lists background equivalent concentration (BEC) and DLs (i.e., analyte concentration necessary to give a net signal equivalent to three times the standard deviation of the background) for various lines in the following scenarios. Values were measured using our Optima 3000 spectrometer with the new torch and axial viewing and for the plasma supplied with the same instrument viewed laterally. For comparison, literature values for a different Optima 3000 XL, with Perkin

Elmer's axial viewing option (i.e., a cut-off gas), are also included from the measurements of Ivaldi and Tyson [11] and Brenner et al. [13].

These data support the following general conclusions:

1. The low-flow torch with axial viewing provides better BECs and DLs than a conventional torch viewed laterally, despite the long transfer optics.
2. The BEC and DL values obtained with the new torch and our cooled cone axial viewing method are generally comparable to those obtained from the literature with the Optima 3000XL at a similar power level (1.0 or 0.9 kW). Results for lines close to 200 nm (e.g., the Zn lines and Co (II) 228.616 and 230.786 nm) are poorer with the new torch by factors of two to three, which we attribute to loss of UV photons in the three lenses necessary to transfer light to the spectrometer.
3. The new torch and viewing system provide very good performance for certain lines in the visible, especially Ba (II) 455.403 nm and Ca (II) 393.366 nm. For some unknown reason, the Ca sensitivity is so high that the background was measured off-peak because of Ca in the blank. The DL of 0.9 ppt for Ca is at least as good as that obtainable by ICP-MS and could be of great value in the semiconductor industry. Calcium is a common, easily ionized impurity element that ruins the performance of silicon. It is hardly the best element for ICP-MS. Analysis using the only major Ca isotope ($^{40}Ca$) requires a "cool" plasma [14-16] to suppress $^{40}Ar^{+}$, and use of $^{44}Ca$ requires either high spectral resolution or a cool plasma.
4. Air entrainment could cause problems at the low outer gas flow rate used (7 $L.min^{-1}$). If so, the BEC values for lines like Zn (I) 213.856 nm and V (II) 309.311 nm would be poor because of spectral overlap from NO and OH band components. Instead, the BEC values

from the present work are better than those obtained by lateral viewing and comparable to those obtained in other axial viewing experiments (Table 3). Scans of these spectral regions show the ratio of atomic line intensity / band intensity to be as good or better than those obtained by conventional viewing methods. Furthermore, at high signal levels the signal precision is ~1 to 2% RSD (Table 2), only moderately worse than that seen with this device using conventional viewing methods. Finally, the tail plume of the plasma can be seen to flow around and isolate the tip of the sampling cone from air entrainment.

These observations indicate that the cone interface collects emission signals from the plasma before it suffers from air entrainment. To prevent this potential problem, it is important to position the cone tip close to the end of the torch, as shown in Fig. 1.

*3.4. Matrix effects*

The effects of Na matrix on sensitivity for Ca (II) and Ba (II) lines are shown in Fig. 6. There is a slight enhancement of signal at 100 $\mu g.mL^{-1}$ Na followed by a suppression of between 4% and 8% at 1000 $\mu g.mL^{-1}$. The general shapes of these interference curves and the extent of the matrix effect are similar to those seen in our early axial viewing experiments [5,6]. The matrix effect induced by Na is more severe than would be seen in lateral viewing if the observation height is optimized properly, as often seen in the axial viewing experiment [11,13,17]. The similarity of the matrix effect seen here to that usually observed in axial viewing is further evidence that this low-flow plasma has similar properties as a conventional one.

## 4. Conclusions

When viewed axially in the proper fashion, the performance of this low-flow torch is comparable to that of a regular torch and is actually better for Ca and Ba. Performance near 200 nm is believed to be limited by the transmission of the three lenses used. The torch housing and optical system could be rebuilt to move the plasma closer to the normal object position of the spectrometer to mitigate this problem. This externally-cooled torch is readily interchangeable with conventional torches, at least in those instruments equipped for axial viewing with a sampling cone inside the plasma. At low flow the plasma does not stream far out of the end of the torch, but this is not a problem because of the cooled cone interface. Axial sampling of ions (for MS)[4] or photons (for AES) before the low-flow plasma is exposed to air is the key to this concept for reducing argon consumption without compromising performance.

## Acknowledgements

Ames Laboratory is operated by Iowa State University for the U. S. Department of Energy under Contract No. W-7405-Eng-82. This research was supported by the Molecular Processes Program, Division of Chemical Sciences, Office of Basic Energy Sciences. The authors thank Perkin Elmer for loan of the spectrometer, Trond Forre for constructing the torches, and Spex CertiPrep for providing standards.

**References**

1. G. M. Hieftje, "Mini, micro, and high-efficiency torches for the ICP – Toys or Tools?" Spectrochim. Acta. Part B, 38B (1983) 1465-1481.

2. P. W. J. M. Boumans and G. M. Hieftje, Torches for Inductively Coupled Plasmas. Inductively Coupled Plasma Emission Spectroscopy, Ed. P. W. J. M. Boumans, Part 1, Methodology, Instrumentation and Performance, Chap. 5, p 258. Wiley, New York, 1987

3. L.de Galan and P. S. C. Vander Plas, Low gas-flow torches for ICP. *Inductively Coupled* Plasmas in Analytical Atomic Spectrometry, Ed. A. Montaser and D. W. Golightly, Chap. 14. V. C. H. Publishers, New York, 1987

4. N. Praphairaksit, D. R. Wiederin and R. S. Houk, "Externally cooled low flow torch for ICP-MS," Spectrochimica Acta Part B, 55B (2000) accepted.

5. R. S. Houk, V. A. Fassel and B. R. LaFreniere, "Direct detection of vacuum ultraviolet radiation through an optical sampling orifice: spatially resolved emission studies of argon resonance lines from an ICP," Appl. Spectrosc., 40 (1986) 94-100.

6. B. R. LaFreniere, R. S. Houk, and V. A. Fassel, "Direct detection of vacuum ultraviolet radiation through an optical sampling orifice: analytical figures of merit for nonmetal emission from an ICP," Anal. Chem., 59 (1987) 2276-2282.

7. S. H. Tan and G. Horlick, "Matrix-effect observations in ICP-MS," J. Anal. At. Spectrom., 2 (1987) 745-763.

8. M. W. Blades, G. Horlick, "The vertical spatial characteristics of analyte emission in the ICP," Spectrochim. Acta Part B 36 (1981) 861-880.

9. N. Furuta, G. Horlick, "Spatial characterization of analyte emission and excitation temperature in an ICP," Spectrochim. Acta Part B 37 (1982) 53-64.

10. J. M. Mermet, "Use of magnesium as a test element for ICP atomic emission spectrometry diagonstics," Anal. Chim. Acta., 250 (1991) 85-94.

11. J. C. Ivaldi and J. F. Tyson, "Performance evaluation of an axially viewed horizontal ICP for optical emission spectrometry," Spectrochimica Acta Part B, 50 (1995) 1207-1226.

12. Optima 3000 operating manual, Perkin Elmer.

13. I. B. Brenner, M. Zischka, B. Maichin and G. Knapp, "Ca and Na interference effects in an axially viewed ICP using low and high aerosol loadings," J. Anal. At. Spectrom., 13 (1998) 1257-1264.

14. N. S. Nonose, N. Matsuda, N. Fudagawa and M. Kubota, "Some characteristics of polyatomic ion spectra in ICP-MS," Spectrochimica Acta Part B, 49 (1994) 955-974.

15. K. Sakata and K. Kawabata, "Reduction of fundamental polyatomic ions in ICP-MS," Spectrochimica Acta Part B, 49 (1994) 1027-1038.

16. S. D. Tanner, "Characterization of ionization and matrix suppression in inductively coupled 'Cold' plasma mass spectrometry," J. Anal. At. Spectrom., 10 (1995) 905-921.

17. D. R. Demers, "Evaluation of the axially viewed (end-on) inductively coupled argon plasma source for atomic emission spectroscopy," Appl. Spectrosc., 33 (1979) 584-591.

Table 1: Effect of sampler cone diameter on collection efficiency

| Cone diameter | RF power: 1kW, Aerosol flow: 0.9 L/min | Zn(I) 213. 856 (1μg/mL) | Zn(II) 202. 580 (1μg/mL) | Mg(II) 279.553 (200 ng/mL) | Mg(I) 285.213 (200 ng/mL) |
|---|---|---|---|---|---|
| 1 mm | Signal | 1400 | 1250 | 21400 | 9410 |
| | Background | 64 | 65 | 323 | 281 |
| | S/B Ratio | 21.9 | 19.3 | 66.2 | 33.5 |
| 2 mm | Signal | 2530 | 1630 | 32300 | 12300 |
| | Background | 114 | 81 | 370 | 293 |
| | S/B Ratio | 22.2 | 20.1 | 87.3 | 41.8 |
| 3mm | Signal | 3410 | 1860 | 46800 | 18000 |
| | Background | 162 | 109 | 428 | 349 |
| | S/B Ratio | 21.0 | 17.1 | 109 | 51.5 |

Table 2: Sensitivity, background, relative standard deviation of background (RSDB), and signal RSD with the low flow, axially viewed ICP[a]

| Element | Line wavelength, nm | Background signal . 1 % $HNO_3$ or DI water, counts/s | Emission signal counts $s^{-1}$ / ppm | RSDB / Signal RSD[b] % |
|---|---|---|---|---|
| V | 270.094(II) | 226 | 2120 | 0.37 |
| | 292.402(II) | 712 | 23700 | 0.62 |
| | 309.311(II) | 1640 | 61600 | 0.31 |
| | 310.230(II) | 57000 | 72000 | 0.56 |
| Zn | 202.580(II) | 85 | 1560 | 1.11 / 1.7 |
| | 213.856(I) | 126 | 3930 | 0.87 / 1.6 |
| Co | 228.616(II) | 56 | 611 | 1.04 |
| | 230.786(II) | 79 | 724 | 1.08 |
| | 236.379(II) | 302 | 2940 | 0.74 |
| | 238.892(II) | 264 | 5980 | 0.82 |
| Mn | 257.610(II) | 167 | 24400 | 1.15 |
| | 260.569(II) | 201 | 18700 | 0.98 |
| | 279.482(II) | 381 | 3450 | 0.54 |
| | 294.920(II) | 428 | 12700 | 0.38 |
| | 403.076(II) | 803 | 9280 | 0.52 |
| Ba | 230.424(II) | 114 | 2880 | 1.67 |
| | 233.527(II) | 340 | 7960 | 0.68 |
| | 413.066(I) | 2560 | 50300 | 0.23 |
| | 455.403(II) | 3070 | 1070000 | 0.21 |
| Mg | 279.079(II) | 668 | 4030 | 1.36 |
| | 279.553(II) | 430 | 236000 | 0.36 |
| | 280.270(II) | 473 | 92800 | 0.41 |
| | 285.213(I) | 1200 | 29100 | 1.38 |
| Ca | 393.366(II) | 2210[c] | 17000000 | 0.24 / 1.2 |
| | 396.847(II) | 568[c] | 1700000 | 0.52 / 1.4 |
| Fe | 234.349(II) | 284 | 1980 | 1.28 |
| | 238.204(II) | 144 | 2030 | 0.75 |
| | 239.562(II) | 273 | 3170 | 1.14 |
| | 259.940(II) | 363 | 6880 | 0.43 |
| | 273.955(II) | 187 | 908 | 0.86 |
| Ti | 334.941(II) | 640 | 49100 | 0.32 |
| | 336.121(II) | 616 | 37200 | 0.28 |
| | 337.280(II) | 1110 | 42800 | 0.44 |
| | 368.520(II) | 606 | 16700 | 0.36 |

[a]Cone diameter: 0.3 mm, length of torch (distance between inner tube and outer tube): 40 mm, outer gas flow rate : 7 L/min, auxiliary flow rate: 0.2 L/min, aerosol flow rate: 0.9 L/min, RF power: 1.0 kW

[b]1 ppm Zn & 2 ppb Ca, n=20.

[c]Background measured with deionized water

Table 3: Comparison of BEC and DL for the low flow axially viewed ICP to other Optima ICP devices using lateral or axial viewing

| Element | Line & wavelength | BEC Axial low-flow torch 1.0 kW | BEC / DL Lateral viewing, 1.0 kW[ 12 ] | BEC Axial viewing, 0.9 / 1.4kW [ 11,13 ] | DL Axial low-flow torch 1.0 kW | DL Axial viewing, 1.0 kW [11] (0.9/1.4 kW) [13] |
|---|---|---|---|---|---|---|
| | nm | ppb | ppb | ppb | ppb | ppb |
| V | 270.094(II) | 106 | 590 | | 1.2 | 1.6 |
| | 292.402(II) | 30.0 | 250 | | 0.5 | 0.25 |
| | 309.311(II) | 26.7 | 170 / 1 | 92 / 304 | 0.2 | (0.4 / 0.6) |
| | 310.230(II) | 786 | 210 | | 13 | |
| Zn | 202.580(II) | 54.6 | 130 | | 1.8 | 1.0 |
| | 213.856 (I) | 32.0 | 60 / 0.8 | 21 / 114 | 0.8 | (0.35 / 0.9) |
| Co | 228.616(II) | 91.6 | 230 / 13 | | 2.9 | 1.3 |
| | 230.786(II) | 109 | 320 | | 3.5 | 0.95 |
| | 236.379(II) | 103 | 370 | | 2.3 | |
| | 238.892(II) | 44.2 | 200 | | 1.1 | |
| Mn | 257.610(II) | 6.8 | 50 / 3 | 6.9 / 53 | 0.2 | (0.06 / 0.14) |
| | 260.569(II) | 10.7 | 70 | | 0.3 | 0.14 |
| | 279.482(II) | 110 | 420 | | 1.8 | |
| | 294.920(II) | 33.7 | 260 | | 0.4 | |
| | 403.076(II) | 86.5 | 1470 | | 1.3 | |
| Ba | 230.424(II) | 39.6 | 140 | | 1.9 | |
| | 233.527(II) | 42.7 | 130 | | 0.8 | |
| | 413.066(I) | 50.8 | 1100 | | 0.4 | |
| | 455.403(II) | 2.86 | 40 / 0.2 | 5.6 / 87 | 0.02 | (0.01 / 0.04) |
| Mg | 279.079(II) | 165 | 1000 | | 6.7 | 2.5 |
| | 279.553(II) | 1.82 | 10 / 0.2 | | 0.02 | |
| | 280.270(II) | 5.09 | 10 | | 0.06 | 0.13 |
| | 285.213(I) | 41.2 | 50 | | 1.7 | 0.6 |
| Ca | 393.366(II) | 0.130 | 10 / 0.1 | | 0.0009 | 0.005 |
| | 396.847(II) | 0.335 | 20 | | 0.005 | |
| Fe | 234.349(II) | 144 | 340 | | 5.5 | |
| | 238.204(II) | 70.8 | 150 / 4 | 36 / 209 | 1.6 | (0.36 / 1.0) |
| | 239.562(II) | 86.0 | 170 | | 2.9 | 2.2 |
| | 259.940(II) | 52.8 | 210 | | 0.8 | 1.6 |
| | 273.955(II) | 206 | 670 | | 5.3 | |
| Ti | 334.941(II) | 13.0 | 130 / 0.8 | 17/196 | 0.1 | (0.08/0.24) |
| | 336.121(II) | 16.5 | 180 | | 0.1 | |
| | 337.280(II) | 26.0 | 220 | | 0.3 | |
| | 368.520(II) | 36.3 | 380 | | 0.4 | |

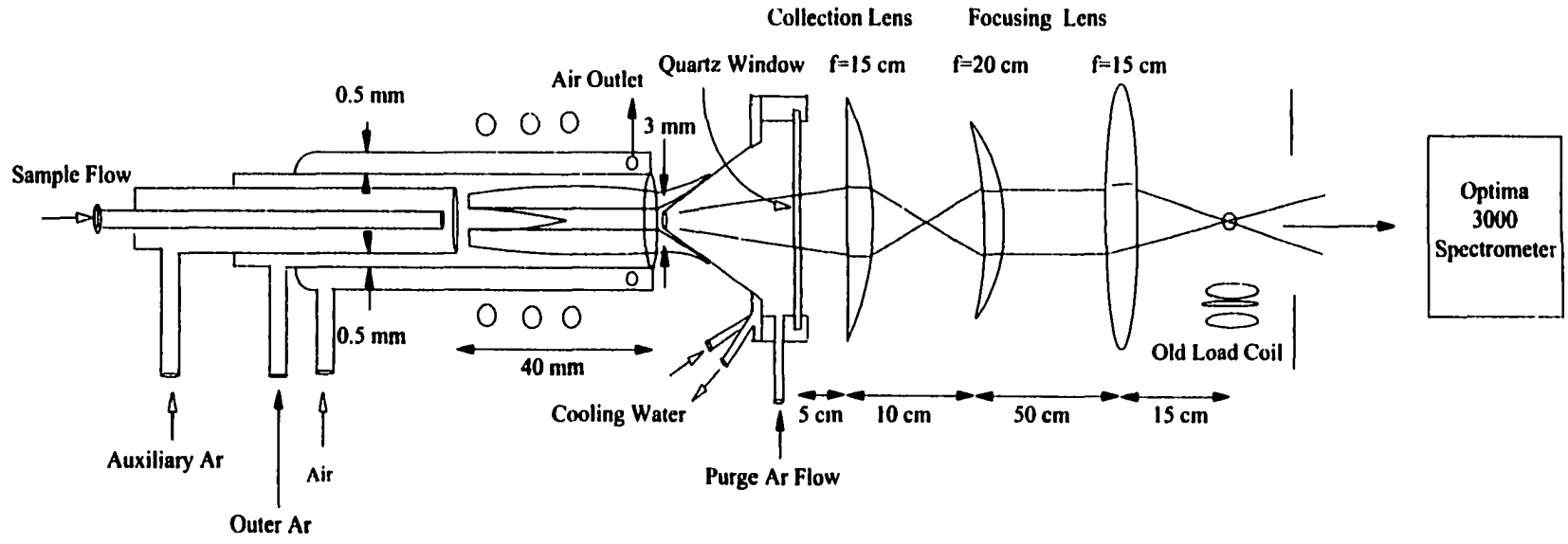


Figure 1: Schematic diagram of the interface for low flow axially viewed plasma to spectrometer

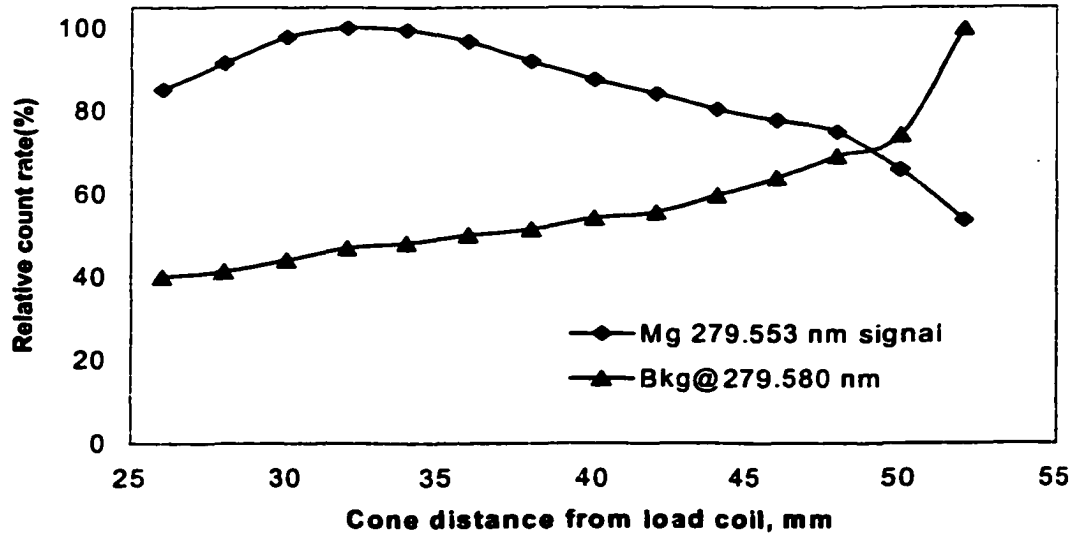


Figure 2: Variation of Mg(II) signal with distance of cone from load coil

200 ng/mL Mg in DI water, RF power: 1.0 kW, aerosol Ar flow: 0.9 L/min, aux. Ar flow: 0.2 L/min, outer Ar flow: 7 L/min

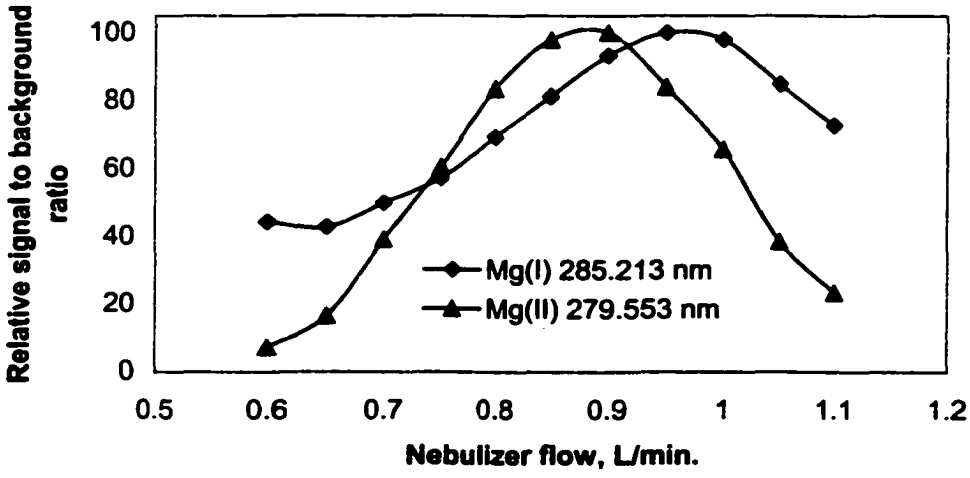


Figure 3: Effect of aerosol gas flow rate on Mg(I) and Mg(II) emission

Conc. of Mg: 200 ng/mL in DI water, RF power: 1.0 kW, aux. Ar flow: 0.2 L/min, outer Ar flow: 7L/min. The actual S/B ratios for Mg (II) are about 5 times greater than those for Mg (I).

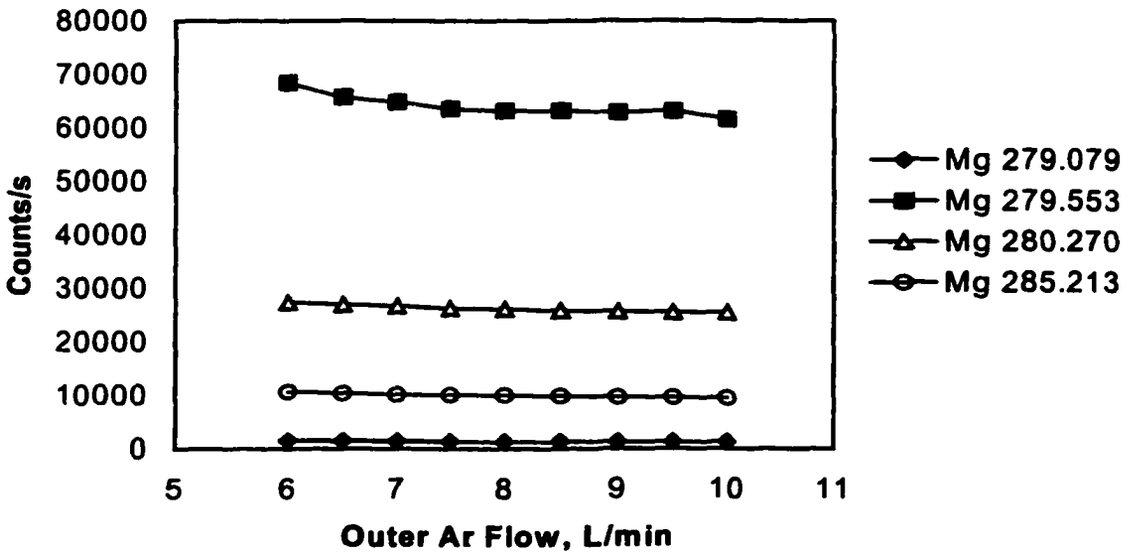


Figure 4: Effect of outer gas flow rate on Mg emission signal

200 ng/mL Mg in DI water, RF power: 1.0 kW, aerosol Ar flow: 0.9 L/min, aux. Ar flow: 0.2 L/min, outer Ar flow: 7 L/min

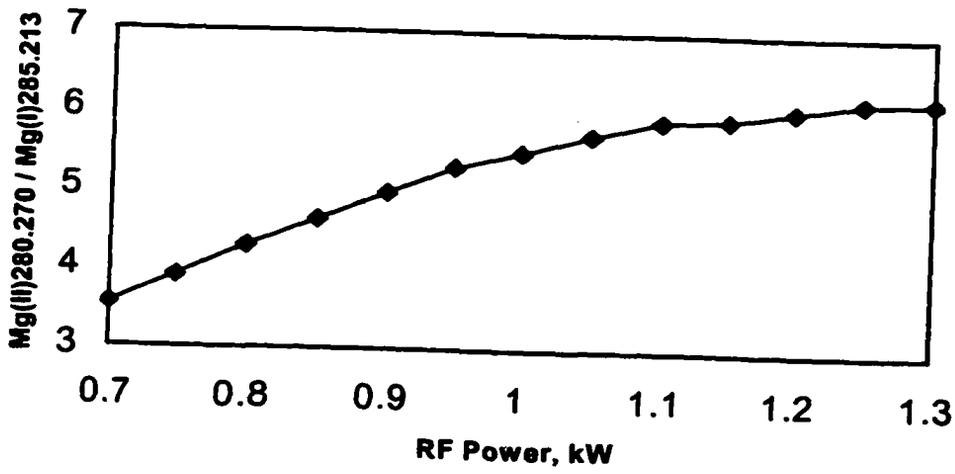


Figure 5: An indicator of plasma robustness: effect of RF power on Mg(II) / Mg(I) intensity ratio

[Mg(II)/Mg(I) ratio is corrected for grating efficiency]
200 ng/mL Mg in DI water, RF power: 1.0 kW, aerosol Ar flow: 0.9 L/min, aux. Ar flow: 0.2 L/min, outer Ar flow: 7 L/min

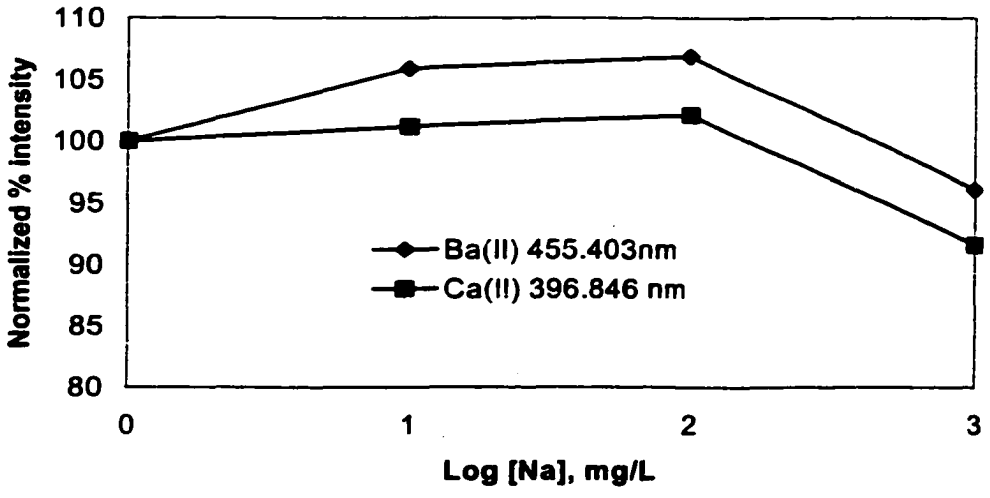


Figure 6: Interference of Na concomitant on Ca (II) 396.846 and Ba(II) 455.403 signal

Ca Conc.: 100 ng/mL, Ba Conc.: 100 ng/mL, Na Conc.:1000 mg/L in 2% HNO3 and diluted, RF power: 1.0 kW, outer Ar flow:7 L/min, aerosol` Ar flow: 0.95 L/min, aux. Ar flow: 0.2 L/min

# CHAPTER 3. MEASUREMENT OF SILICON CONCENTRATION AND ISOTOPE RATIOS IN ORGANIC MATRICES BY INDUCTIVELY COUPLED PLASMA MASS SPECTROMETRY AT RESOLUTION 300 AND 4000

A paper to be submitted to the Journal of Analytical Atomic Spectroscopy

Towhid Hasan and R. S. Houk*

## Abstract

Silicon is measured at m/z 28, 29 and 30 by reducing the spectral interference caused by $N_2^+$, $CO^+$, $COH^+$ and $NO^+$. Cryogenic desolvation of the wet droplets from a low flow nebulizer removes most of the solvent and makes silicon determination possible at m/z = 28 at the parts per million level by low resolution ICP-MS. Xenon and krypton can be added at 1-3 mL/min to the aerosol gas flow of plasma for further removal of polyatomic ions. Isotope ratios can be measured by medium resolution (m/Δm=4000) ICP-MS by direct nebulization. To avoid deposition of carbon on the interface cone, oxygen is added to the spray chamber and the $O_2$ flow rate is adjusted to titrate carbon in the plasma. Despite the sharply pointed peaks at m/Δm = 4000, ratio precision of ± 0.1% relative standard deviation (RSD) can be obtained using approximately 1 μg of silicon.

Keywords: *inductively coupled plasma, ICP, inductively coupled plasma mass spectrometry, ICP-MS, silicon, isotope ratio, high resolution, solvent removal*

---

*Corresponding author

## INTRODUCTION

Measurement of silicon by ICP-MS is hindered by interference from polyatomic ions e.g., $N_2^+$, $CO^+$ at m/z 28, $COH^+$ at m/z 29, and $NO^+$ at m/z 30. With organic matrices the polyatomic interferences are even more severe than those seen from aqueous solutions. The high background due to these polyatomic ions complicates the measurement of even 10 to 100 ppm level silicon by low resolution ($m/\Delta m$ =300) ICP-MS. For accurate measurement of silicon, it is imperative that signal at m/z 28, 29 and 30 should be interference free.

In addition, introduction of organic matrices into inductively coupled plasma (ICP) generates a number of other drawbacks. Adverse effects of volatile organic substances on ICP have been reported in the literature [1-6]. Organic solvents overload the plasma, thus sensitivity and detection limits for analyte ions are usually worse than those obtained from aqueous solution [7,8]. Carbon from organic solvents deposits and clogs the sampler and skimmer cones. Carbon containing polyatomic ions e.g., $ArC^+$, $CO_2^+$ etc. become more abundant and interfere with a number of important analyte elements.

Removal of interference is usually more effective than correction. For isotope ratio measurements, all the isotopes of interest should be free of interferences. Removal of solvent from the aerosol generated by the nebulizer is an effective solution as shown by Maessen et al. [4] for ICP emission spectrometry. Reducing the solvent load to the plasma can attenuate many polyatomic ions, avoid clogging of plasma cones, improve stability and hence give relatively interference free analyte ion signals. Cooling the spray chamber is the most common way of reducing the solvent load [9]. Cooling is done by employing a jacket outside the spray chamber or by condenser with coolant flow at 0 to $-10^{\circ}C$ after the spray chamber followed by a heater. Lower temperature desolvation at $-40^{\circ}C$ by Peltier cooling shown by

Hill et al. [10] is very effective for removal of organic solvent. Cryogenic desolvation at –77°C coupled with an ultrasonic nebulizer used by our group [11-15] has been proven very effective tool for desolvation of water, organic solvent, and HCl from aqueous solution. Cryogenic desolvation has also been used to attenuate troublesome $MO^+$ ions to very low levels by removing water and reducing the corresponding concentration of oxygen atoms in the ICP [12].

Several gases, particularly $N_2$, $O_2$, He, $CH_4$, $H_2$, Xe have been introduced into the ICP [13, 16-20]. Carbon deposition can be avoided by titrating carbon with a carefully introduced low flow of oxygen into the spray chamber [7,8,10]. Obviously, addition of oxygen would increase the intensity of those polyatomic ions that contain O atom.

The effect of Xe added to the axial channel of an Ar ICP was reported earlier by our group [16,17]. Polyatomic ions, such as $Ar^+$, $ArH^+$, $ArN^+$, $ArO^+$, $ArCl^+$, $Ar_2^+$, and $ClO^+$ were attenuated substantially upon addition of Xe at 1-2 mL/min in the Ar flow [17]. Addition of Xe causes little change in the visual appearance of the ICP. Analyte ions from elements with low to moderate ionization energy (like $Fe^+$, $K^+$, $V^+$) are also attenuated, but less so than the polyatomic ions and $Ar^+$ if the Xe flow rate is carefully adjusted. Higher Xe flow eventually attenuates all analyte ions from elements with high ionization energy (like $As^+$ or $Se^+$) and polyatomic ions (like $Ar_2^+$, $ArCl^+$, $CO^+$, $NO^+$ etc.) signal.

Isotope ratio measurements using ICP-MS are of a widespread interest in environmental and geochemical research. ICP-MS is increasingly being implemented as a tool for fast precise and accurate isotope ratio measurement [21]. Quadrupole ICP-MS instruments have been used for isotope ratio measurement. Typically relative standard deviation (RSD) is 0.1 % for interference free isotope signals. However, the precision is

substantially poorer particularly for very large or very small isotope ratios [22-25]. With the advent of magnetic sector mass spectrometer with the ICP, the precision of 0.05% RSD value can be attained at low resolution mode for isotope ratios near unity [26, 27]. Isotope ratio measurements at high resolution are the most recent study found in the literature [28]. Sulfur isotope ratio were measured at resolution 4000 with a precision better than 0.1% RSD. Silicon isotopes at m/z 28, 29 and 30 can be separated from the major polyatomic ion interferences at resolution of 4000 (Table 1). In the present work, a method for isotope ratio measurement of silicon in organic solvents has been developed.

Silicon has also been determined in organic solvents by low-resolution quadrupole ICP-MS using cryogenic desolvation and inert gas (Xe and Kr) introduction into the plasma. In the earlier cryogenic desolvation experiment with ultrasonic nebulizer [15], an additional desolvation chamber was used to remove most of the water or organic solvent. In this work the first desolvation chamber has been avoided as solvent load with low flow nebulizer is significantly smaller. A very low flow (20 μL) self-aspirating micro-nebulizer minimizes the solvent load.

## EXPERIMENTAL

### Low Resolution Experiments

Instrumentation: Hewlet Packard HP 4500 ICP mass spectrometer with quadrupole mass analyzer was used for low-resolution experiments. A PFA 20 self-aspirating teflon nebulizer, teflon spray chamber and sapphire injector from Elemental Scientific (Omaha, NE) were used.

The cryogenic desolvation system is shown in Figure 1. Part of this apparatus is similar in principle to regular condenser used with nebulizer. A detailed description was given in a previous paper from our group [14]. The bulk of the organic solvent condensed in the first loop and was removed as liquid through the drain. The aerosol was then heated and cooled repeatedly in the glass loops. Periodic heating and cooling removes most of the solvent from the aerosol. The temperature of the heating tube was kept ~40°C above the boiling points of the solvents. The heater temperature was kept at 152°C and 125°C for butanol and propanol respectively. Without these repetitive heating cycles, solvent condenses back from the vapor phase onto the particles and recreates wet droplets in the cooled portion of the tubes [11]. To transport solvent free dry aerosol to the plasma, the tube is therefore heated after every cooling cycle.

Introduction of inert gases into the plasma was done with a custom made torch. The schematic diagram of the torch is shown in Figure 2. A capillary tube is inserted through the side tube into the sample flow stream, so that the added inert gas (Xe or Kr) does not distort the sample flow. A pre-calibrated mass flow controller controls the flow of inert gases through the capillary. Operating parameters for the low resolution HP4500 instrument for direct measurement of silicon in organic solvent are summarized in Table 3.

**High Resolution Experiments**

For high resolution, Finnigan MAT Element ICP mass spectrometer with double focussing magnetic sector mass analyzer was used. Silicon isotope ratios were measured at resolution 4000. Operating parameters for isotope ratio measurement are shown in Table 4. Oxygen was added to the spray chamber at 10 ml/min rate for direct analysis of organic solvent. A PFA

20 self-aspirating teflon nebulizer (Elemental Scientific, Omaha, NE) and quartz injector were used. The average of 100 scans was integrated for each m/z. After subtracting background signal at each m/z level, isotope ratios were calculated from the integrated signal.

Organosilicon standards were prepared from tetramethoxysilane (99%) procured from Alfa Aesar (Johnson Mathey Company, MA, USA). Silicon isotopic standards (shown in Table 2) were prepared from pure natural $SiO_2$ and isotopically enriched $SiO_2$ (Oak Ridge National Laboratory). $SiO_2$ standards were dissolved in the minimum volume of 10 % aqueous hydrofluoric acid (Fisher Scientific, A.C.S. grade) and then diluted with organic solvent. Oxygen gas (99.9%) was introduced into the spray chamber by a mass flow controller (Matheson, Model 8284). HPLC grade 1-butanol and 1-propanol (Fisher Scientific, Pittsburgh, PA, U.S.A.) were used for all experiments.

## RESULTS AND DISCUSSIONS

### Direct Silicon Measurement in Organic Solvent at Low Resolution

Direct nebulization of pure butanol and propanol from even a micro-flow nebulizer causes instability in the ICP. At high forward power, it is possible to keep the plasma running. But within a short period of time, the silicon signal drops and the cones glow red due to carbon deposits. However, with oxygen flow the cones can be kept clean. Over 20 ml/min of oxygen flow extinguishes the plasma. Oxygen flow at 10-12 mL/min keeps the plasma cones clean and signal stable. Signal at m/z 28, 29, and 30 can be recorded at low electron multiplier voltage without saturating the detector response. Because of polyatomic interference, background equivalent concentration (BEC) of silicon at m/z 28 and 30 is about 50-100 ppm

and at m/z 29 is about 300- 800 ppm, as shown in Table 5 for butanol and Table 6 for propanol. The intensity of background due to polyatomic ions tends to decrease as the plasma conditions approach "cool" mode [29]. However sensitivity of silicon signal also decreases with decreasing plasma robustness.

**Silicon Measurement in Organic Solvent at Low Resolution with Cryogenic Desolvation**

Most of the organic solvent can be removed from the aerosol by cryogenic desolvation. The background signal from polyatomic ions is reduced by one order of magnitude. Tables 5 and 6 show the improvement of background equivalent concentration and detection limit obtained from cryogenic desolvation. Decreasing heater temperature shows higher background of polyatomic ions and increasing heater temperature above the optimum temperature does not significantly change the sensitivity of silicon signal or background. Figure 3(a, b) shows linearity of silicon signal at m/z 28, 29 and 30 over three order of magnitude concentrations in pure butanol. However the background signals at all much range are still high as observed from the intercept in Figure 3(a, b).

**Silicon Measurement at Low Resolution with Cryogenic Desolvation and Inert Gases**

Although cryogenic desolvation removes most of the solvent, polyatomic ion interferences still persist, so that detection limits are only ~ 1ppm. In addition nitrogen and nitrogen oxide ionic species, which are abundant enough to overlap ppm level of silicon signal, are not fully removed by cryogenic desolvation. Introduction of inert gases, Xe and Kr, has been observed to prevent formation of most of the polyatomic ions at m/z 28, 29 and 30. The effect of Xe introduction on the background signal of polyatomic ions along with effect on silicon signal

is shown in figure 4. The intensity of polyatomic ions drops exponentially with increasing Xe flow. Silicon signal also drops significantly. However the lowering of silicon signal is relatively less than that of polyatomic ion signal resulting in overall signal to background ratio (S/B) gain. Figure 4 also shows the effect of Xe flow rate on signal to background ratio of silicon. The best of S/B for m/z 28 occurs at somewhat higher value of Xe flow. Introduction of krypton into the plasma shows similar effects (Figure 5), but approximately twice as much Kr is necessary. Similar effects were observed with silicon in propanol solvent. Figure 6 shows standard calibration curves at low ppm level concentration of silicon in butanol at 0.2 % Xe flow. Tables 5 and 6 show the improvement in signal to background ratio and detection limit of silicon. Both BEC and detection limit are observed to be improved by one order of magnitude for introduction of Xe or Kr, compared to those obtained using cryogenic desolvation alone.

**Silicon Isotope Ratio Measurement by High Resolution (m/Δm=4000) ICP-MS**

Figure 7 shows that there are various polyatomic ions at m/z = 28, 29, and 30; that all can be separated from $Si^+$ at m/m =4000. Mass bias toward higher m/z value was observed at higher concentration (more than 10 ppm) at the conditions described in table 4. However mass bias was corrected with an isotope standard at the same level of concentration. With lower (<0.1s) settling time, increased mass bias and lower precision of isotope ratios were observed. Less mass bias was observed at analog detection than counting detection. Silicon signals were steady for considerable period of time with the low flow self aspirating nebulizer. However, at higher concentration silicon tends to deposit on the cones resulting in poorer precision. In addition, the nebulizer can clog at high concentration of silicon. Silicon sometimes suffers

from memory effect in ICP-MS because of its tendency to stick to the surface wall of nebulizer, spray chamber and cones. As a result the precision of isotope ratio is degraded in sequential mass device with scanning electron multiplier detector.

To authenticate the measurement method, series of standards were prepared with increasing $^{28}Si$ isotope abundance in 5% butanol. Figure 8, 9 and 10 show actual and measured Si isotope abundances in different standards prepared using mixtures of natural ($^{28}Si = 92.25\%$) and enriched ($^{28}Si = 99.94\%$). The agreement ($R^2 > 0.999$) confirms that the measured silicon isotope ratios are close to the actual values in the standard solutions.

Direct isotope ratio measurements were done in pure butanol and propanol with the addition of oxygen into the spray chamber. Table 7 shows isotope ratios found in pure butanol, propanol, water and 5% butanol. The precision for isotope ratios is 3 to 5 times better in aqueous solution than in organic solvent. Relative standard deviation (RSD) is close to 0.5% in both butanol and propanol, whereas in water it is near to 0.1%. Lower precision in organic solvent might be due to instability of plasma caused by carbon deposition and turbulence caused by the addition of oxygen in plasma.

## CONCLUSION

The present study shows that silicon can be measured quantitatively by ICP-MS with even quadrupole mass analyzer by reducing polyatomic ion interference at m/z 28 to 30. Cryogenic desolvation removes most of the solvent from the aerosol and enables silicon measurement at low parts per million levels. With the advantage of low flow nebulizer with high efficiency and less solvent load, polyatomic ions can be reduced further by adding Xe or

Kr into the plasma. Detection limit of silicon with few ml/min of Xe and Kr with the aerosol flow can be further improved one order of magnitude to ~100 ppb level.

Although double focussing sector ICP-MS is reported to provide precision of 0.05% RSD value at low resolution for isotope ratios near unity [26, 27], but at higher resolution and at higher isotope ratio the precision better than 0.1% RSD value is less likely. At higher resolution, the peak is triangular rather than flat top occurred in the case of low resolution. Isotope ratio of silicon with its adverse memory effect is unlikely to provide better precision than above-mentioned RSD value. In our present study, the precision we obtained is about 0.1% for aqueous and low concentration organic solution whereas in concentrated organic solvent the precision is close to 0.5%.

## SAFETY NOTE

Heater temperature (150°C) is above the flash point of organic solvents used in the work. The flammable vapors must be kept inside the tube with inert gas flow. Care should also be taken to handle oxygen. Oxygen flow from cylinder was passed through an arrestor valve.

## ACKNOWLEDGEMENTS

Ames Laboratory is operated by Iowa State University for the U. S. Department of Energy under Contract No. W-7405-Eng-82. Part of this research was supported by the Molecular Processes Program, Division of Chemical Sciences, Office of Basic Energy Sciences. The authors thank Dan Weidem for his suggestions, and Spex CertiPrep for providing standards.

## REFERENCES


1. Boorn, A. W., Browner, R. F., *Anal. Chem.* 1982, **54**, 1402-1410
2. Hausler, D. W., Taylor, L. T., *Anal. Chem.*, 1981, **53**, 1223-1227
3. Hausler, D. W., Taylor, L. T., *Anal. Chem.*, 1981, **53**, 1227-1231
4. Maessen, F. J. M. J., Kreuning, G., Balke, J., *Spectrochim. Acta.*, Part B, 1986, **41**, 3-25
5. Maessen, F. J. M. J., Seeverens, P. J. H., Kreuning, G., *Spectrochim. Acta.*, Part B, 1984, **39**, 1171-1180
6. Brotherton, T., Barnes, B., Vela, N., Caruso, J., *J. Anal. At. Spectrosc.*, 1987, **2**, 389-396
7. Hutton, R. C., *J. Anal. At. Spectrosc.*, 1986, **1**, 259
8. Hausler, D., *Spectrochim. Acta.*, Part B, 1987, **42**, 63
9. Hutton, R. C., Eaton, A. N., *J. Anal. At. Spectrom.*, 1987, **2**, 595
10. Hill, S. J., Hartley, J., Ebdon, L., *J. Anal. At. Spectrom.*, 1992, **7**, 895
11. Wiederin, D. R., Houk, R. S., Winge, R. K., D'Silva, A. P., *Anal. Chem.*, 1990, **62**, 1155
12. Alves, L. C., Wiederin, D. R., Houk, R. S., *Anal. Chem.* 1992, **64**, 1164
13. Alves, L. C., Allen, L. A., Houk, R. S., *Anal. Chem.* 1993, **65**, 2468
14. Alves, L. C., Minnich, M. G., Wiederin, D. R., Houk, R. S., *J. Anal. At. Spectrom.*, 1994, **9**, 399- 403
15. Minnich, M. G., Houk, R. S., *J. Anal. At. Spectrom.*, 1998, **13**, 167- 174
16. Bricker, T. M.; Smith, F. G.; Houk, R. S.; *Spectrochimica Acta*, Part B, 1995, **50**, 1325-1335
17. Smith, F. G., Wiederin, D. R., Houk, R. S., *Anal. Chem.*, 1991, **63**, 1458
18. Evans E. H., Ebdon, L, *J. Anal. At. Spectrom.*, 1990, **5**, 425-430

19. Sheppard, B. S., Shen, W. L., Caruso, J. A., *J. Am. Soc. Mass Spectrom.*, 1991, **2**, 355-361

20. Shibata, N., Fudagawa, N., Kubota, M., *Anal.Chem.*, 1991, **63**, 636-640

21. Vanhaecke, F., Moens, L., Dams, R., *Anal. Chem.*, 1996, **68**, 567

22. Serfass, R. E., Thomson, J. J., Houk, R. S., *Anal. Chim. Acta.*,1986, **188**, 73

23. Jarvis, K. E., Gray, A. L., Houk, R. S., Handbook of ICP-MS (Blackie, London, 1991), pp. 225, 235, 312, 326

24. Whittaker, P. G., Barrett, J. F. R., Williams, J. G., *J. Anal. At. Spectrom.*, 1992, **7**, 109

25. Begley, I. S., and Sharp, B. L., *J. Anal. At. Spectrom.*, 1999, **12**, 395

26. Becker J. S., Dietze, H. –J., *J. Anal. At. Spectrom.*, 1998, **13**, 1057

27. Latkoczy, C., Prohaska, T., Stingeder, G., Teschler- Nicola, M., *J. Anal. At. Spectrom.*, 1998, **13**, 561

28. Prohaska, T., Latkoczy, C., Stingeder, G., *J. Anal. At. Spectrom.*, 1999, **14**, 1501-1504

29. Jiang, S-J., Houk, R. S., and Stevens, M. A., *Anal. Chem.*, 1988, **60**, 1217

Table 1: Spectral interferences at m/z 28, 29 and 30

| Isotope | Natural Abundance | Interferences* | m/Δm |
|---|---|---|---|
| $^{28}Si$ | 92.25 % | $CO^+$ | 1600 |
| | | $N_2^+$ | 930 |
| $^{29}Si$ | 4.65 % | $^{28}SiH^+$ | 3600 |
| | | $COH^+$ | 1200 |
| | | $N_2H^+$ | 780 |
| $^{30}Si$ | 3.10 % | $NO^+$ | 1200 |

*Other very low abundant polyatomic ions of C, O, N, H minor isotopes can also be separated at mass resolution 4000

Table 2: Silicon standards

| | % By Mass | | |
|---|---|---|---|
| Silicon Isotopes | m/z 28 | m/z 29 | m/z 30 |
| Enriched $SiO_2$ | 99.94 | .04 | .02 |
| Natural $SiO_2$ | 92.251 | 4.651 | 3.098 |

Table 3: Operating parameters for the HP4500 for silicon measurements

| **ICP-MS parameters:** | |
|---|---|
| RF power | 1450 kW |
| Sampler & skimmer cone | Nickel |
| Guard Electrode | Pt made on |
| Injector | Quartz |
| Sample gas flow rate | 0.86 L/min |
| Sample uptake rate | 20-30 μL/min |
| Optimum Xe flow rate | 1.2 mL/min |
| Optimum Kr flow rate | 2.1 mL/min |

| **Cryogenic system parameters:** | |
|---|---|
| Heater temperature (Butanol) | 152°C |
| Heater temperature (Propanol) | 125°C |
| Cryogenic Cooling temperature | -77°C |

Table 4: Operating parameters for the Finnigan Mat Element optimized for Silicon isotope ratio measurement

| | |
|---|---|
| **Instrumental setup:** | |
| RF Power | 1200 watts |
| Sample gas flow rate | 0.95 L/min |
| Sample uptake rate | 20-30 μL/min |
| Sampler and Skimmer cones | Nickel |
| Injector | Sapphire |
| Guard Electrode | Pt made on |
| Acquisition mode | EScan |
| Resolution (m/Δm) | 4000 |
| Oxygen flow rate | 10 mL/min |
| **Parameter for analysis:** | |
| Mass window | 80% |
| Settling time | 0.3 s |
| Sample time | 10 ms |
| Number of samples | 1x100 |
| Analysis Time | 2 min |
| Dead time correction | none |
| Replicate measurements | 5 |

Table 5: Performance Comparison of Si Analysis in 1-Butanol

| **Techniques for Si analysis** | **Background Equivalent Concentration(BEC), ppm** | | | **Detection Limit(DL)*, ppm** | | |
|---|---|---|---|---|---|---|
| | **Si 28** | **Si 29** | **Si 30** | **Si 28** | **Si 29** | **Si 30** |
| With $O_2$ Titration | 63 | 301 | 51 | 4.8 | 13 | 2.0 |
| Cryogenic Desolvation (No $O_2$) | 13 | 18 | 15 | 0.8 | 1.2 | 1.0 |
| Cryogenic + Xenon (No $O_2$) | 1.6 | 1.3 | 1.4 | 0.11 | 0.07 | 0.1 |
| Cryogenic + Krypton (No $O_2$) | 3.1 | 2.0 | 1.6 | 0.2 | 0.10 | 0.08 |

*Detection limit is the concentration equivalent to the signal equal to 3s of background

Table 6: Performance Comparison of Si Analysis in 1-Propanol

| **Techniques for Si analysis** | **Background Equivalent Concentration(BEC), ppm** | | | **Detection Limit(DL)*, ppm** | | |
|---|---|---|---|---|---|---|
| | **Si 28** | **Si 29** | **Si 30** | **Si 28** | **Si 29** | **Si 30** |
| With $O_2$ Titration | 64 | 807 | 52 | 8 | 80 | 3.3 |
| Cryogenic Desolvation (No $O_2$) | 26 | 47 | 34 | 1.7 | 2.8 | 2.1 |
| Cryogenic + Xenon (No $O_2$) | 2.7 | 6.8 | 4.5 | 0.23 | 0.14 | 0.2 |
| Cryogenic + Krypton (No $O_2$) | 5 | 8.4 | 6 | 0.4 | 0.3 | 0.24 |

*Detection limit is the concentration equivalent to the signal equal to 3s of background

Table 7: Silicon isotope ratios measured in organic matrices

| | $^{28}Si$ / $^{29}Si$ | | $^{28}Si$ / $^{30}Si$ | | $^{29}Si$ / $^{30}Si$ | |
|---|---|---|---|---|---|---|
| **Solvent** | **Ratios** | **RSD** | **Ratio** | **RSD** | **Ratio** | **RSD** |
| 1-Butanol with $O_2$ flow | 19.82 | 0.6% | 29.72 | 0.4% | 1.497 | 0.5% |
| 5% butanol | 19.84 | 0.2% | 29.76 | 0.2% | 1.495 | 0.15% |
| Water | 19.85 | 0.15% | 29.75 | 0.15% | 1.496 | 0.1% |
| 1-Propanol | 19.84 | 0.5% | 29.75 | 0.4% | 1.496 | 0.4% |
| Expected natural Ratios | 19.84 | | 29.76 | | 1.500 | |

RSD values were calculated for n = 5

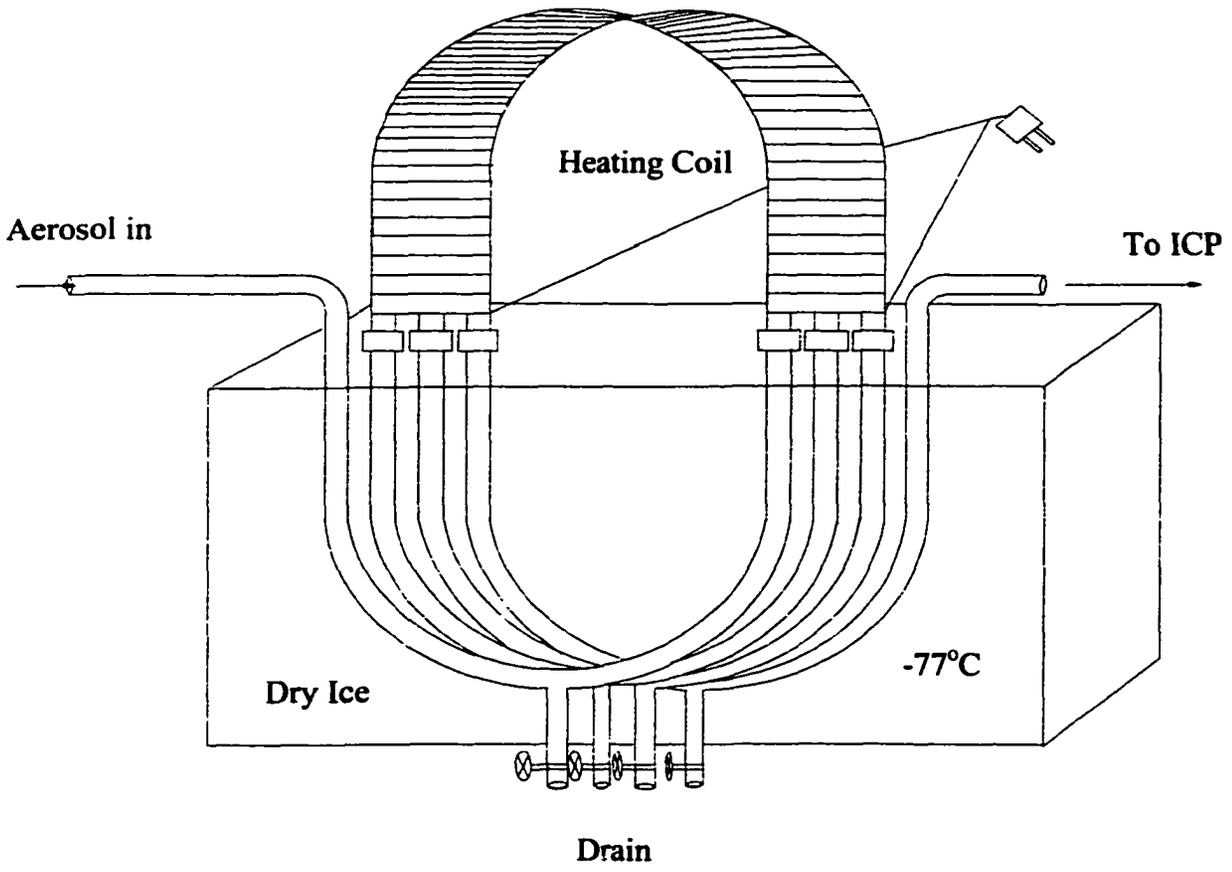


Figure 1: Schematic of cryogenic desolvation system

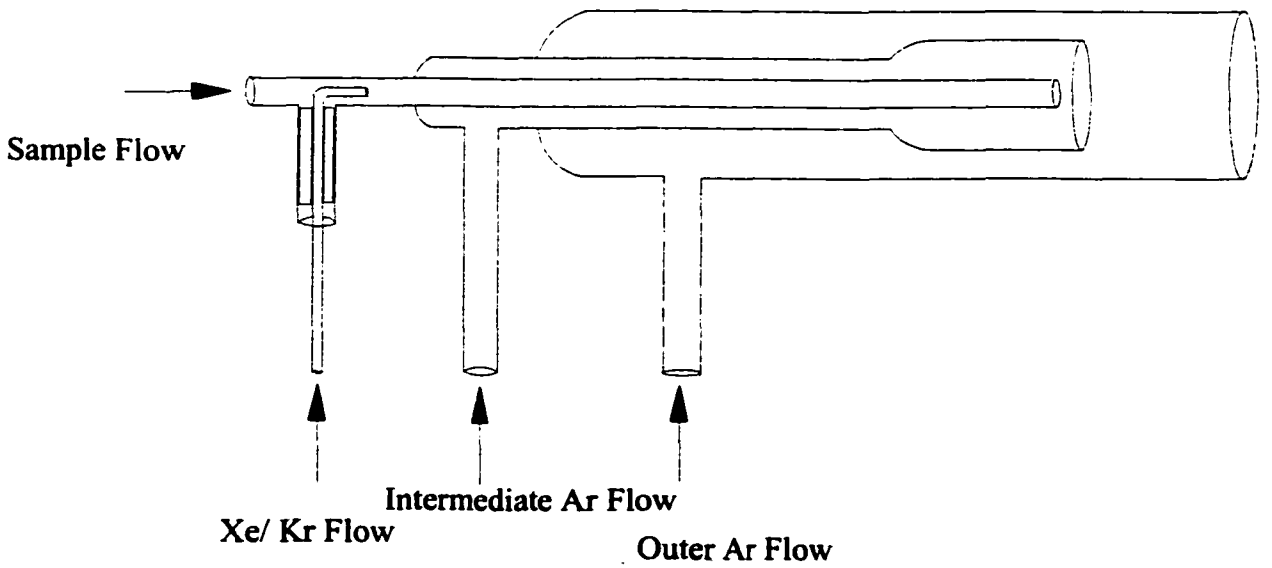


Figure 2: Scheme for introduction of Xe and Kr gases in the ICP

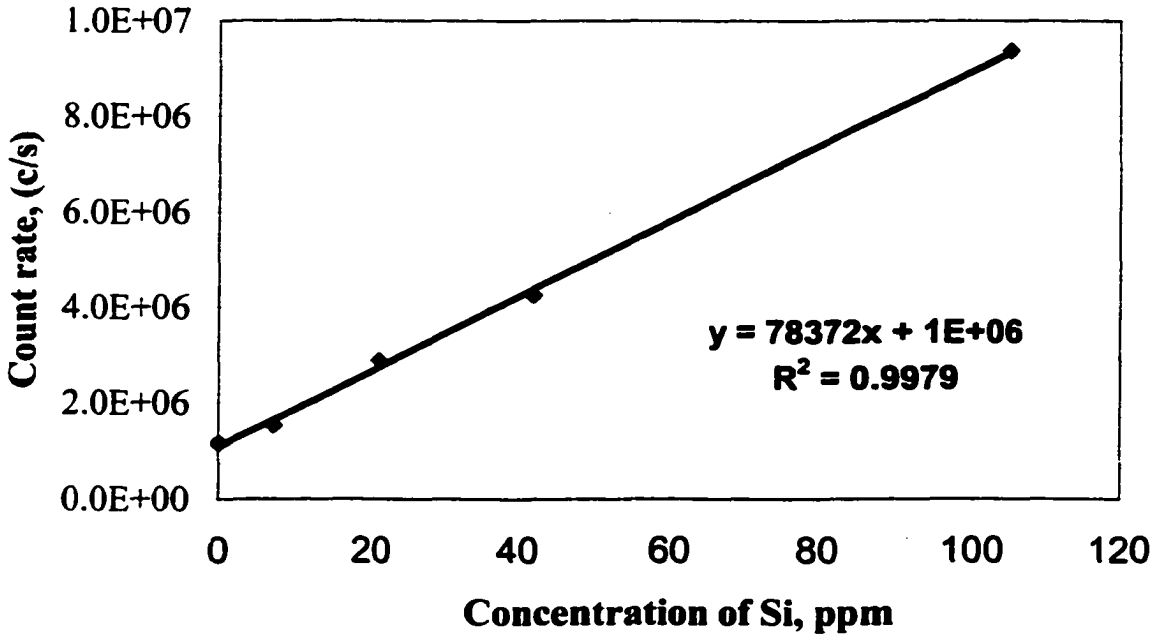


Figure 3a: Standard calibration curve for $^{28}Si$ in 1-butanol with cryogenic desolvation

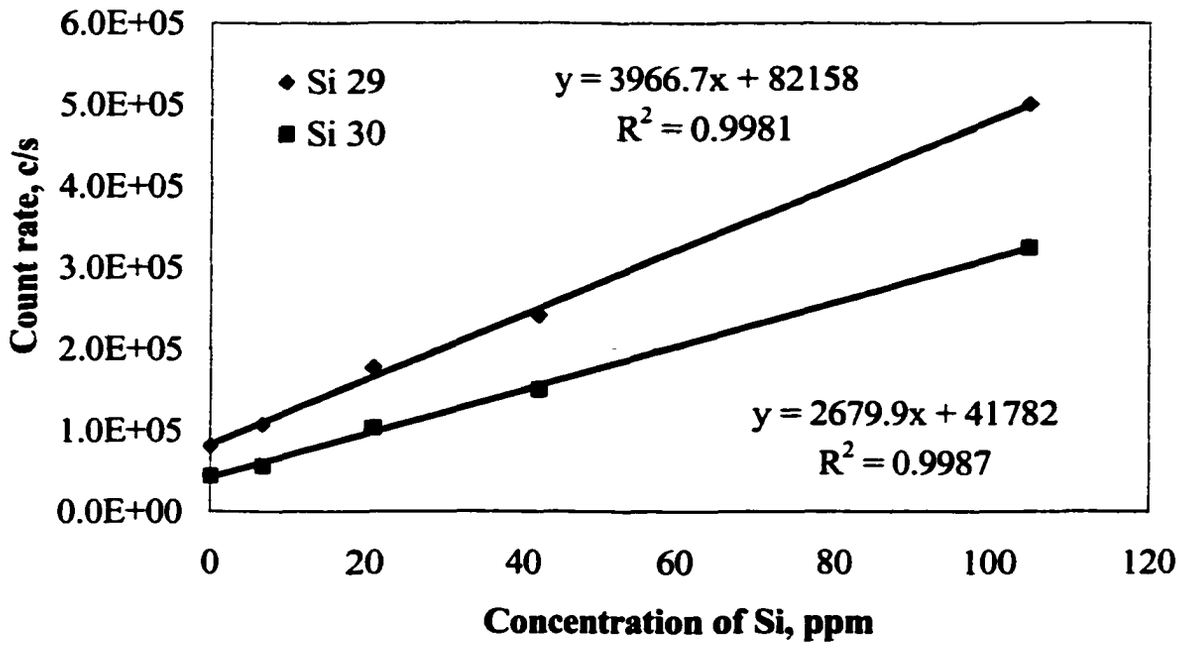


Figure 3b: Standard calibration curve for $^{29}Si$ and $^{30}Si$ in 1-butanol with cryogenic desolvation

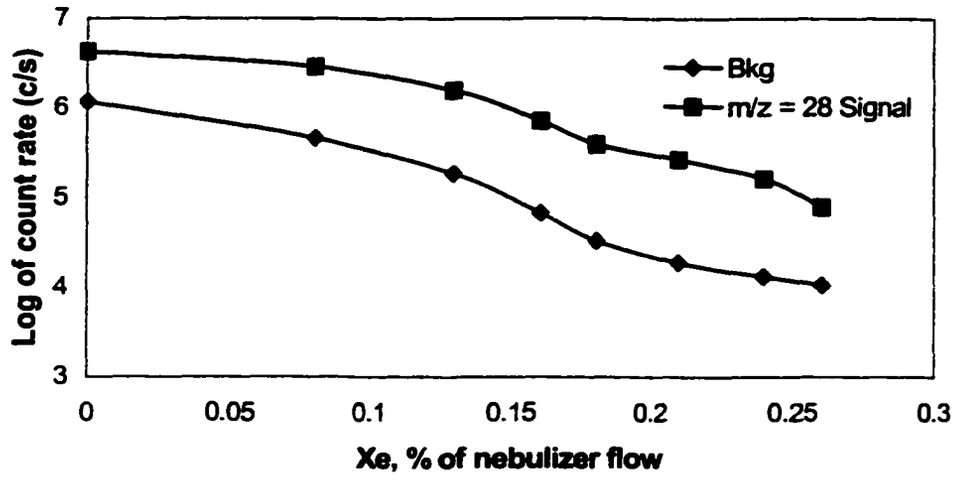


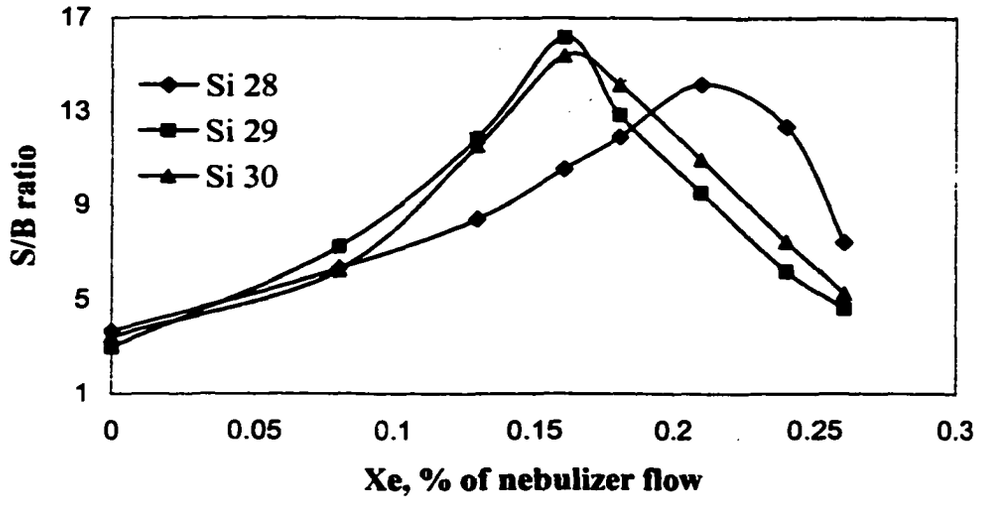


Figure 4: Effect of Xe on silicon (21 ppm) signal and background in 1-butanol

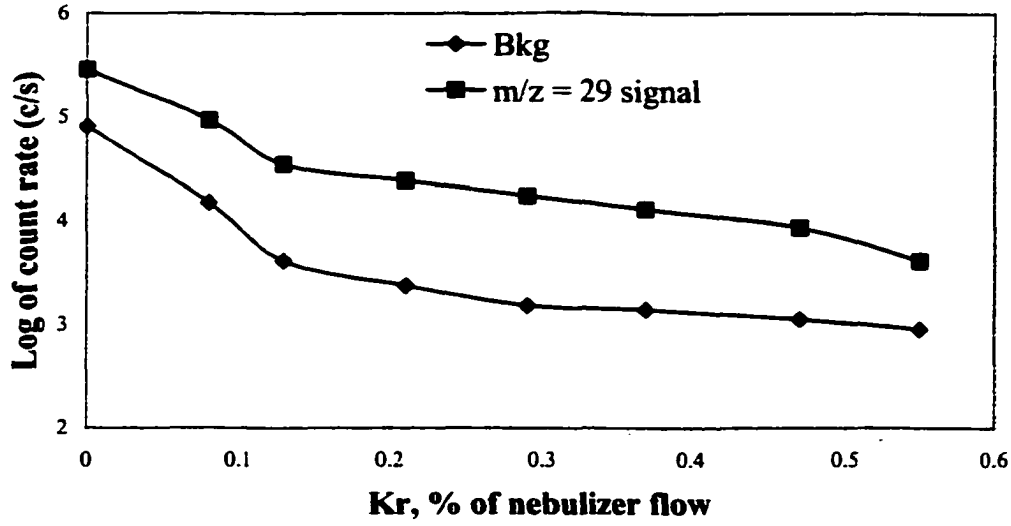


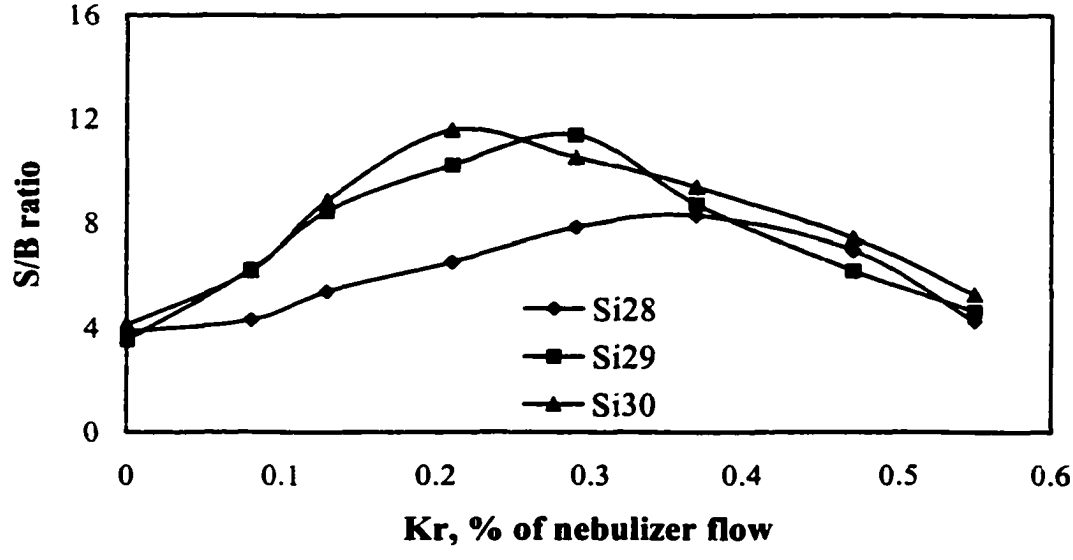


Figure 5: Effect of Kr on silicon (21 ppm) signal and background in 1-butanol

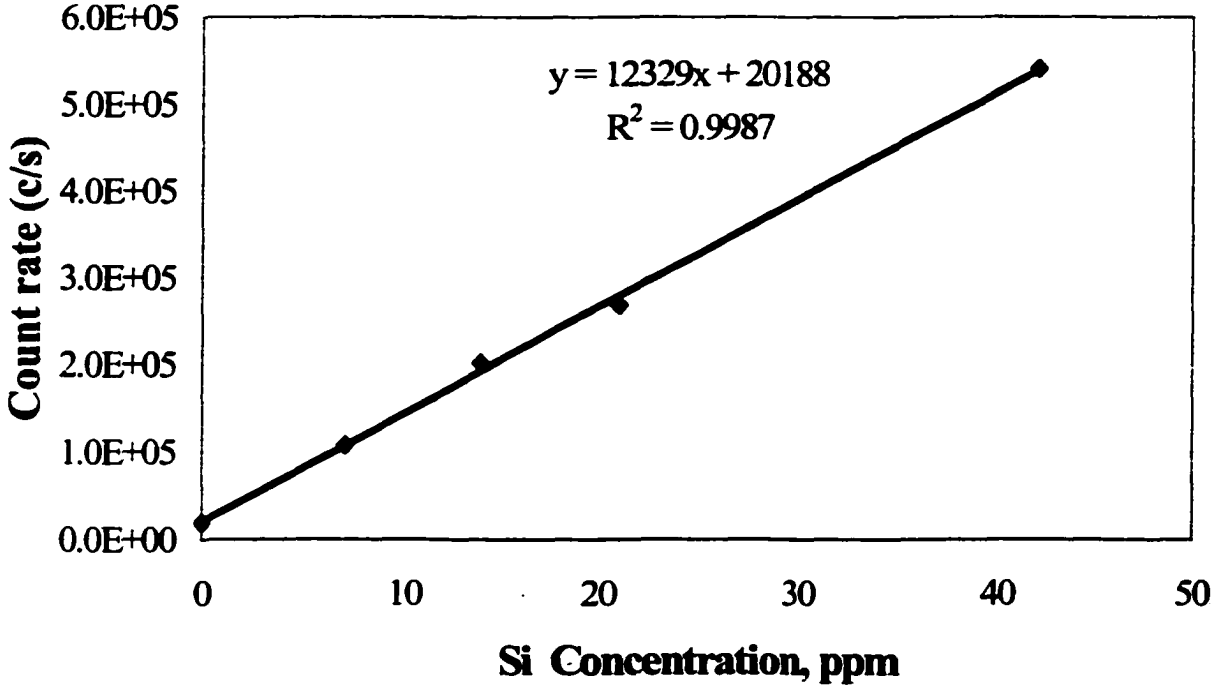


Figure 6a: Standard calibration curve for $^{28}Si$ in 1-butanol with 0.2% Xe flow after cryogenic desolvation

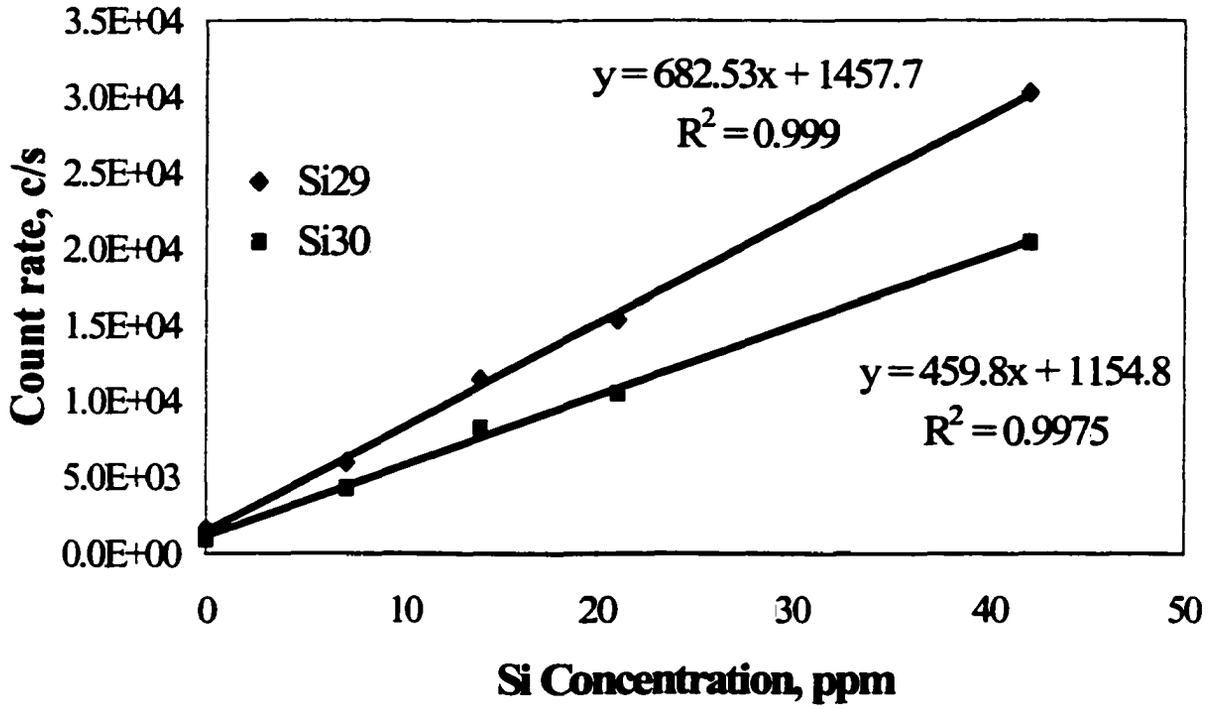


Figure 6b: Standard calibration curve for $^{29}Si$ and $^{30}Si$ in 1-butanol with 0.2% Xe flow after cryogenic desolvation

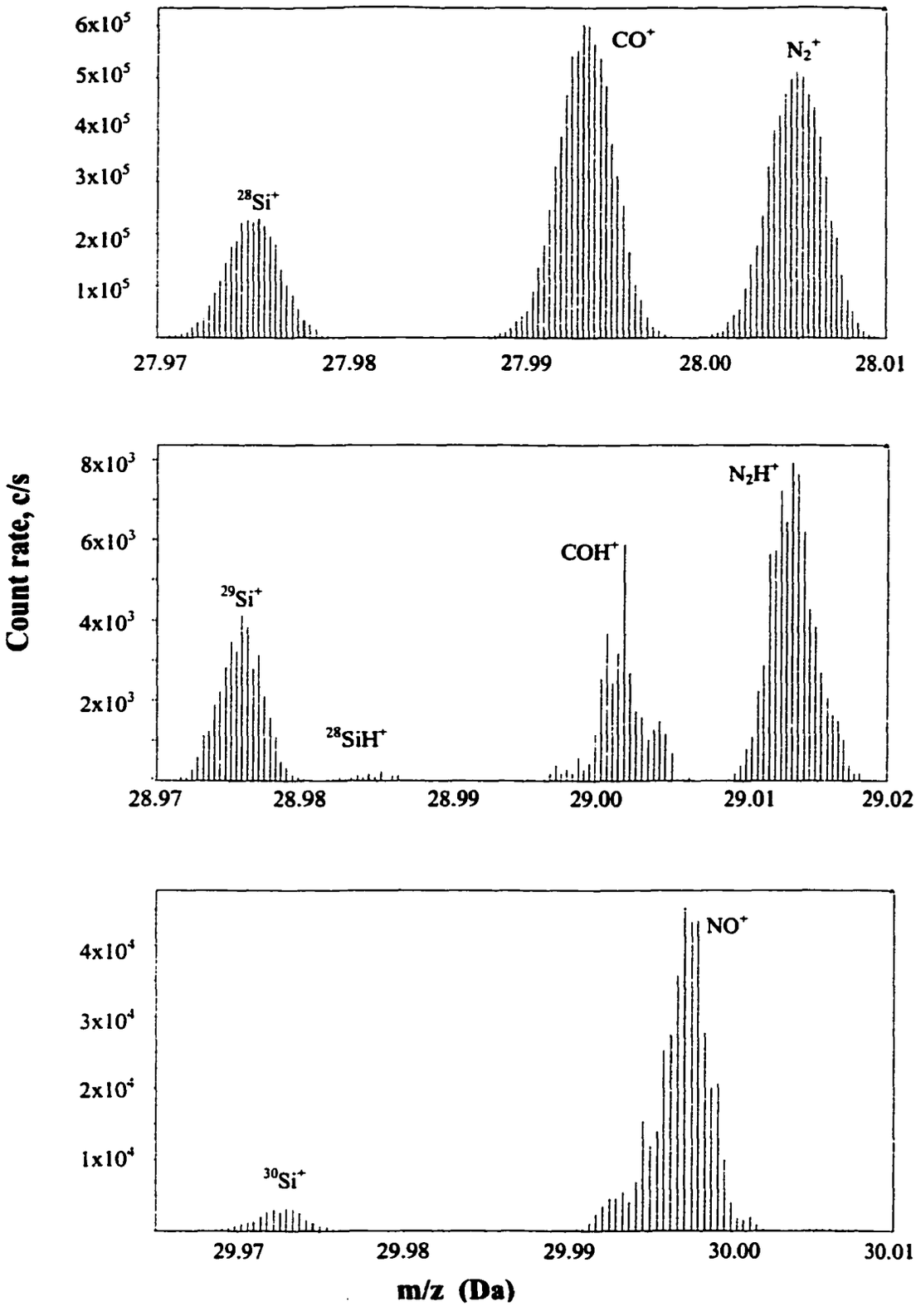


Figure 7: Interference on silicon mass signal by polyatomic ions at m/z 28 to 30

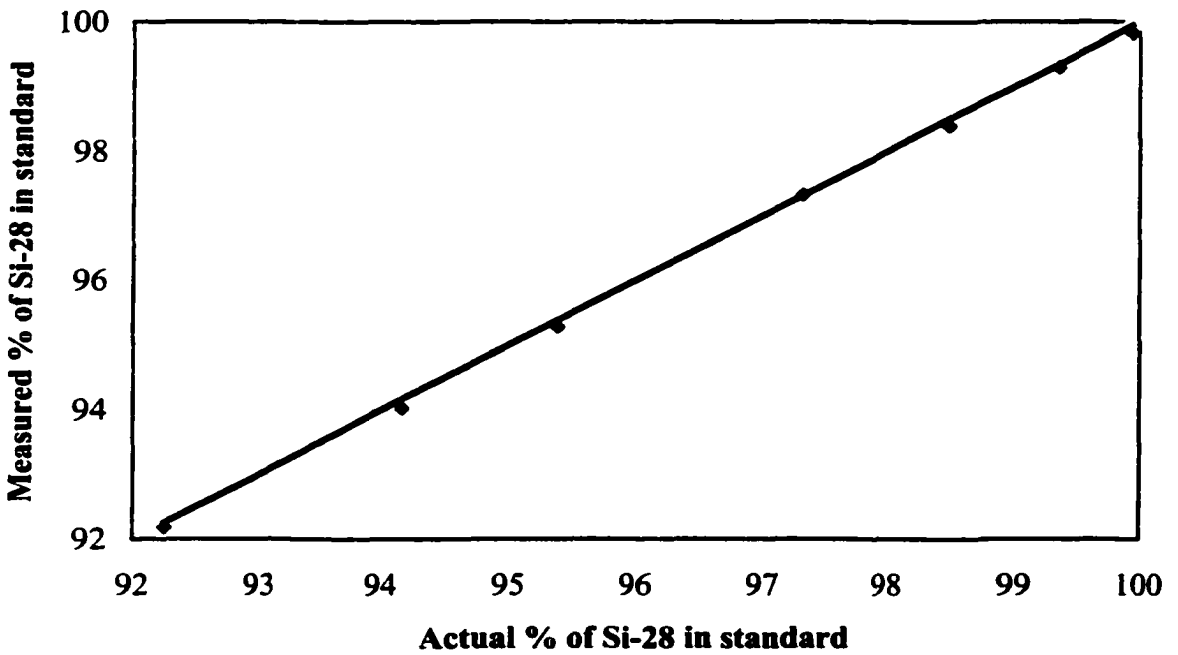


Figure 8: Si isotope calibration curve for m/z 28

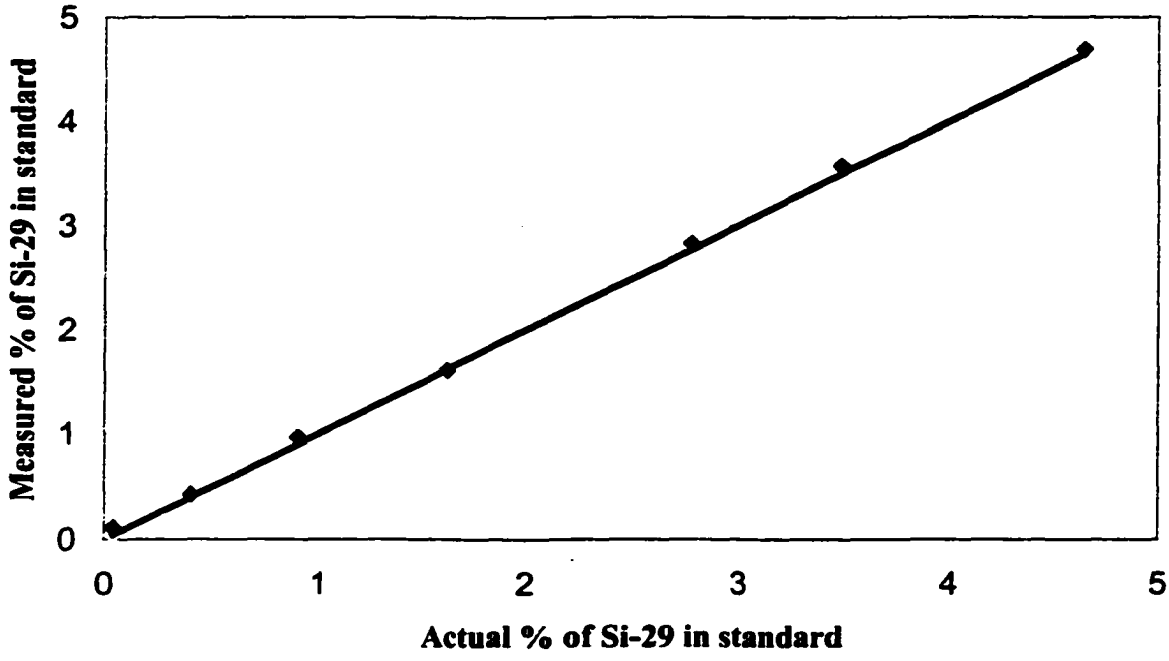


Figure 9: Si isotope calibration curve for m/z 29

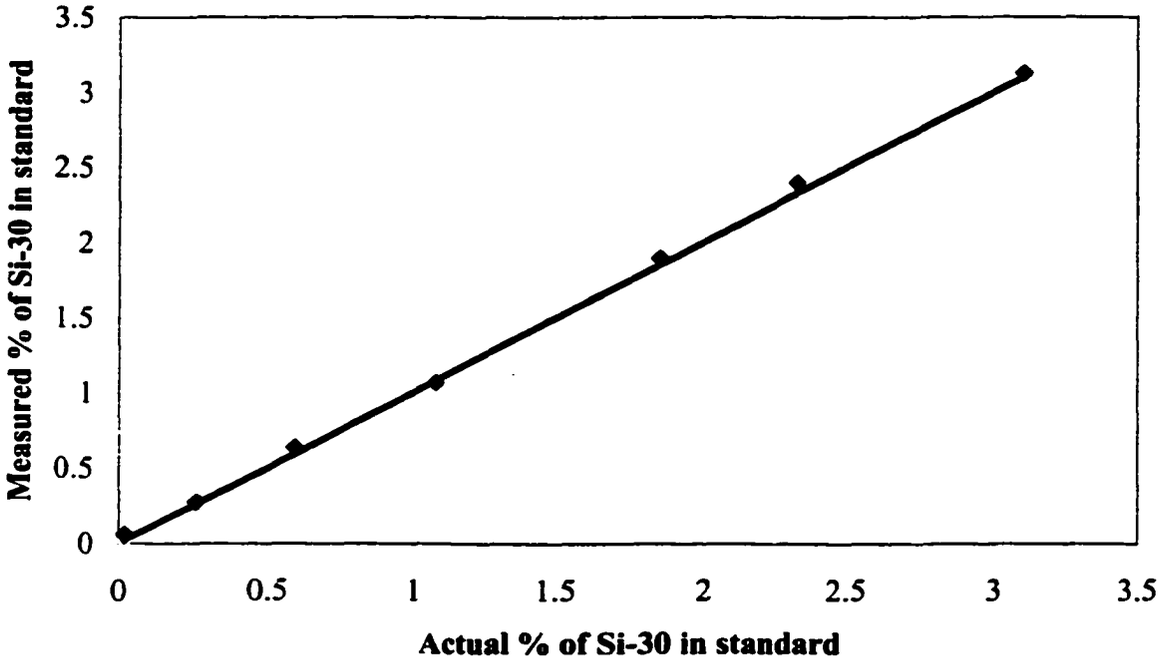


Figure 10: Si isotope calibration curve for m/z 30

# CHAPTER 4: ONLINE CLEAN UP OF BLANKS FOR ICP-MS BY ELECTROCHEMICALLY MODULATED LIQUID CHROMATOGRAPHY

A paper to be submitted to the journal of Analytical Chemistry

Towhid Hasan, Daniel Gazda, Marc. D. Porter and R. S. Houk*

## ABSTRACT

Electrochemically modulated liquid chromatography (EMLC) column has been adopted online with ICP-MS to clean up blanks to reduce background signals and thereby improve detection limits of analyte elements. Metal ions can be retained from the flow of blank in the micrometer size glassy carbon particle packing with appropriate negative potential. A Ag/AgCl (satd. NaCl) reference electrode in dilute nitric acid supporting electrolyte was used for electrochemical cell combination. Supporting electrolyte is placed outside the porous stainless steel column with a Nafion ion exchange resin coating inside, so that supporting electrolyte does not contaminate the stream of blank flow through the column. Several metal ions have found to be retained with >99% extraction efficiency from the blank solution. Cleaning of the column can be done easily by stripping the deposited metal with high positive potential.

Keywords: *inductively coupled plasma, ICP, inductively coupled plasma mass spectrometry, ICP-MS, electrochemically modulated liquid chromatography, EMLC, blank clean, background reduction*

---

* Corresponding author

## INTRODUCTION

Detection limits in ICP-MS are generally limited by the purity of the blank solution, so cleaning up the blank is the best way to improve these important figures of merit. Passing the blank through conventional ion exchange packing in a completely metal free column is one approach for cleaning up deionized water or organic solvents on-line. The clean blank is then sent on-line to the ICP-MS device and analyzed immediately before it is re-contaminated by storage. The hypothesis is that leaching of metals back into the purified solution will be less severe if there is no storage of bulk solutions. In this scheme, the sample bypasses the blank column and goes directly to the nebulizer so the trace elements in the sample do not contaminate the stationery phase. The column can thus be cleaned thoroughly by rigrous washing with very clean reagents. A separate column for analyte preconcentration could be employed for the sample, if desired. Using organic chelating agent and ion exchange resin metals can be accumulated selectively from the flow stream [1,2]. This traditional method of accumulating analyte from sample solution is useful for separating analyte from detrimental matrix. However, chelating agents or ion exchange resins containing protonated groups show low capacity for metal ions at the extreme pH, especially at very low pH. In addition, chelating agents or resins are usually used for complexing analyte from sample not for cleaning the blanks. Regeneration of chelating agents is complicated for the fact that additional solvents or acids need to be used that might contribute further contamination to the blank.

A second approach for on-line purification of acidic or basic solvents employs electrochemically modulated chromatography. The concept is similar to anodic stripping voltammetry, which has been used to clean up water [3,4] and to preconcentrate metals for

ICP-MS analysis [5]. Adsorptive stripping voltammetry, where the analyte is complexed with an chelating ligand at applied potential, was also used for accumulation of analyte metals from the solution [6-8]. Pretty et al. [9] incorporated mercury plated or gold plated reticulated vitreous carbon (RVC) working electrode in anodic stripping voltammetry coupled online with ICP-MS for separating several biologically important elements from the matrix. A similar flow cell system was used for the determination of Cu, Cd and Pb in biological systems by Hwang et al.[10]

Using carbon particles as a chemically reactive stationary phase, it should be possible to reduce and deposit metal ions to purify the blank solution. For blank solutions that are already very clean removal of the remaining ultra-trace elements may require batch type electrolysis for several minutes. The carbon stationery phase can be purged periodically by reversing the potential to remove the deposited metals. Carbon has several desirable features for this application: it is already reasonably clean, a wide range of applied potentials are possible, and it can tolerate extremes of pH, which is necessary for analysis of the acids typically used in elemental analysis. Previous work with carbon stationery phases for on-line electrolysis and chromatographic separation of analytes has shown that a wide variety of metals can be stripped simultaneously by application of a high negative potential [4]. Metals can be deposited even from non-aqueous solvent with appropriate supporting electrolyte and applied potential [11]. In ICP-MS work, Van Berkel and co-workers [12] show that the deposition efficiency on a single glassy carbon disk can be as high as 99%, especially at low liquid flow rate. Low flow rate of such a column can be conveniently coupled with ICP-MS with micro-nebulizer. Instead of using thin layer cell [13], which was used for anodic stripping, micrometer size glassy carbon particle packed column provides much larger

surface area and hence is expected to provide higher deposition efficiency of elements from the solution flow.

Van Berkel et al. also found that the glassy carbon electrode could be conditioned to enhance deposition of ions like $UO_2^{2+}$ and $Th^{4+}$ that are not normally accessible. [8,13] The surface chemistry of such radio-nuclides is of great environmental interest in the nuclear waste remediation effort, reduction of the blank levels for these elements is therefore desirable. Unlike anodic stripping voltammetery, electrochemical separation of individual metals is not necessary, simple removal of as many metals as possible is sufficient.

At present, electrochemically modulated chromatography requires a supporting electrolyte, which will naturally be present from the aqueous inorganic acid. The reference electrode is outside the flow channel, so contamination from it should not be problem. Again it is important to note that the blank column is never exposed to the sample with its much higher analyte levels. Great care should be taken to use only the cleanest, most metal free transfer lines; PFE Teflon is the material of choice. Application of this clean up methodology to low conductivity samples such as deionized water or organic solvents will require either addition of a supporting electrolyte or the development of low current columns that do not need one, thus the optional use of ion exchange described above. Incidentally, this same methodology will also be invaluable to help ICP-MS provide the detection limits necessary to meet the purity specs projected for the next generation of semiconductor chips.

## EXPERIMENTAL

### Instrumentation

Mass spectra data were acquired with Finnigan MAT Element I magnetic sector ICP-MS fitted with PFA 50 μL micro-nebulizer and teflon spray chamber. Conditions for time resolved data acquisitions are listed in Table 1. A HPLC pump (Model 222D, Scientific system Inc., PA) injects the solution into the nebulizer through the column. A schematic diagram of the column and delivery of sample solution to ICP-MS is shown in figure 1. All delivery tubing (Alpha Wire Corp.) is teflon made. Two six-port teflon valve (Rheyodyne, Cotati, CA) were used for sample delivery and routing through the column and to the ICP-MS. DI water is continuously pumped to the sample valve and the flow can be bypassed or passed through the sample loop. Similarly, in the column valve, the flow can be made through the column and bypassing the column. For EMLC column, PAR Model 173 potentiostat (Princeton Applied Research, NJ) was used as a source of electric potential.

### EMLC column

Electrochemically modulated liquid chromatography (EMLC) column is described in figure 2. The design of the EMLC column has been reported elsewhere [14]. In short, a Nafion® (Permapure) ion exchange membrane (outer diameter: 0.280 cm, inner diameter: 0.216 cm) is inserted into a porous stainless steel tube (pore size ~2 μm) and the ends are then flanged to secure it into position. A porous stainless steel frit is placed in the lower end fitting and the column is slurry packed with glassy carbon (GC) particles suspended in a 50:50 acetonitrile:dibromomethane mixture at 8000 psi. The upper end fitting contains a non-conducting PAT frit. The porous stainless steel housing serves as the counter electrode and

the carbon stationery phase as the working electrode in a three-electrode electrochemical cell. A Ag/AgCl( Satd. NaCl) reference electrode is placed in an electrolyte reservoir external to the column. All applied potentials are given with respect to this electrode. The supporting electrolyte used was 0.1 % $HNO_3$. Supporting electrolyte being in the external reservoir is separated from the working electrode by Nafion membrane. The column is washed with 100 μL/min 0.1% $HNO_3$ acid at +0.75 volt positive potential for an hour followed by washing with deionized water for another hour.

### Solvents

Distilled deionized water from Milli-Q purification system (Millipore Corp., Bedford, MA) was used as the primary flow from HPLC pump and to prepare standards. Dilute $HNO_3$ solution was prepared from Ultrex II grade $HNO_3$ (J. T. Baker, Phillipsburg, NJ). Standard metal ion solutions were prepared from 1000 μg/mL ICP standard stock solution (SPEX CertiPrep).

## RESULTS AND DISCUSSIONS

### Supporting Electrolyte

Different supporting electrolytes in the external reservoir were investigated including $LiNO_3$ and various concentrations of nitric acid. Although with 1 % $LiNO_3$, a number of metal ions were observed to accumulated from the flow stream, but it introduces a high level of $Li^+$ ion into the ICP. Due to extreme negative reduction potential, $Li^+$ ion can not be reduced or retained in the column. However with $LiNO_3$ supporting electrolyte the accessible negative applied potential is −1.0 V. Concentrated nitric acid (>1%) showed release of metal

ions from stainless steel construction material of the column especially at higher positive potential. In addition at higher concentration of nitric acid the evolution of $H_2$ occurs at –0.5 V. The cyclic voltamogram obtained with 1% nitric acid mobile phase and supporting electrolyte shows oxidation current above +0.9 V and reduction current below –0.5V. Excessive hydrogen evolution can break the Nafion coating and hence damage the column. With 0.1% nitric acid metal accumulation was observed to be as effective as with 1% nitric acid and also the safe end negative potential can be stressed further to 0.06.

**Online clean up of Cd, Cu and Ag**

Commercial grade nitric acid contains parts per billion levels of Cd and Cu. Figure 3a shows the $^{114}Cd$ signal for 0.1 % $HNO_3$ through the EMLC column at open circuit. Figure 3b shows intensity of $^{114}Cd$ signal with –0.45 V potential applied for the 0.1% $HNO_3$, which is less than 500 cps. Figure 3c demonstrate the effect of potential applied on $^{114}Cd$ signal. Potential positive than -0.40 V does not remove Cd from the solution stream and potential negative than -0.45 V does not increase deposition of Cd either. Stripping Cd ion form the column with positive potential (+0.7 V) is observed at later part of the time scan. Bypassing the column Cd provides 3 times higher intensity of signal ($^{114}Cd$ signal through the column is $2x10^5$ cps, bypassing the column $6x10^5$ cps) which proves that GC carbon has affinity for Cd even without potential.

Copper and Ag can also be removed from the blank with –0.2 V or higher negative applied potential. However retention of Cu in the GC stationary phase is not as high as Cd. Occasional release of Cu from the stationary phase was observed as spike of Cu signal appeared in the time scan of $^{65}Cu$ signal. Accumulation of Ag on the GC from a synthetic

blank with 1 ppb of Ag was also observed at negative potential. But still high background of Ag was observed as result of Ag leaching from the reference electrode. Therefore practical clean up of Ag blank will only be possible with a reference electrode other than Ag/AgCl , which was used in the present system.

**Online clean up of Tl from DI water blanks**

A thallium standard of 500 parts per trillion (ppt) was prepared in DI water. Intensity of $^{205}Tl$ signal for the standard solution is shown in figure 4a. The standard was then injected through the EMLC column. Figure 4b shows the level of $^{205}Tl$ signal in the DI water and upon application of –0.4 V potential the signal goes below 200 cps. Tl can be deposited from DI water below -0.35 V. Stripping can be done at higher positive potential ( +0.75 V) as shown in figure 4c. Although the Tl standard was in DI water, nitric acid from the supporting electrolyte in the external reservoir can leach into the column through the porous stainless steel column wall and Nafion ion exchage membrane. Therefore it confirms that metal ions even in DI water sample flow can also be accumulated in the GC stationary phase.

**Online clean up of U from blanks**

For very low detection limit of uranium, clean up of blank is necessary. Uranium is an important element in semiconductor materials. It decays and ruins band gap if it is present even in very trace amount. Accumulation of uranium from 0.1% nitric acid is shown in figure 5. The GC particles tend to adsorb uranium even at open circuit (figure 5b). However the adsorbed uranium can be stripped of the stationary phase with high positive potential. Maximum accumulation of uranium was observed between –0.2 V to -0.25 V. With higher

negative potential, uranium tends to accumulate less than the above potential. Exact mechanism of uranium deposition is yet to be fully explained. Pretty et al [13] suggested that the following electrochemical reactions take place in an acidic matrix.

$$UO_2^{+} + 4H^{+} + e^{-} = U^{4+} + 2H_2O \quad (E^{\circ}_{red} = 0.42\ V) \qquad (1)$$

$$UO_2^{2+} + 4H^{+} + 2e^{-} = U^{4+} + 2H_2O \quad (E^{\circ}_{red} = 0.13\ V) \qquad (2)$$

$$UO_2^{2+} + e^{-} = UO_2^{+} \quad (E^{\circ}_{red} = -0.15\ V) \qquad (3)$$

U(IV), not U(VI), is assumed to be accumulated. U(IV) is more susceptible to hydrolysis and forms hydrous oxides in aqueous solution even at low pH (<2)[15,16]. Presence of nitric acid as a supporting electrolyte may contribute to formation of oxygen functionalities (C-O groups) on GC particle surface, which may provide complexation sites for U(IV) [17]. Our observation of maximum uranium accumulation at –0.2 V from nitric acid media support the hypothesis. Too negative potential makes the complexes unstable resulting in decrease of uranium accumulation.

**Online clean up of Cr, Pb and Sn from blanks**

Accumulation of Cr(III), Pb(II) and Sn(IV) follow similar behavior as uranium. Pb, Cr and Sn can be accumulated from the blank at potentials between –0.15 volt and –0.30 volt, and further negative potential strip accumulated metal from the stationary phase. Background signal from $ArC^{+}$ at m/z =52 was also investigated by using medium resolution (m/Δm =4000). Intensity of $ArC^{+}$ was found twice higher when the flow through the column than the flow bypassing the column.

**Online clean up of Co, Fe, V and Zn from blanks**

Transition metals can be deposited on GC particles with adequate negative potential. Potential lower than –0.45 V makes accumulation of Co, V, Fe and Zn possible from both neutral water and dilute acid. Figure 6 shows deposition of Co from 0.1% nitric acid. The intensity $^{59}Co$ signal at –0.5 V is observed to be less than 100 cps compared to $10^5$ cps without potential. V and Fe shows similar behavior but the background signal could not be reached as low as observed in case of Co. Figure 7 shows the background $^{51}V$ signal of 500 cps, which is due to $^{38}Ar^{12}C^{1}H^{+}$ and $^{35}Cl^{16}O^{+}$ polyatomic ions. At higher resolution ($m/\Delta m$ =4000) the presence of those polyatomic ions were confirmed. Fe can also be removed from the blank, but significant intensity of Fe still was observed due to dissolution of the stainless steel construction material with nitric acid supporting electrolyte. 1% $LiNO_3$ was used instead of nitric acid for Fe deposition, but the accumulation efficiency was not as good as with nitric acid. Besides with $LiNO_3$, an undesirable high Li background was observed in the ICP-MS, which might interfere with the measurement of other analyte. Zn was observed to be removed from the flow stream from both neutral water and 0.1% $HNO_3$. Figure 8 shows deposition of Zn from the DI water upon application of negative potential at –0.5V.

## CONCLUSION

Electrochemically modulated GC particle packing has demonstrated the ability of cleaning metal ions from both neutral water and dilute acid. Column packing material is resistant to nitric acid; but at higher concentration of the acid, the stainless steel frit can be damaged. Possibility of damage of column-wall, made of stainless steel, is minimal as it is separated from the packing material by Nafion coating. The concentration in the range of

0.1% nitric acid flowing through the column showed insignificant leaching of metals (e.g., V, Cr or Mn, constituents of stainless steel) except iron at high positive potential. The accumulation efficiency of metal ions investigated was > 99%. Cd, Tl, Zn, Co, V, Ag and Cu metal ions can be accumulated from the flow stream with the same set of applied negative potential. Other metal ions require adjustment of appropriate negative potential for their deposition into the column. Alkai and alkaline earth metals having extreme negative reduction could not be retained in the column. The lower limit of negative potential before hydrogen evolution is–0.55 V with 0.1% nitric acid supporting electrolyte. A number of other metal ions are believed to accumulated on this GC packed column with proper application of potential. Decreasing the particle size of the GC particles and hence increasing the surface area are supposed to further enhance the efficiency of retention of metal ions. A metal free construction material other than stainless steel is supposed to eliminate the problem of leaching metal ions into the column.

## ACKNOWLEDGEMENTS

Ames Laboratory is operated by Iowa State University for the U. S. Department of Energy under Contract No. W-7405-Eng-82. This research was supported by the Molecular Processes Program, Division of Chemical Sciences, Office of Basic Energy Sciences. The authors thank for Spex CertiPrep for providing standards.

## REFERENCES

1. Fang, Z., *Spectrochim. Acta. Rev.* 1991, **14**, 235-29
2. Evans, E. H., Giglio, J. J., *J. Anal. At. Spectrom.* 1993, **8**, 1-18

3. Hills, G. "*Electrochemistry [in water purification]*", *Chem. Britain*, 1976, **12**, 291-293
4. Blaedel, W. J., Strohl, J. H., "*Continuous quantitative electrolysis*", *Anal. Chem.*, 1964, **36**, 1245-1251
5. Wang, J., "Stripping Analysis", VCH, Deerfield Beach, 1985
6. Wang, J. Setiadji, R., *Anal. Chim. Acta.*, 1992, **264**, 205
7. Zhou, F., Van Berkel, G. J., Morton, S. J., Ducworth, D. C., Adeniyi, W. K., Keller, J. M., "*Applications of Inductively Coupled Plasma-Mass Spectrometry to Radionuclide Determinations*", ASTM STP 1291, Morrow, R. W., Crain, J. S. (Eds.), American Society for Testing and Materials, West Conshohocken, 1995, pp82-98
8. Pretty, J. R., Duckworth, D. C., Van Berkel, G. J., *Intl. J. Mass spectrometry* ,1998, **178**, 51-63
9. Pretty, J.R.; Evans, E. H.; Bluebaugh, E. A.; Shen, W. L.; Caruso, J. A.; Davidson, T. M.; *J. Anal. Atomic Spectrom.* 1992, **7**, 1131-1137
10. Hwang, T. J., Jiang, S. J., *J. Anal. At. Spectrom.* 1996, **11**, 353-7
11. Pretty, J. R., Van Berkel, G. J., *Rapid Commun. Mass Spectrom.*, 1998, **12**, 1644-1652
12. Pretty, J. R., Duckworth, D. C., Van Berkel, G. J., *Anal. Chem.*, 1997, **69**, 3544-3551
13. Pretty, J. R., Duckworth, D. C., Van Berkel, G. J., *Anal. Chem.*, 1998, **70**, 1141-1148
14. Yting, E., Porter, M. D., *Anal. Chem.*, 1998, **70**, 94
15. Baes, C. F. Jr., Mesmer, R. E., *The Hydrolysis of Cations*, John Wiley, New York, 1976
16. Cotton, F. A., Wilkinson, G., *Advanced Inorganic Chemistry*, John Wiley, New York, 1980
17. McCreery, R., In *Electroanalytical Chemistry*; Bard, A. J., Ed., Marcel Dekker, New York, 1990, Vol. 17, pp 221-374

Table 1: Operating parameters for the Finnigan Mat Element ICP-MS

| | |
|---|---|
| **Instrumental setup:** | |
| RF Power | 1200 watts |
| Sample gas flow rate | 0.95 L/min |
| Sample uptake rate | 50-80 μL/min |
| Sampler and Skimmer cones | Nickel |
| Injector | Quartz |
| Guard Electrode (Pt) | Grounded |
| Acquisition mode | EScan |
| Resolution (m/Δm) | 4000/300 |
| **Parameter for analysis:** | |
| Mass window | 100% |
| Integration window | 100% |
| Sample time | 10 ms |
| Number of samples per unit mass | 20 |
| Analysis Time | 60 min |

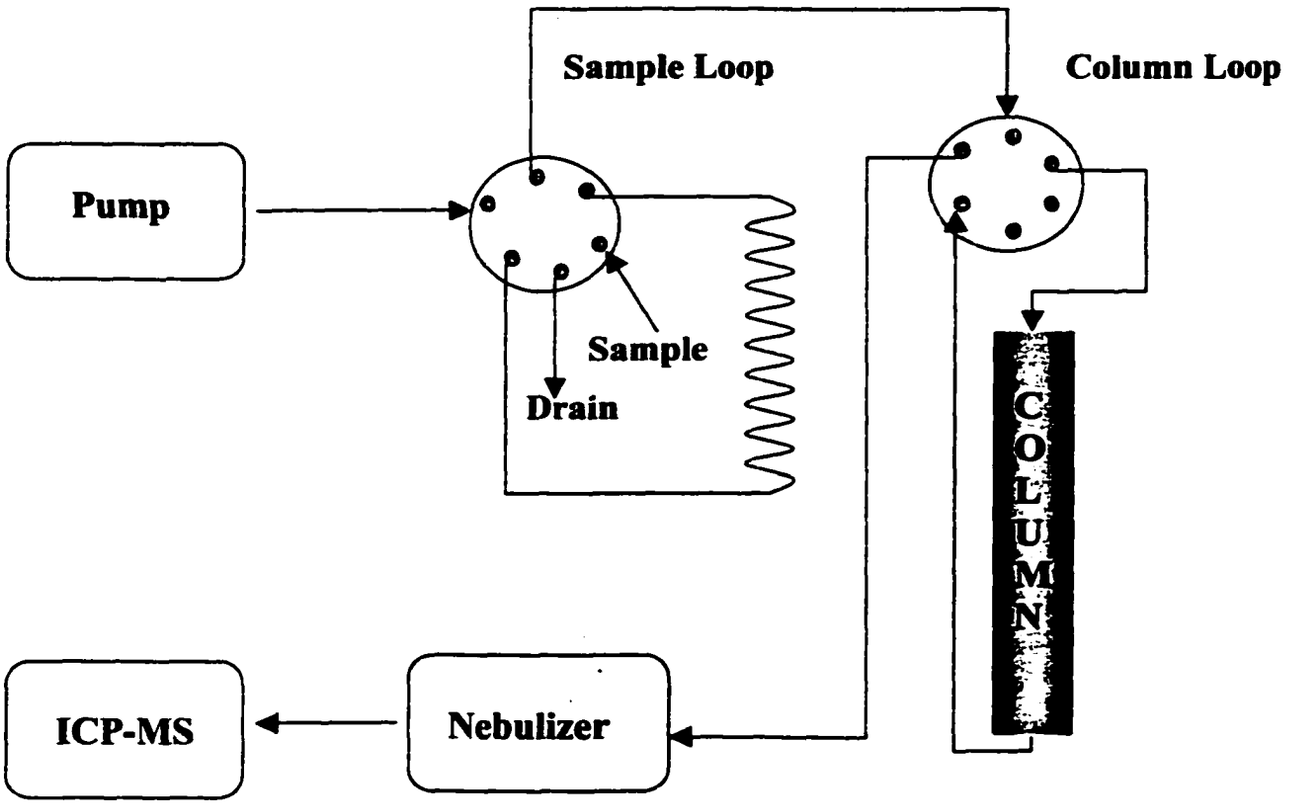


Figure 2: Schematic Diagram of EMLC - ICPMS Interface

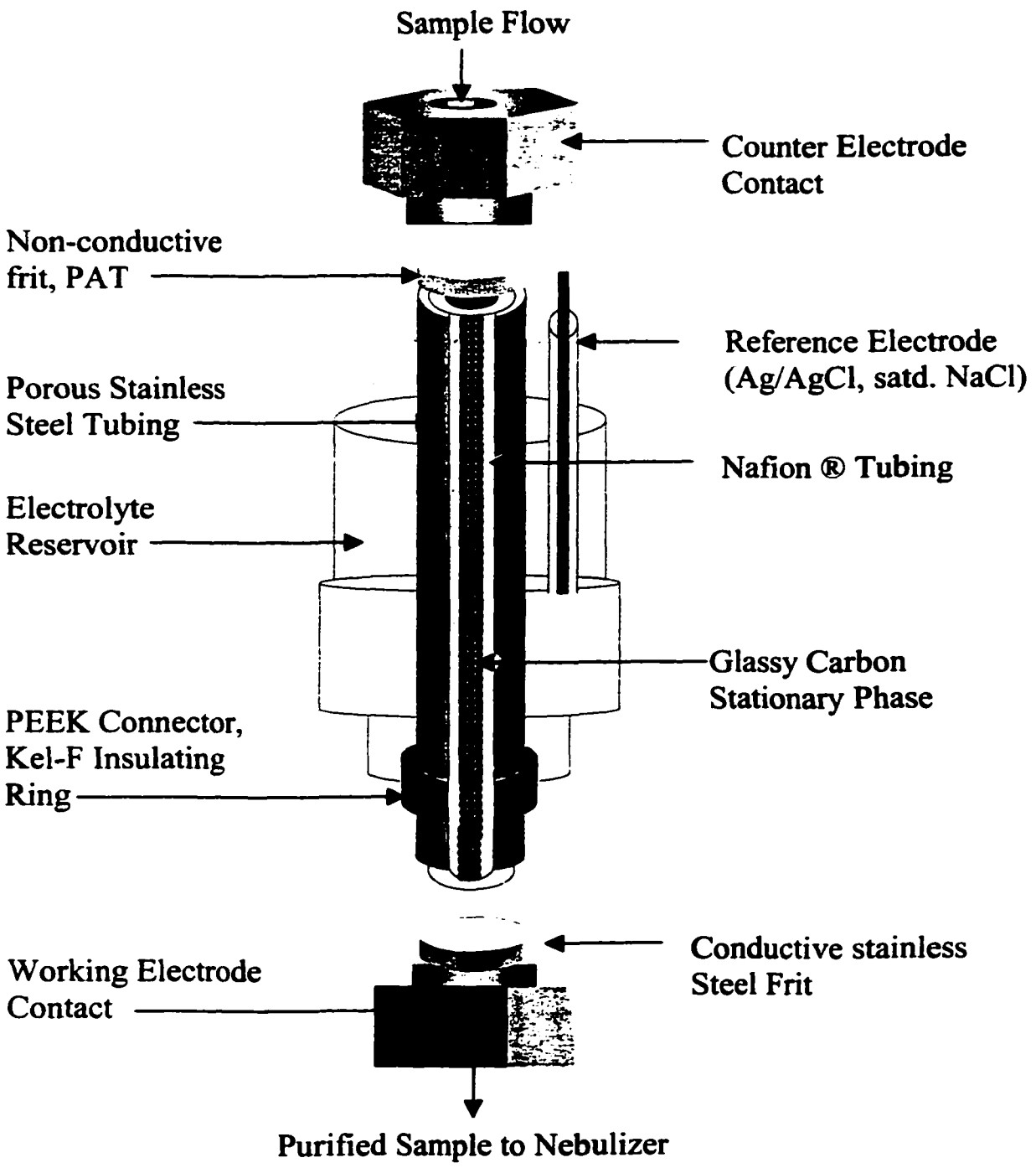


Figure 2: Construction of Electrochemically Modulated Liquid Chromatograph

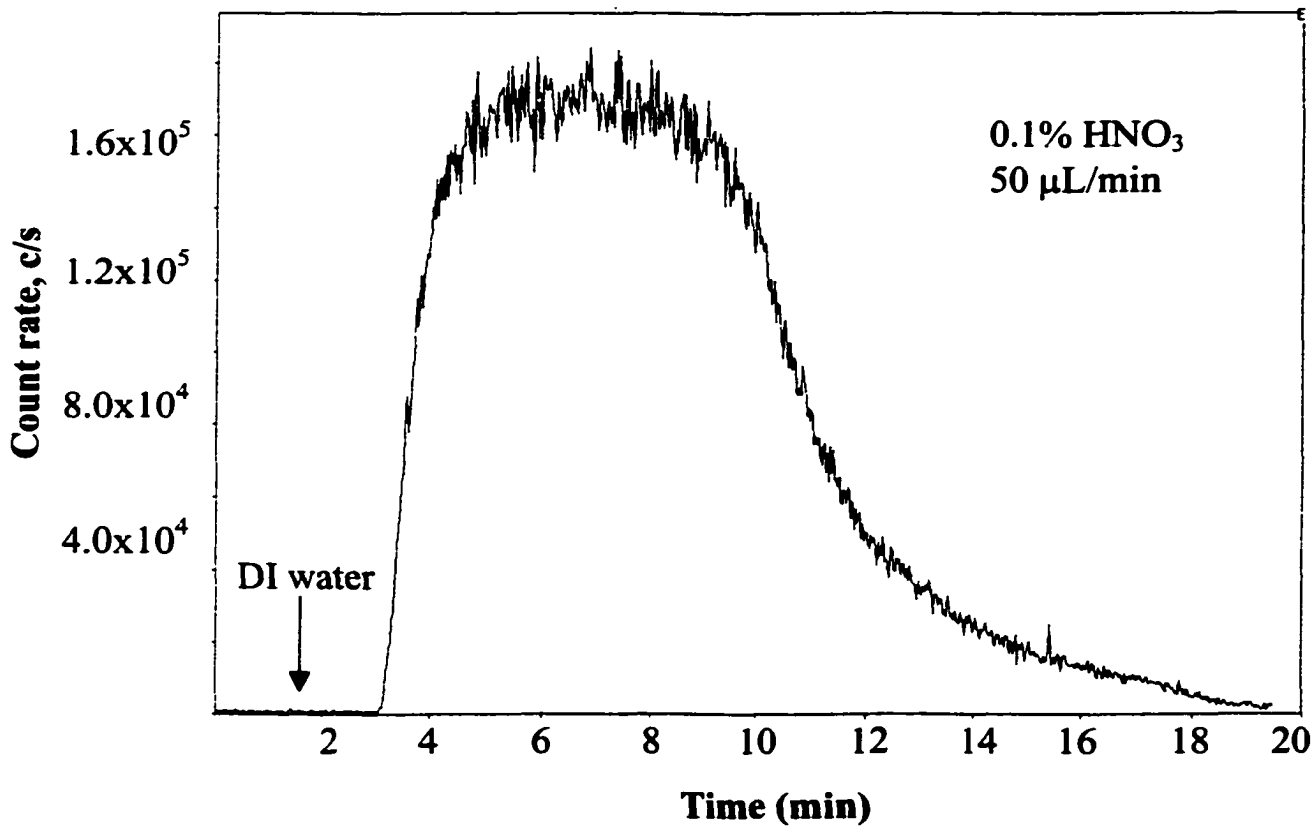


Figure 3a: $^{114}Cd$ signal for 0.1% $HNO_3$ blank (~1 ppb of Cd) at 50 µL/min through a 0.5 ml loop through the EMLC column at open circuit

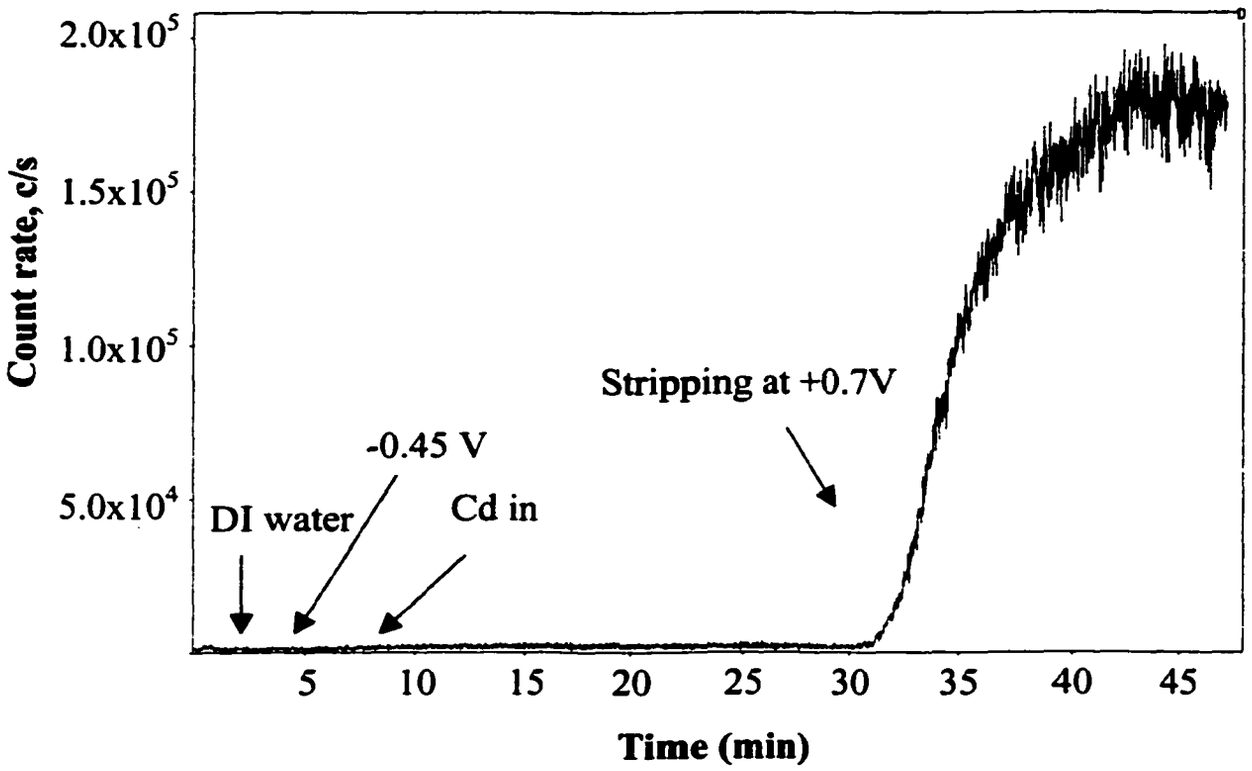


Figure 3b: Cd in 0.1 % HNO3 through the column; deposition of Cd at with -0.45 V potential and stripping at +0.7 V

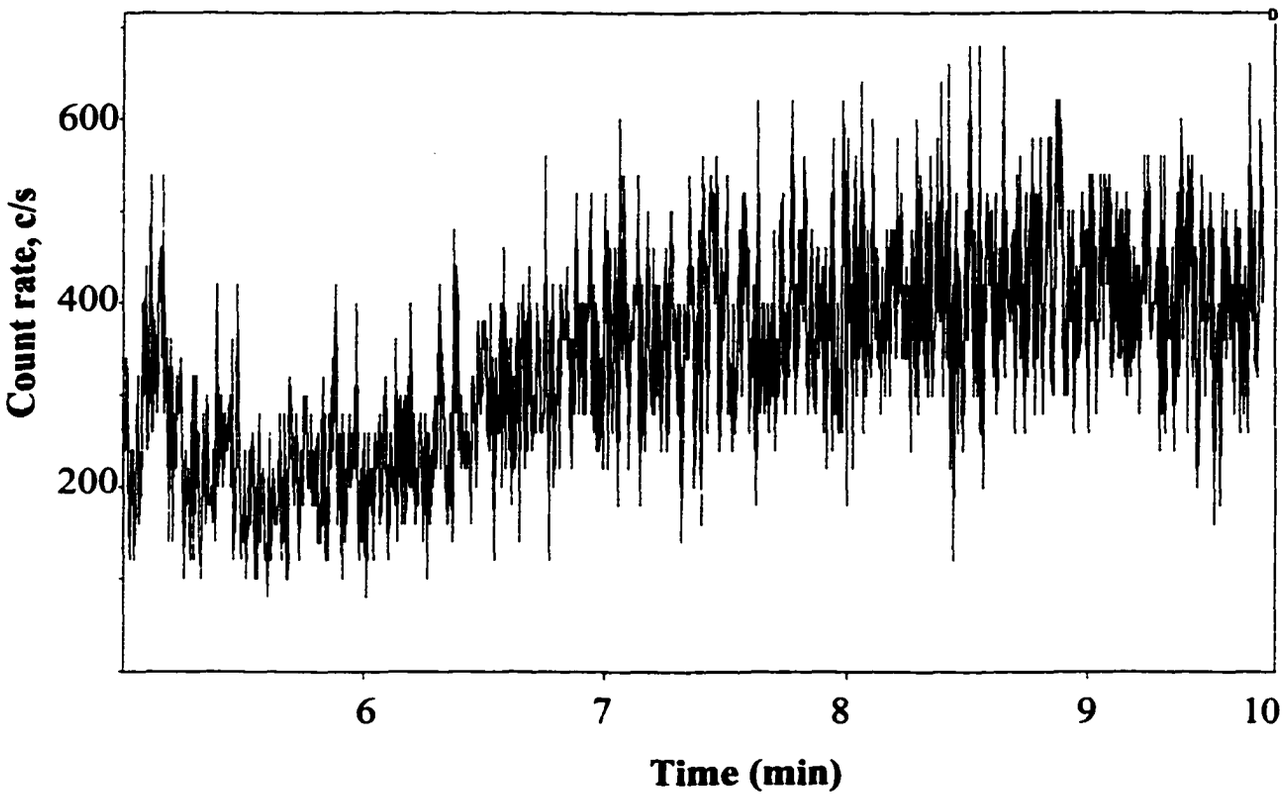


Figure 3c: Cd through the column during the moment of introduction and applied potential

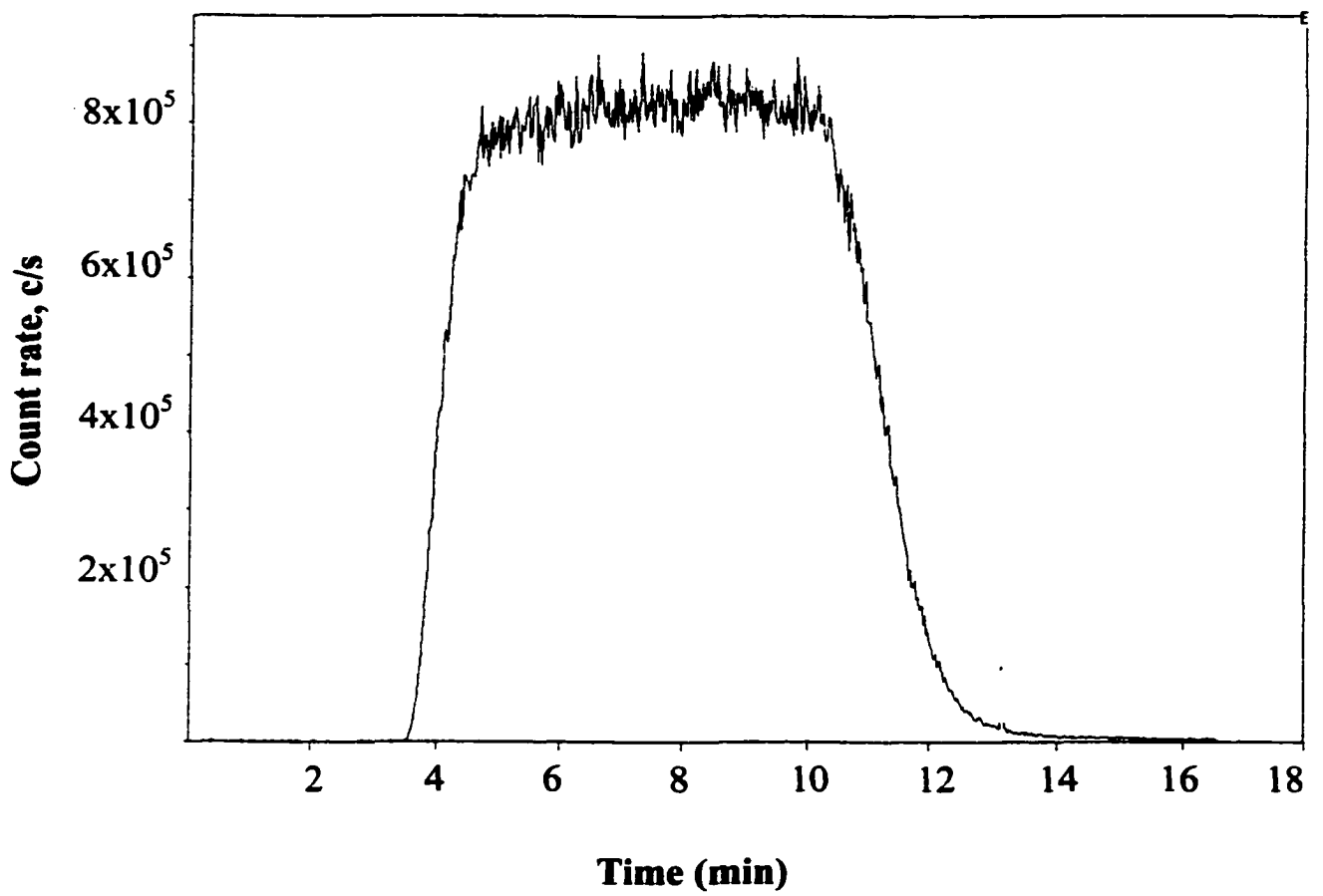


Figure 4a: $^{205}Tl$ signal for 500 parts per trillion (ppt) in DI water bypassing the column at 50 μL/min flow rate

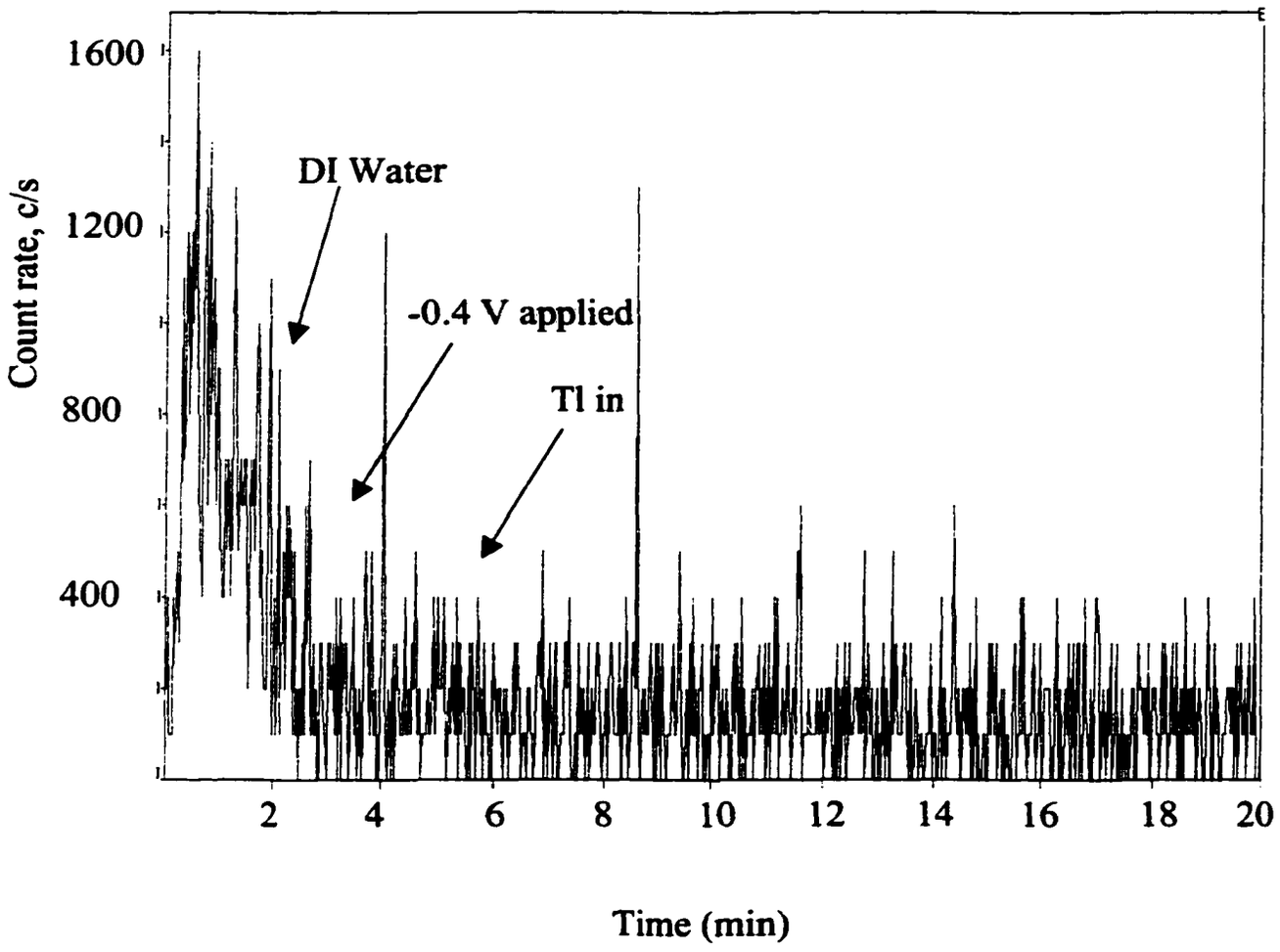


Figure 4b: Deposition of Tl in EMLC column at –0.40V

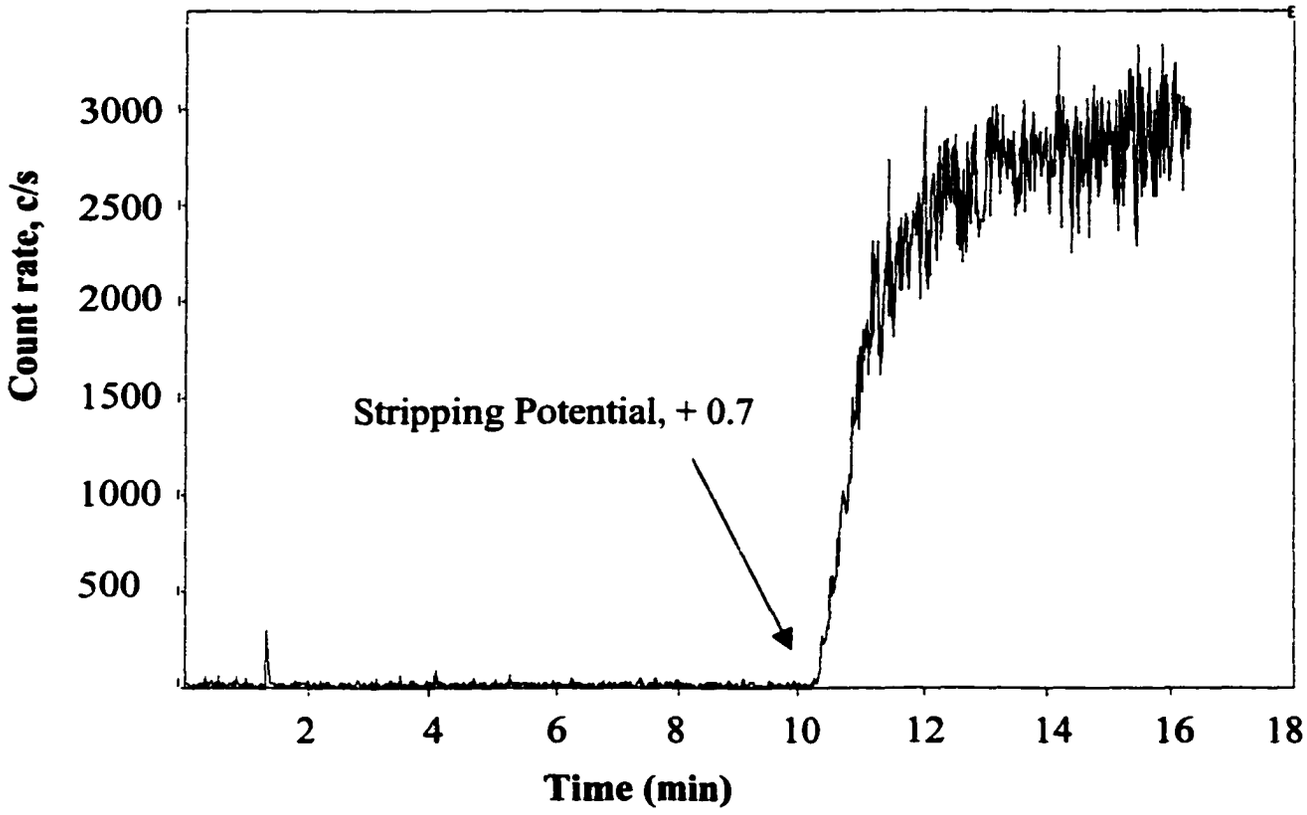


Figure 4c: Stripping of Tl from EMLC Column by applying +0.7 Volt.

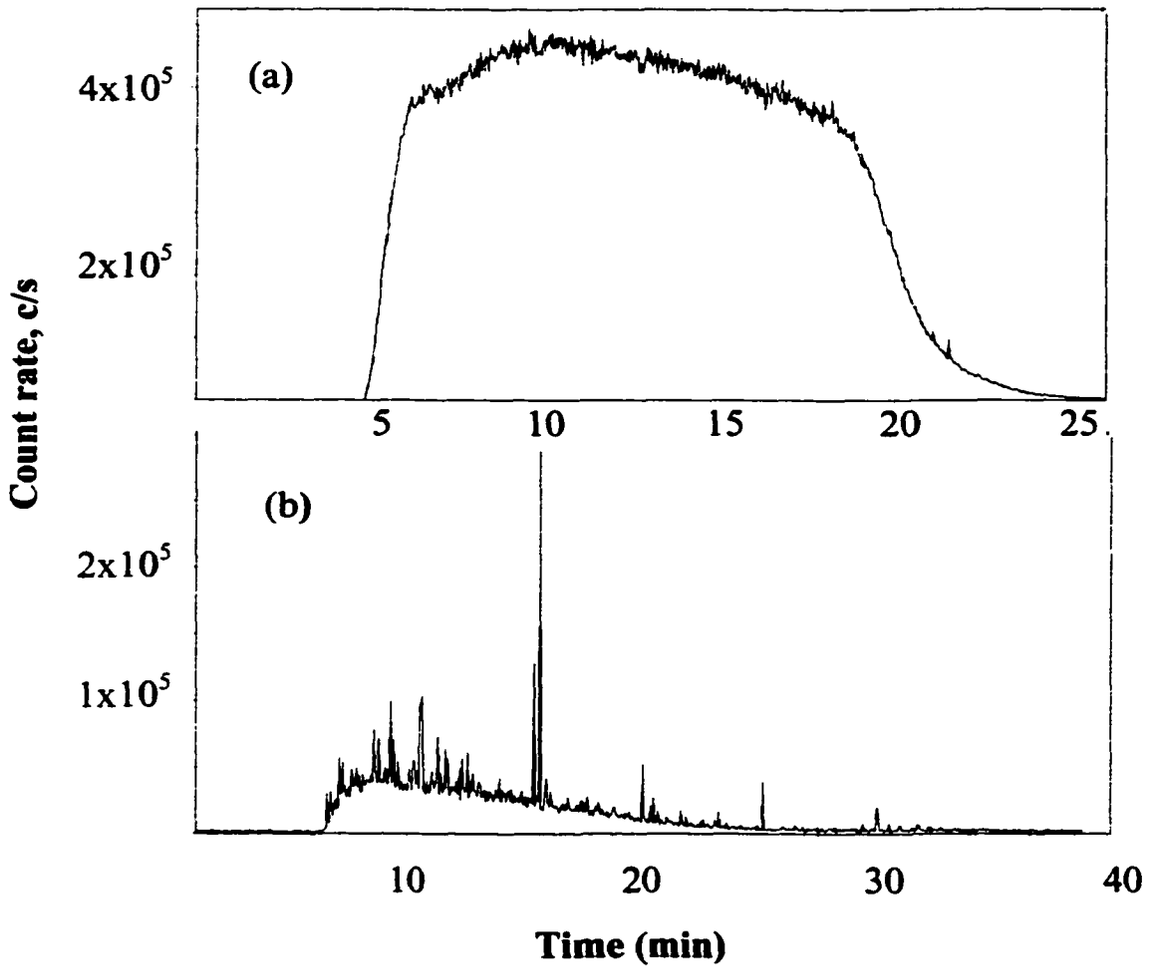


Figure 5 (a,b): $^{238}U$ signal of 500 ppt U in 0.1% nitric acid, a) bypassing the EMLC column; b) through the column at open circuit

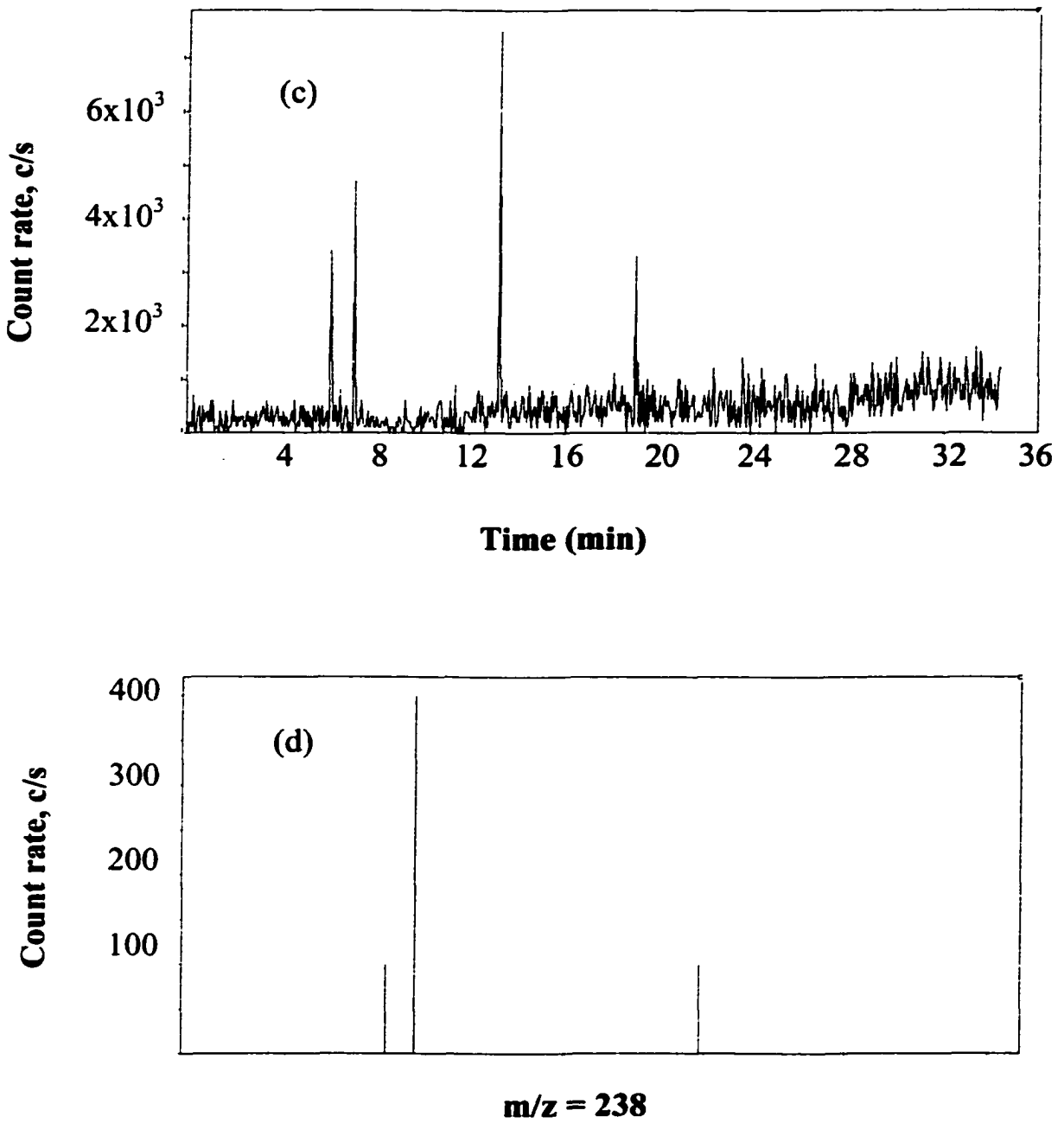


Figure 5 (c,d): $^{238}U$ signal of 500 ppt U in 0.1% nitric acid c) through column at –0.25 V, d) mass spectrum at –0.25 V applied potential

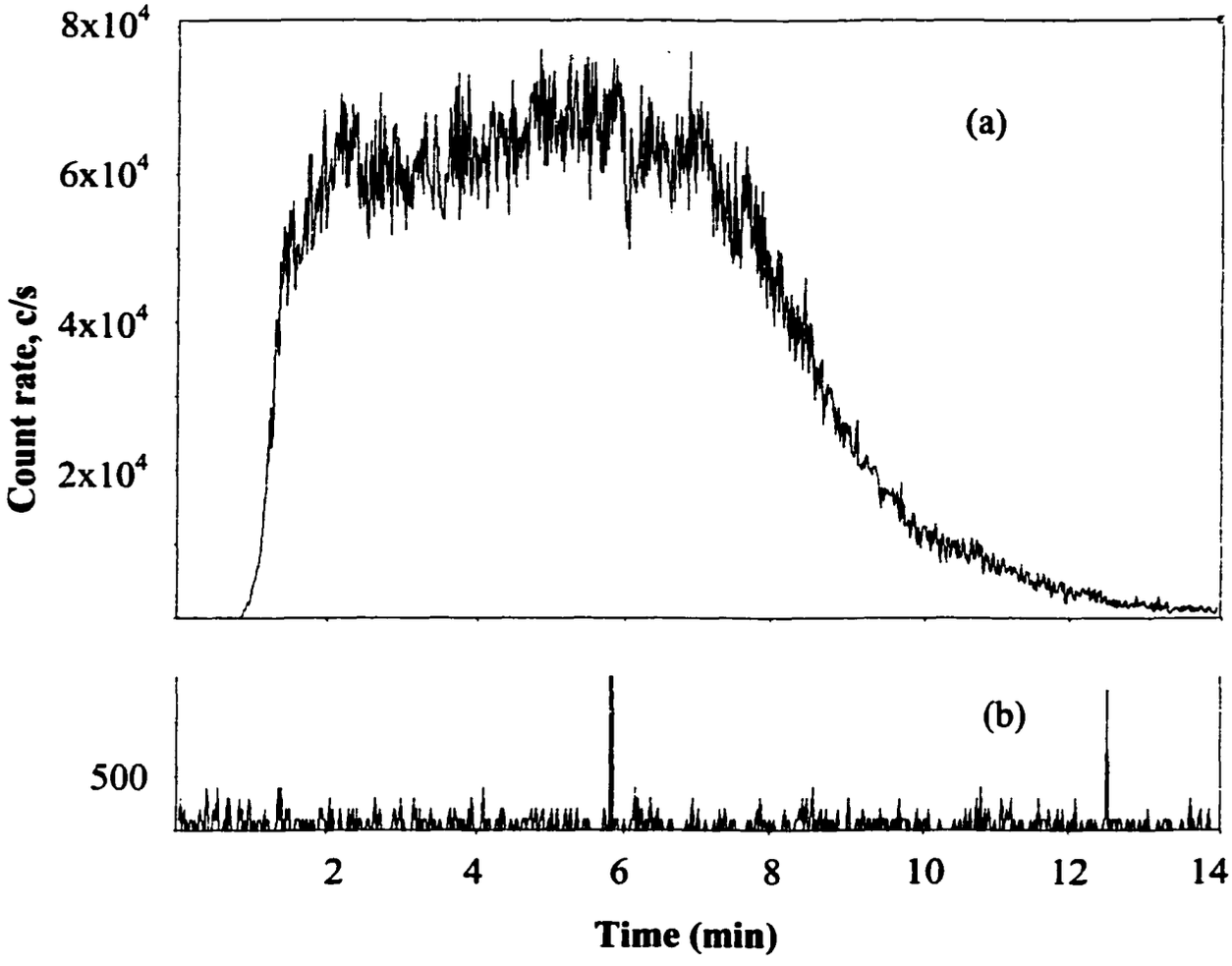


Figure 6: $^{59}Co$ signal a) 0.1 % $HNO_3$ blank, containing less than ppb of Co, at open circuit; b) through the EMLC column at –0.45 V

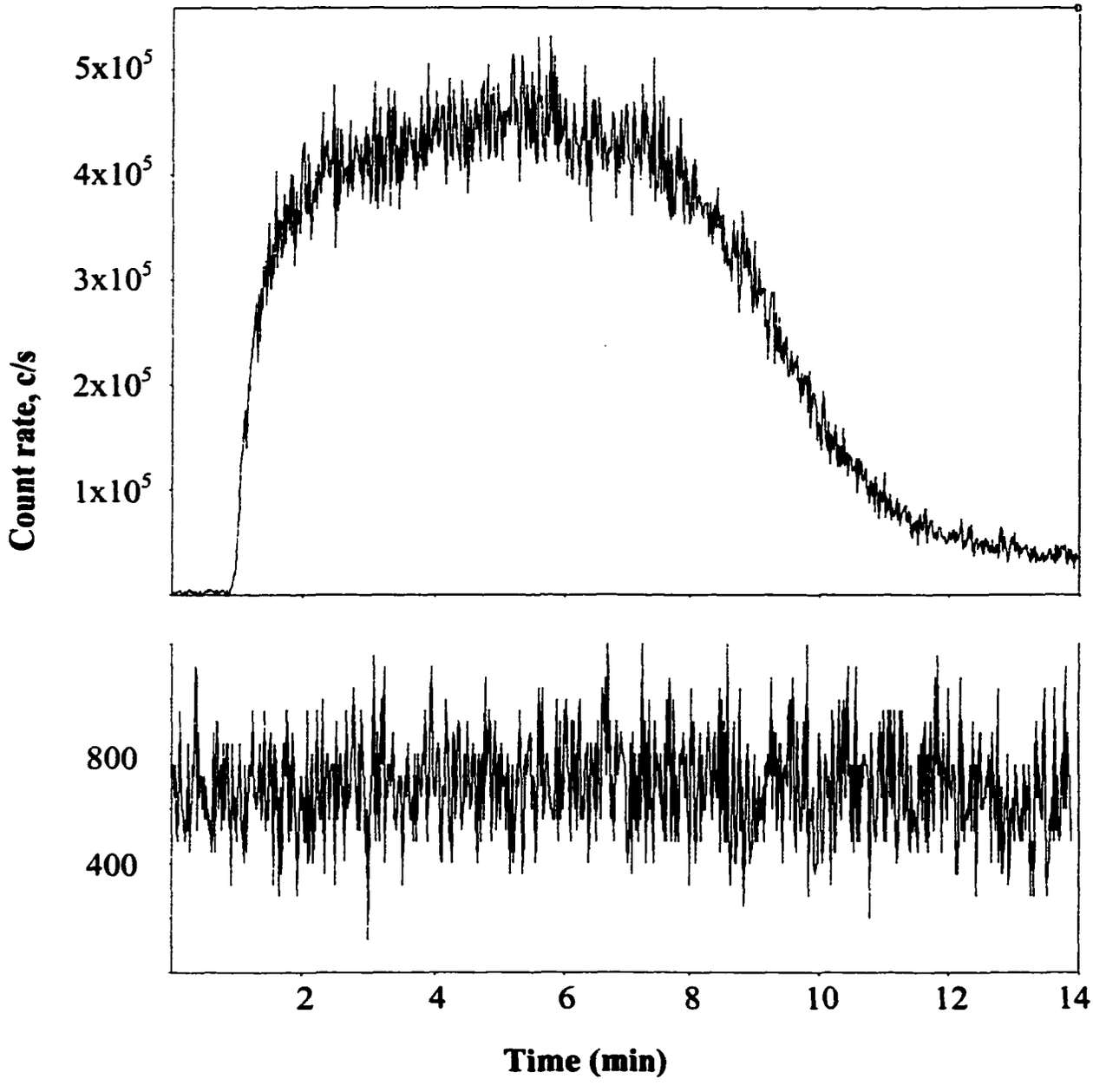


Figure 7: $^{51}V$ signal a) for 0.1 % $HNO_3$ through the EMLC column at open circuit; b) through the EMLC column at –0.45 V

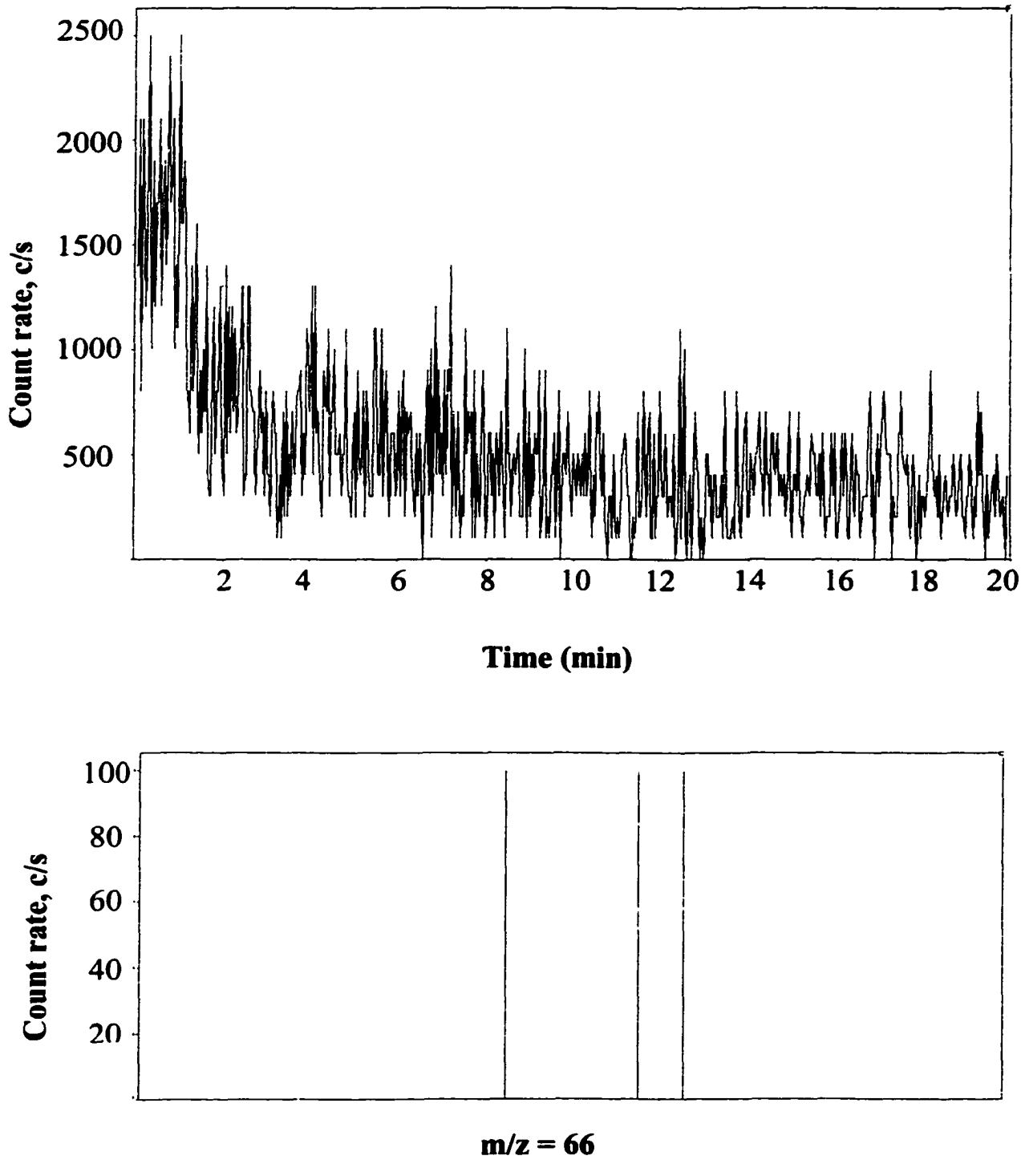


Figure 8: Zn clean up from DI water with 0.1% HNO3 supporting electrolyte at –0.5 V

# CHAPTER 5: FUTURE WORK AND CONCLUSION

High operating cost of ICP instruments largely due to the high argon consumption (15-20 L/min) can be minimized by the proposed externally air-cooled low flow torch. Outer argon flow can be lowered to less than 6 L/min with no risk of melting the torch or loosing analytical performance. Low flow ICP can be viewed axially with the cooled cone interface. At low flow the plasma does not stream far out of the end of the torch, but this is not a problem because of the cooled cone interface. Axial sampling of photons before the low-flow plasma is exposed to air is the key to this concept for reducing argon consumption without compromising performance. Such a torch –cone combination combines the improved detection limits of axial viewing with low argon consumption. The performance of this low-flow torch is comparable to that of a regular torch and is actually better for Ca and Ba. The new torch and viewing system provide very good performance for certain lines in the visible, especially Ba (II) 455.403 nm and Ca (II) 393.366 nm. The DL of 0.9 ppt for Ca is at least as good as that obtainable by ICP-MS and could be of great value in the semiconductor industry. Calcium is a common, easily ionized impurity element that ruins the performance of silicon. It is hardly the best element for ICP-MS. Performance near 200 nm is believed to be limited by the transmission of the three lenses used. The torch housing and optical system could be rebuilt to move the plasma closer to the normal object position of the spectrometer to mitigate this problem. This externally-cooled torch is readily interchangeable with conventional torches, at least in those instruments equipped for axial viewing with a sampling cone inside the plasma.

Both quantitative and isotope ratio measurement of silicon are becoming very important for quality assurance in semiconductor manufacturing. Measurement of silicon by ICP-MS is interfered by the presence of polyatomic ions at m/z range 28 to 30. The polyatomic ion interferences are more severe in measurement of silicon in organic solvents in addition to other adverse effects of organic solvents in ICP-MS. The present study shows that silicon can be measured quantitatively by ICP-MS with a quadrupole mass analyzer by reducing polyatomic ion interference at m/z 28 to 30. With the advantage of low flow nebulizer with high efficiency and less solvent load, cryogenic desolvation removes most of the solvent from the aerosol and enables silicon measurement at low parts per million levels. However the background due to polyatomic ions is still high that prevents measurement of silicon lower than ppm level. Further removal of polyatomic ions is possible by adding Xe or Kr into the plasma. Detection limit of silicon with few ml/min of Xe and Kr with the aerosol flow can be further improved one order of magnitude to ~100 ppb level. Although Isotope ratio measurement by quadrupole instrument is reported to provide high precision (0.1% RSD) for a number of interference free elements, the present technique with cryogenic desolvation and Xe/Kr introduction does not provide precision better than 0.5 % RSD. Lower precision is largely due to incomplete removal of polyatomic ion interferences and differential effect of Xe/Kr on the background at different m/z. Unsteady flow of Xe/Kr gas might contribute to the higher RSD value in isotope ratio measurement.

Although double focussing magnetic sector ICP-MS is reported to provide precision of 0.05% RSD value at low resolution for isotope ratios near unity, but at higher resolution and at higher isotope ratio the precision better than 0.1% RSD value is less likely. At higher resolution, the peak is triangular rather than flat top occurred in the case of low resolution. Isotope ratio of silicon with its adverse memory effect is unlikely to provide better precision

than above-mentioned RSD value. In our present study, the precision we obtained is about 0.1% for aqueous and low concentration organic solution whereas in concentrated organic solvent the precision is close to 0.5%.

ICP-MS has already shown its tremendous advantage of ultra-trace detection limits for metal elements. However the practical detection limits are limited by the purity of the blanks. Electrochemically modulated glassy carbon particle packed column online with ICP-MS has shown the capability of cleaning a number of metal ions from the DI water or dilute nitric acid blanks. The deposition efficiency of some metal ions was more than 99%. Fortunately a single set of applied potential was observed to work for retention of different metal ions. However, some metals need appropriate adjustment of applied potential for their accumulation in the column.

Glassy carbon column packing material is resistant to strong acid. But in this study, the column used was made of stainless steel. At higher concentration of the acid, there would be possibility of damage of column-wall, made of stainless steel. Although 0.1% nitric acid flowing through the column showed insignificant leaching of metal ions, a metal free construction material of the column would be a better choice in future.

Metals having extreme negative reduction could not be retained in the column. At negative potential lower than –0.55 V, hydrogen evolution occurs. Excessive hydrogen evolution may damage the Nafion coating of the column. A release system of hydrogen gas formed in the column can alleviate this problem and help to increase the applied potential to further negative range. Decreasing the particle size of the GC particles and hence increasing the surface area can further enhance the efficiency of retention of metal ions.

# ACKNOWLEDGMENTS

I would like to express my sincere appreciation and thanks to my major professor, Dr. R. S. Houk. His guidance, support, patience and enthusiasm made this work possible. I express my utmost respect to him not only as a professor, but also as a person for his kindness, friendliness and broadminded attitude to his students. I have been very fortunate to have him as my supervisor for my graduate studies at Iowa State University.

Sincere thanks are also extended to Dr. Marc Porter, Dr. Denis Johnson, Dr. Keith Woo and Dr. David Laird, who serve as committee members. The effort of their critical reading of this manuscript, interest and suggestions are greatly appreciated. I owe the members of the Houk group (Narong Praphairasksit, Maan Amad, David Acshiliman, Yongjin Hou, and Fumin Li) deep appreciation not only for their help in scientific discussions, but also for the friendship they have extended to me during my stay at Iowa State University. I especially want to thank Dan Gazda, doctoral student with Dr. Porter, for his kind support and advice to do the EMLC experiment.

I owe a great deal to Dr. Dan Weiderin, founder of Elemental Scientific Inc., for his guidance and advice to complete this work. I would like to thank the chemistry machine shop and glass blowing shop, especially Trond Forre. Thanks go to all my friends who have made the years in graduate school bearable and enjoyable.

I am indebted to my research advisor Dr. A. I. Mustafa at University of Dhaka, and Dr. M. A. Wechter at University of Massachusetts Dartmouth, for their continuing encouragement and help in building my career in analytical chemistry.

Most importantly, I would like to thank my parents and my sisters and brothers for their support during all the years of my education. Finally, I thank my wife, Salma, for making everything unbearable to bearable in my graduate student life.